

**COMPUTER-GENERATED FRACTALS WITH MEDICAL
APPLICATION IN TRABECULAR BONE STRUCTURE**

HIZMAWATI MADZIN

**FACULTY OF COMPUTER SCIENCE & INFORMATION
TECHNOLOGY
UNIVERSITY OF MALAYA
KUALA LUMPUR**

2006

COMPUTER-GENERATED FRACTALS WITH MEDICAL
APPLICATION IN TRABECULAR BONE STRUCTURE

HIZMAWATI MADZIN
WGC030035

This project is to submitted to
Faculty of Computer Science and Information Technology
University of Malaya
In partial fulfillment of requirement for
Degree of Master of Software Engineering
Session 2006/2007

ABSTRACT

Fractal can be described as a self-similarity, irregular shape and scale independent object. The generation of each fractal is dependent on the algorithm used. The fractal is generated using a form of computer-generated process to create complex, repetitive, mathematically based geometric shapes. There are two main aims of this research, one of which is to develop a prototype known as Fractal Generation System (FGS) whereby each type of fractal is generated by practical implementations of the theories with some adaptation in the following algorithms: IFS Iteration, Formula Iteration and Generator Iteration. FGS also caters for the calculation of the fractal dimension (F_D) parameter using Box Counting Method (BCM). This parameter enables the system to characterize the irregularity and self-similarity of fractal shapes. FGS generates four types of fractals, which are Julia set, Mandelbrot set, Sierpinski Triangle and Koch Snowflake based on the three iterations. The F_D values computed and fractal patterns generated by FGS agree well with theoretical values and existing fractal shapes. The second main aim is in relation to the importance of fractal application in the real world whereby it focuses on analyzing trabecular bone structure. Bone has fractal characteristics. CT-scan images of trabecular bones of 27 males and 26 females ranging between 25 to 81 years were analyzed. The CT-scan images were digitized to convert it to binary images. The images were then processed to obtain the F_D parameter. The differences of the values due to gender and age are discussed in this thesis. There is a decrement of the F_D values when the age increases for both male and female. This is due to an age-associated reduction in number of fine trabecular network. Male F_D is generally higher than female F_D . The rate of decrease in F_D with age for male and female depends on the puberty, pre-menopausal and post-menopausal stages.

ABSTRAK

Fraktal boleh dijelaskan sebagai objek yang mempunyai persamaan antara satu sama lain, mempunyai bentuk yang tidak tentu dan skala yang tersendiri. Pembentukan fraktal adalah bergantung kepada algoritma yang digunakan dan fraktal yang dibangunkan menggunakan proses pengkomputeran akan menghasilkan bentuk fraktal yang kompleks, berulang dan corak berbentuk geometri berdasarkan teori matematik. Terdapat dua tujuan utama bagi penyelidikan ini. Salah satu daripadanya adalah untuk membangunkan prototaip sistem bernama 'Fractal Generation System' (FGS), di mana fraktal akan dibentuk dengan mengadaptasi teori di dalam penggunaan algoritma-algoritma berikut: 'IFS Iteration', 'Formula Iteration' dan 'Generator Iteration'. Prototaip sistem FGS juga mempunyai modul untuk mengira parameter dimensi fraktal menggunakan kaedah 'Box-Counting Method' (BCM). Parameter dimensi ini membolehkan sistem untuk membuat pencerian bentuk yang tidak tentu dan persamaan yang ada pada bentuk fraktal. Prototaip sistem FGS telah dibangunkan untuk membentuk empat jenis fraktal iaitu Julia set, Mandelbrot set, Sierpinski Triangle dan Koch Snowflake. Nilai parameter dimensi bagi empat jenis fraktal ini dan corak fraktal yang dihasilkan daripada FGS adalah sama dengan nilai teori dan bentuk corak bagi fraktal yang sedia ada. Tujuan penyelidikan yang kedua adalah berkaitan aplikasi fraktal dengan objek sebenar dan untuk penyelidikan ini memfokus kepada penganalisaan struktur tulang trabekular. Struktur tulang mempunyai ciri-ciri fraktal. 53 keping imej pengimbas CT bagi 26 lelaki dan 27 perempuan berumur lingkungan 25 hingga 81 tahun dianalisa bagi tujuan tersebut. Imej pengimbas CT ini diproses untuk ditukar kepada imej berformat binari. Kemudian imej ini dianalisa bagi memperolehi nilai parameter dimensi bagi setiap imej struktur tulang trabekular tersebut. Perbezaan nilai parameter dimensi di antara jantina dan juga umur turut dibincang di dalam tesis ini. Nilai parameter dimensi bagi struktur tulang trabekular didapati menurun apabila umur meningkat dan nilai parameter dimensi bagi tulang lelaki adalah lebih besar berbanding dengan nilai parameter dimensi tulang perempuan. Ini adalah disebabkan umur berkait rapat dengan pengurangan penghasilan tulang yang baik. Kadar penurunan parameter dimensi yang dinilai adalah bergantung kepada peringkat umur baligh, sebelum dan selepas monopus.

ACKNOWLEDGEMENTS

First and for most, I would like to thank my supervisor, Associate Professor Dr. Roziati binti Zainuddin for her constant support and guidance. She gave me enough time to start my research and trusted that I would accomplish something. She gave me as much freedom as I needed to get my research work done.

I also would like to thank to Cik Hanizan Ahamad, from Radiology Department of University Hospital, for her willingness to share her knowledge on matters regarding to this research field.

A big thank you to both of my parents, Mr. Madzin Majid and Mrs. Halimah Ahmad and the rest of the family for giving me all the support that I need and have been always encouraging me to pursue my studies until this far.

My thanks are also extended to my entire friends who have helped me in this research work directly or indirectly.

Last but not least, a very big thank you to my beloved husband, Mr. Mohd Faizal Aziz for all the guidance, ideas, time, support, attention, motivation, and encouragement.

Hizmawati Madzin

2007

LIST OF TABLES

Table		Page
Table 3.1:	Comparison of parameters in Julia set and Mandelbrot set	33
Table 3.2:	Evaluation of the method to determine fractal dimension	41
Table 5.1:	Generation of Sierpinski Triangle using separately of affine transformations 1,2 and 3	68
Table 5.2	Comparison of fractals images between Crownover and FGS	76
Table 5.3	Analytical fractal dimension values for Koch Snowflake and Sierpinski Triangle	77
Table 5.4	Sierpinski Triangle data acquisition	78
Table 5.5	Koch Snowflake data acquisition	79
Table 6.1	Fractal dimension values for patients in the age range from 20 to 80 years	84

LIST OF FIGURES

Figure		Page
Figure 2.1	: Fern leaf, one of fractal's examples in our natural surrounding	10
Figure 2.2	: Image of rugged terrain photographed from the side of a mountain	14
Figure 2.3	: Example of Sierpinski Triangle in nature object. The picture (a) appears as the generator of the whole tree. Which mean small branch of a tree reminds one of the entire tree.	17
Figure 2.4	: Example of naturally occurring fractal in human body. (a) The folds on the surface of the brain (b) The branching of blood vessels in the human body	18
Figure 2.5	: An example of fractal in computer graphic used in science-fiction movie Star Trek.	19
Figure 2.6	: An example of space 'A' in a unit of square	20
Figure 2.7	: Richardson method in the coastline of Great Britain	22
Figure 2.8	: Minkowski sausage method	23
Figure 3.1	: Procedure of Generating Sierpinski Triangle	34
Figure 3.2	: Affine transformations used in generating Sierpinski Triangle	35
Figure 3.3	: Initial point of Sierpinski Triangle is plotted	36
Figure 3.4	: Construction of Koch Curve	37
Figure 3.5	: Process of Koch Snowflake	37
Figure 3.6	: Five points in line segment	38
Figure 3.7	: p3 point execute as generator	38
Figure 3.8	: The upper and lower bound limit to define fractal dimension	43
Figure 3.9	: Conversion of a CT-scan image to a grayscale image	47
Figure 3.10	: Figure 1 shows the selection of ROI of the CT-scan image and figure 2 is the result of output image after the cropping	47
Figure 3.11	: Conversion of grayscale image to binary format. The white structure represents the bone structure to be measured	48

Figure	Page
Figure 4.1 : DFD Level '0' of FGS	53
Figure 4.2 : DFD Level '1' of FGS	54
Figure 4.3 : DFD Level '2' of FGS	55
Figure 4.4 : DFD Level '3' of FGS	56
Figure 4.5 : Use case diagram of FGS	58
Figure 4.6 : Class Diagram of FGS	59
Figure 4.7 : Sequence diagram of FGS	60
Figure 5.1 : Main Screen	62
Figure 5.2 : Fractal image of Julia set	63
Figure 5.3 : Julia set using same fractal generation equation with different parameter values of real number and imaginary number.	65
Figure 5.4 : The zoom-in of Julia set. The layers of colors represent number of iterations that has been reached before executing next orbit.	65
Figure 5.5 : Fractal image of Mandelbrot set	66
Figure 5.6 : White circle shows the Mandelbrot set in variety size based on the fractal generated in previous figure	67
Figure 5.7 : Figure (a) shows the generation of Sierpinski Triangle with initial point. Figure (b) shows the generation of Sierpinski Triangle without initial point.	69
Figure 5.8 : Screenshots of Sierpinski Triangle via FGS	69
Figure 5.9 : Fractal image of Koch Snowflake	70
Figure 5.10 : The sequence of Koch Snowflake generation	71
Figure 5.11 : Screen shot for data acquisition phase	72
Figure 5.12 : The system interface after the structure measurement	73
Figure 5.13 : The system interface for fractal dimension calculation phase	74
Figure 5.14 : Sierpinski Triangle	78

Figure		Page
Figure 5.15 :	Scatter plot to obtain fractal dimension value of Sierpinski Triangle	78
Figure 5.16 :	Koch Snowflake	79
Figure 5.17 :	Scatter plot to obtain fractal dimension value of Koch Snowflake	79
Figure 6.1 :	Graph presentation of BMD value and age versus fracture risk.	82
Figure 6.2 :	Image (a) is the ct-scan images. Image (b) is the grayscale image before it's been crop to ROI. Image (c) shows the ROI of the image with binary format.	84
Figure 6.3 :	F_D value for patients range age 25 to 29; male $F_D = 1.863$ and female $F_D = 1.843$	85
Figure 6.4 :	F_D value for patients range age 30 to 35; male $F_D = 1.816$ and female $F_D = 1.781$	85
Figure 6.5 :	F_D value for patients range age 38 to 48; male $F_D = 1.760$ and female $F_D = 1.746$	86
Figure 6.6 :	F_D value for patients range age 50 to 58; male $F_D = 1.735$ and female $F_D = 1.726$	87
Figure 6.7 :	F_D value for patients range age 62 to 67; male $F_D = 1.698$ and female $F_D = 1.682$	87
Figure 6.8 :	F_D value for patients range age 69 to 81; male $F_D = 1.693$ and female $F_D = 1.678$	88
Figure 6.9:	Measurement of trabecular bone structure for male patient age range 20 – 80 years.	89
Figure 6.10:	Measurement of trabecular bone structure for female patient age range 20 – 80 years	89

Content	TABLE OF CONTENTS	Page
ABSTRACT		i
ABSTRAK		ii
ACKNOWLEDGEMENT		iv
DECLARATION		v
LIST OF TABLES		vi
LIST OF FIGURES		vii
CHAPTER 1: INTRODUCTION		
1.1 Research Background		1
1.2 Statement of Problems		2
1.3 Project Specification		3
1.3.1. Research Motivation and Importance of Study		3
1.3.2. Main Aims and Objectives		4
1.4 Research Contributions and Publications		5
1.5 Dissertation organization		7
CHAPTER 2: TYPES OF FRACTALS AND APPLICATIONS		
2.1 Overview on Fractals		9
2.2 Types of Fractal Patterns		11
2.2.1 Formula Iteration		12
2.2.2 IFS Iteration		12
2.2.3 Generator Iteration		13
2.3 Fractal Characteristics		13
2.4 Fractals in Real World		16
2.4.1 Fractals in Nature		16
2.4.2 Fractals in Biological Science		17
2.4.3 Fractals in Computer Graphics		18
2.5 Fractal Dimension		19
2.5.1 Notion of Dimension		20
2.5.2 Fractal Dimension Computation		21

Content	Page
2.6 Fractal Analysis in Medical Field	24
2.6.1 Osteoporosis and Trabecular Bone Structure	25
2.7 Summary	27

CHAPTER 3: PROBLEM ANALYSIS AND SOLUTION APPROACHES

3.1 Classification of Problems	28
3.2 Proposed solutions approaches	29
3.3 Fractal Algorithms	30
3.3.1 Formula Iteration	31
3.3.2 IFS Iteration	33
3.3.3 Generator Iteration	36
3.4 Fractal Dimension Measurement	39
3.4.1 Comparison of Various Fractal Dimension Measurement Methods	39
3.4.2 Box-counting Method	41
3.5 Application of Fractal Analysis in Trabecular Bone Structure	44
3.5.1 Conversion of CT-scan Image to Grayscale	46
3.5.2 Selection Region of Interest (ROI)	47
3.5.3 Conversion of Image to Binary Format	48
3.6 Summary	49

CHAPTER 4: REQUIREMENT ANALYSIS AND DESIGN

4.1 FGS Requirement Analysis	50
4.1.1 Functional Requirements	50
4.1.2 Non-Functional Requirements	51
4.2 System Design	52
4.2.1 Structural Analysis Modeling	52
4.2.2 Object-oriented Analysis Modeling	57
4.2.2.1 Use Case Diagram	57
4.2.2.2 Class Diagram	58
4.2.2.3 Sequence Diagram	60

Content	Page
CHAPTER 5: IMPLEMENTATION RESULTS AND DISCUSSION	
5.1 Fractal Generation Phase	63
5.1.1 Julia set	63
5.1.2 Mandelbrot set	66
5.1.3 Sierpinski Triangle	67
5.1.4 Koch Snowflake	70
5.2 Fractal Dimension Phase	71
5.2.1 Data acquisition phase	72
5.2.2 Fractal dimension measurement	73
5.3 System Validation	75
5.4 Summary	80
CHAPTER 6: RESULTS AND DISCUSSION OF FRACTAL ANALYSIS IN TRABECULAR BONE ARCHITECTURE	
6.1 Bone Mineral Density (BMD) and Bone Architecture	81
6.2 Fractal analysis in Trabecular Bone Structure	83
6.3 Summary	90
CHAPTER 7: SYSTEM EVALUATION	
7.1 Strengths of FGS	91
7.2 FGS Weaknesses	93
CHAPTER 8: CONCLUSION AND FUTURE ENHANCEMENT	
8.1 Conclusion	94
8.2 Future Enhancements	96
8.3 Summary	97
BIBLIOGRAPHY	98
APPENDIX I : Julia Set Fractals	103
APPENDIX II : CT-scan Images	105

CHAPTER 1

INTRODUCTION

This chapter gives a general background of this research project with statement of problems. Project specifications on the importance of the study, aims and objectives are spelled out. The last part of this chapter is on the dissertation organization for this research project.

1.1 Research Background

Due to advancement of multimedia technology, there has been an increasing interest in studies of fractal patterns. A fractal is an irregular fragmented figure which consists of the identical pattern undergoing repeated geometric transformation of scaling down and rotation. It can be subdivided into parts, whereby each part is a reduced-size copy of the original whole shape. Such characteristics imply that fractals are generally self-similar and scale independent. Fractals are created by an iterative process of a positive feedback loop whereby input data undergoes a modification and the output is fed back into the system as input. There are different approaches and algorithms to generate various types of fractals. For this research project, a prototype system is developed to generate and compare different types of fractals by using the different iteration techniques.

There are many instances that can be related between fractals and nature surroundings. Nowadays fractals are often describing the real world better than traditional mathematics and physics. Scientists have investigated that many natural structures are better characterized using fractal geometry.

There are many fields in science that can use fractals in domain understanding and their analysis. As cited by Hasting and Sugihara (1994:4): “..1991, the Science Citation Index listed amount of 400 papers with the word fractal in their title.” These titles span fields ranging from nature, cosmology and the developmental biology.

In recent years, the importance of fractal applications has gained interest in medical field. This field ranges from pathology, radiology and largely on physical anthropology. Osteology, which is a study on bone structure, is a subfield of anthropology. In the past decade, the use of fractal analysis has been widely used and shown its capability for properly describing the characteristics of the natural forms in human biology. Therefore, there is a research motivation to design and develop a system for fractal analysis in medical images.

1.2 Statement of Problems

The following problems have to be addressed to develop a prototype system in this research:

I. Generation of each type of fractal using a corresponding algorithm.

- Differentiate various types of fractals using different algorithms.
- There are three algorithms used in this research project to generate fractals, namely Formula Iteration algorithm, IFS Iteration algorithm and Generator Iteration algorithm.

II. Identifying a suitable method of calculating fractal dimension

- Various methods need to be compared to identify a suitable method for this research such as Richardson method, Minkowski method, Mass method and Box-counting method (BCM).
- BCM has many advantages compared to other methods due to its flexibility, ease for application and suitability for medical image analysis.

III. Selection of an appropriate biomedical application, which can be related to fractal pattern and analyzing, the medical images.

- Fractal approaches are relevant to demonstrate real world applications. Structural patterns in nature cannot be described by using Euclidean geometry. Hence, fractal approach is needed to describe fractal properties of self-similarity, complexity and iterative characteristic.
- Conventionally BMD approach is used to characterize trabecular bone structure. Fractal analysis is an alternative technique to determine the bone strength based on the value of fractal dimension.

1.3 Project Specification

This section explains the main aims and objectives of the research project with the proposal solution approaches. The significant contributions of the research project are also listed.

1.3.1 Research Motivation and Importance of Study

The advancement of multimedia technology drives interest in more detail studies of fractal patterns. Therefore a prototype system is developed to generate various types of fractal patterns and intended to provide a foundation for further experimentation. The generation

of each fractal is dependent on the approach and algorithm used. Thus it is important to understand the properties of each type of fractal, as this will influence the procedure during the generation of fractals.

Recently, the application of fractal analysis has become an important study in medical field. Fractal characteristics such as self-similarity, irregularity, scale independence and complexity are particularly suited to the properties of medical images. Therefore the fractal properties of these images are important variables in understanding the nature of biological materials. Such reasons motivate the study of fractal application in medical field.

1.3.2 Main Aims and Objectives

There are two main aims for this research project namely:

- I) To generate fractals and to quantify the fractal structure.
- II) To study fractal application in biomedical field. In relation to each aim there are several objectives that need to be achieved.

(I) Generation of fractals and measurement quantification of fractal structure.

- a. To study fractal patterns and their properties.
 - i) This study includes the classification of various types of fractals and the corresponding algorithms to generate them.
 - ii) A method to calculate fractal dimension is determined to quantify fractal structure.
 - iii) Types of fractals are identified for various real world applications.

- b. To build a prototype of fractal generation system (FGS)
 - i) The system can produce four types of fractals, which are Mandelbrot, Julia, Koch Snowflake and Sierprinski Triangle.
 - ii) The system is able to measure the dimension of fractal generated.
 - iii) The system can display the results of the data in the form of tables and graphs for better illustrations and interpretation of the results.

(II) Fractal application in biomedical field.

- a. To implement the FGS prototype in studying fractal patterns in trabecular bone structure.
 - i) CT-scan images, which undergo various stages of image processing, are input into FGS.
 - ii) The system provides the application of fractal analysis towards medical images.
 - iii) Comparative studies can be made between the images.

1.4 Research Contributions and Publications

Based on the solution approaches, this section states the contributions for the research project. The contributions are two-fold. The first contribution is the research product of a prototype system to generate fractals. FGS will generate four types of fractals, which are Julia set and Mandelbrot set from Formula Iteration, Sierpinski Triangle from IFS Iteration and Koch Snowflake from Generator Iteration. Moreover this system provides a module to measure the fractal dimension value. FGS performance will be discussed based on the comparison of fractal dimension values of fractals generated with the theoretical fractal

dimension values. Furthermore the fractal-generated image will be matched with the existing fractal image.

The second contribution is the analysis of trabecular bone structure using FGS. In this analysis the results of fractal dimension values in trabecular bone structure will be discussed and related with osteoporosis based on gender and range of age. The purpose of the analysis is to justify that fractal analysis of trabecular bone structure can be a reliable technique to measure the architecture of trabecular bone. It is important to analyze the architecture of trabecular bone as it can prevent or diagnose osteoporosis.

Publications for the research work are as follows:

Proceedings

1. **Hizmawati Madzin, Roziati Zainuddin** 2006. "Computer Simulation in Generating Fractals." *Proc. International Conference on Geometric Modelling and Imaging:IEEE (GMAI'06)* pg 47-50, London, United Kingdom.
2. **Hizmawati Madzin, Roziati Zainuddin** (2006). "Measurement of Julia Set Fractal Dimension Using FGS." *Proc. Regional Computer Science Postgraduate Conference 2006 (ReCSPC '05)* pg 206-209, Pulau Pinang, Malaysia.
3. **Hizmawati Madzin, Roziati Zainuddin** (2006). "Fractal Dimension Measurement in Bone Architecture." *Proc. International Conference on Information & Communication Technology for the Muslim World 2006 (ICT4M)*,(CD ROM Paper ID: 57) Kuala Lumpur, Malaysia

Exhibition – Gold Medal

1. Roziati Zainuddin, **Hizmawati Madzin**, Nor Sabirin Mohamad, Nurfadhlina Mohd Sharef (2006). “Development Of A Tool To Analyze Trabecular Bone Structure.” *3rd International Biotechnology Trade Exhibition, Conference and Award*, PWTC Kuala Lumpur.

Poster

1. **Hizmawati Madzin**, Roziati Zainuddin (2006.) “Computer-based Comparative Study of Fractal Algorithms” (*Poster presentation*) *University of Malaya Graduate Symposium*, Kuala Lumpur, Malaysia

1.5 Dissertation Organization

Chapter 1 covers the introduction of this research project. It briefly explains the research background. Moreover, this chapter clarifies the aims, objectives, contributions and publications of this research project.

Chapter 2 represents an overview of fractal theory. This chapter gives a literature review on each type of fractal iterations and the algorithm used to generate the fractals. Furthermore, this chapter gives description on the characteristics of fractal and briefly illustrates fractals in real world applications. Lastly this chapter covers the application of fractal analysis in medical field.

Chapter 3 expresses the problem analysis and the solution approaches of this research. This chapter discusses the fractal algorithms to generate fractals and a suitable method to measure fractal dimension value. Moreover the application of fractal analysis in trabecular bone structure is discussed in this chapter.

Chapter 4 describes the analysis and design process of FGS. These include requirement analysis and object-oriented design of FGS. Object-oriented design includes use case diagram and data flow diagrams.

Chapter 5 represents results and discussion of FGS. This chapter illustrates the execution of FGS in generating every type of fractal and the fractal dimension calculation. Screen shots of FGS help in better understanding. The chapter also covers system validation to determine the accuracy and the usability of the system.

Chapter 6 describes the results of fractal analysis in trabecular bone structure. In this research, 53 CT scan images of trabecular bone structure are analyzed based on gender and range of age between 25 to 81 years.

Chapter 7 covers the system evaluation, where we describe the strengths and weaknesses of FGS.

Chapter 8 is the last chapter of this research. It covers conclusion and future enhancements of this research project.

CHAPTER 2

TYPES OF FRACTALS AND APPLICATIONS

The first part of this chapter describes the overview and types of fractals. Important characteristics of fractals are highlighted and compared. This chapter also gives explanation about fractal dimension and techniques to measure the dimension.

2.1 Overview on Fractals

According to Mandelbrot (1983), a fractal can be characterized as a fragmented and rough geometric shape, which can be subdivided into parts whereby each of which is a reduced-size copy or at least approximately copy of the entire shape. The root word of fractal came from Latin adjective "*fractus*". It is equivalent to Latin verb "*frangere*" which means "to break": to create irregular fragments. No matter what the scale level, the occurrence of the component object within memorializes the original structure. Generally a fractal is identified with its main key characteristics. According to McGuire (1991) a fractal looks the same over all ranges of scale.

The application of fractal started in 1970 when the term "fractal" has been widely used to characterize the properties of object that exist in our natural surroundings. The objects are defined as fractal objects when there are fractal characteristics revealed in the objects namely self-similarity, scale independence, irregularity and complexity. For example, a whole fern leaf is a geometry pattern that has many similar irregular shapes, and each of these smaller leaves, in turn, is made from even smaller leaves. The closer one looks the more similar detail one can see. From the Figure 2.1, fern leaf cannot be described using

the traditional Euclidean geometry shape. Hence, fractal has become an important concept of geometry to represent nature objects.

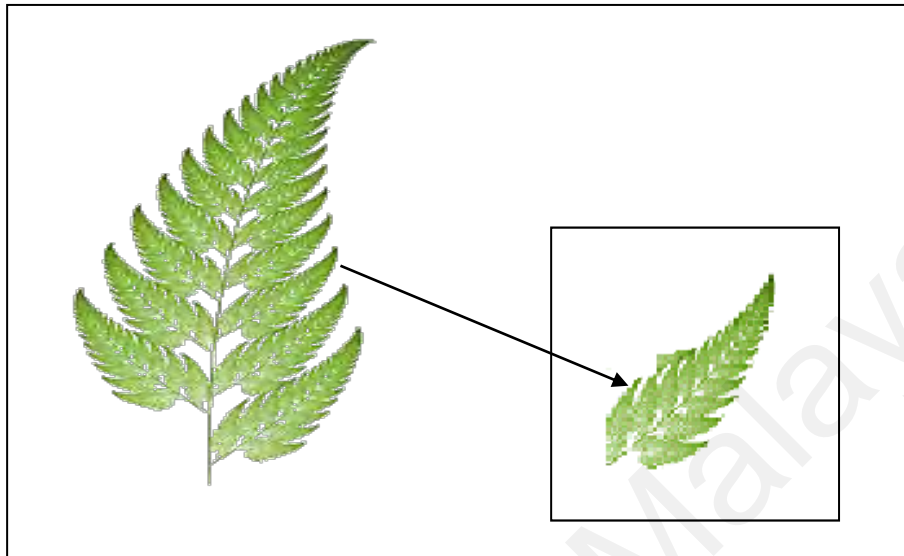


Figure 2.1: Fern leaf, one of fractal's examples in our natural

Euclidean geometry is a widely known type of geometry. Euclidean geometry comprises of lines, planes, rectangular volumes, arcs, cylinders, spheres and others. Almost all of the Euclidean geometries are used to build all kinds of objects. However, people later had discovered that there are certain curves and surfaces that could not be described by the Euclidean geometry. According to Mandelbrot (1983), clouds are not spheres, mountains are not cones, coastlines are not circles, and bark is not smooth, nor does lightning travel in a straight line. According to Kaye (1989) that there are limitations in trying to approximate the shape of natural object with Euclidean geometry. Such limitations include failure to model appropriately the irregularity in shape shown by natural objects. Euclidean geometry is not suitable to describe fractal, as fractal structure is complex, irregular at all levels of magnification and its structure is indefinite. Euclidean geometry is based on the first, second and third dimensions which are not realistic in nature. Fractal geometry is the

geometry of the fourth dimension which is real and comprise of the three dimensions and intervals between them.

According to Deering and West (1992), the shape in fractal geometry is far closer to nature compared to Euclidean geometry. Mandelbrot (1983) invented the term of fractal with advanced and the position of the fractal geometry can be classified as geometry of nature. Hence, this makes fractal analysis a better technique for evaluating form, shape, size and the morphological parameters of objects in our natural surroundings.

In nature, fractals can be related to many real world objects. Recently, the importance of fractal analysis has gained the interest of biomedical field. Traditionally, scientists modeled nature using Euclidean representations of natural object. However, there are many objects that have complex biological structures that are not suitable to model using Euclidean geometry. Typically the most common of such pattern is the branching structure of many biological structures. According to Richardson and Gillespy (1993), branching structures in the human body include regional distribution of pulmonary blood flow, pulmonary alveolar structure, distribution of arthropod body lengths and trabecular bone structure in vertebral specimen.

2.2 Types of Fractal Patterns

There are various iteration techniques that can be used to generate fractals namely Formula Iteration, IFS iteration and Generator Iteration (Crownover, 1995). Each iteration is supported with a particular fractal algorithm. Fractals are generally created by an iterative process of a positive feedback loop whereby input data undergoes a modification to

produce an output which is fed back into the system as input (Cynthia, 1996). The process repeats itself until the stop criteria such as maximum number of iterations is met.

2.2.1 Formula Iteration

Formula Iteration is based on mathematical formula to construct fractal. It might produce the most complex fractal in its geometry pattern by a simple formula. The Formula Iteration technique involves complex numbers for the computation (David, 1994). In this research project, the system developed is able to generate Julia set and Mandelbrot set in presenting fractals of Formula Iteration.

2.2.2 IFS Iteration

Iteration Function System (IFS) is another type of iteration to generate fractals. Many kind of structures in the universe can be represented using IFS Iteration. The generation of fractals using IFS Iteration is by substituting initial object with identical ones as described by a generator (Crownover, 1995). IFS Iteration is composed of a few simple elements such as transformations and probabilities. In every iteration each object in the generator is replaced by using affine transformation. Affine transformations is obtained by applying a linear transformation and followed by a translation. Linear transformation may consists of dilation, rotation, reflection or inversion. Each affine transformation uses several linear transformations to change the coordinate (x,y) to a new coordinate (x_1, y_1) .

IFS Iteration is the best way to reveal the simplicity underlying some complex shapes. By using these affine transformation and after infinite number of iterations, this iteration will produce an image which will have the outline of the original object but an exact self-

similarity of the object. In this research project, Sierpinski Triangle (Gasket) is used as example for IFS Iteration.

2.2.3 Generator Iteration

The generation of fractals using Generator Iteration is by substituting certain geometric shape with other shapes continuously. In other words, there are two main parts in Generator Iteration which are base and generator. Base is the initial shape of the figure. Then, every initial shape of the figure is substituted with another shape called generator. The Koch Snowflake fractal is generated to represent fractal in Generator Iteration.

2.3 Fractal Characteristics

As previously mentioned in section 2.1, the characteristics of fractals are self-similarity, scale-independence, irregularity and complexity. These characteristics are important to describe fractal patterns. Fractals may encompass one or more of these characteristics.

According to Clayton (1994), self-similarity is the main characteristic in defining fractal. Moreover, self-similarity is a crucial property in differentiating between the ideal fractal and natural fractal. Generally the ideal fractal is categorized in strict self-similarity while nature fractal object exhibits a statistical self-similarity behavior (Keith, 1997).

Most of ideal fractals are categorized in strict self-similarity. Types of fractals defined by IFS Iteration and Generator Iteration often display strict self-similarity, which means that, the fractal appears identical at different scales. For instance, Koch Snowflake is a strict self-similarity fractal, that is the development process produces smaller and smaller elements which produces a complex structure. Patterns in Formula Iteration fractals do display strict

self-similarity even though it is in an irregularity shape. Therefore, the structure would look the same at any level of magnification of the fractal.

In contrast to ideal fractal, the natural fractals do not display strict self-similarity behavior. Nevertheless, many natural fractal do display some degree of 'statistical' self-similarity at least over a limited range of magnification or temporal scales. According to Richard (1999), the patterns observed at different magnifications, although not identical and irregularity in shape are described by the same statistics. Moreover, One of the reasons of this statistical behavior, is due to the fact that there are both upper and lower limits to the size range over which objects in nature display the characteristics of fractal Thatcher (1999). As for example lung branching shows statistical self-similarity over 14 dichotomies, and trees branching over 8 dichotomies (Lorimer et al. ,1994).

Thatcher (1999) stated that natural objects are generated randomly rather than exactly or scale symmetric. This means that, instead the properties of natural fractals are within the upper and lower limit bounds; the rough shape revealed at one particular magnification only bears an approximate similarity to the shape at another level of magnification.



Figure 2.2: Image of rugged terrain photographed from the side of a mountain. (Adapted from Paul Bourke, Self-Similarity, 2002)

Shown in Figure 2.2 is a large piece of rugged terrain photographed from the side of a mountain where there are many rough shapes revealed at different levels of magnifications in the surface that need to be measured precisely in order to gain exact comparison at different length scales (level of magnification). According to McNamee (1991), the distribution of shapes at different level of magnification is known as self affinity. In conclusion there are two main contributors to the statistical self-similarity behavior in natural fractal which are upper and lower limit bounds and also self affinity.

In the study of natural fractals, the displayed pattern of nature form is intensely complex but it may exhibit an underlying simplicity through scale invariance up to a certain order. Thus, using the application of natural fractal has attracted the interest of researchers to be able to identify the simple basic structure of natural form and therefore will gain a better understanding of these nature objects. However, as Green (1995) writes: “.. true fractals are an idealization. No curve or surface in the real world is a true fractal; real objects are produced by processes that act over a finite range of scales only.” Furthermore, Green (1995) also explain that the estimates of fractal dimension in natural fractal may vary with scale.

A fractal object is characterized by constant parameter, called fractal dimension. The fractal dimension measures a qualitative features of fractal geometric objects. According to Peterson (1992), while a straight line has a dimension of one, a fractal curve will have a dimension between one and two depending how much space it takes up as it twists and curves. Hence, the more fractal's flat fills the plane, the closer it reaches to two dimensions. While the Euclidean geometry works with objects which exist in integer dimensions, fractal structure deals with objects in non-integer dimensions. Although all fractals have their own

fractal dimensions; these are not the same as the familiar Euclidean dimensions. The purpose to measure the dimension is to distinguish different fractals. The dimension of fractal geometry shapes of curves, surfaces and volumes can be very complex to be measured with the ordinary measurement. There are several notions of dimension, which are related to fractal dimension such as topological dimension and Hausdorff dimension. According to Maurice (2003), Hausdorff dimension is an extended non-negative real number, that is a number in the closed infinite interval $[0, \infty]$ associated to any metric space. Topological dimension is a basic concept of dimension, which a point has topological dimension 0, a line has topological dimension 1, a surface has topological dimension 2 and so on. (Theiler, 1990)

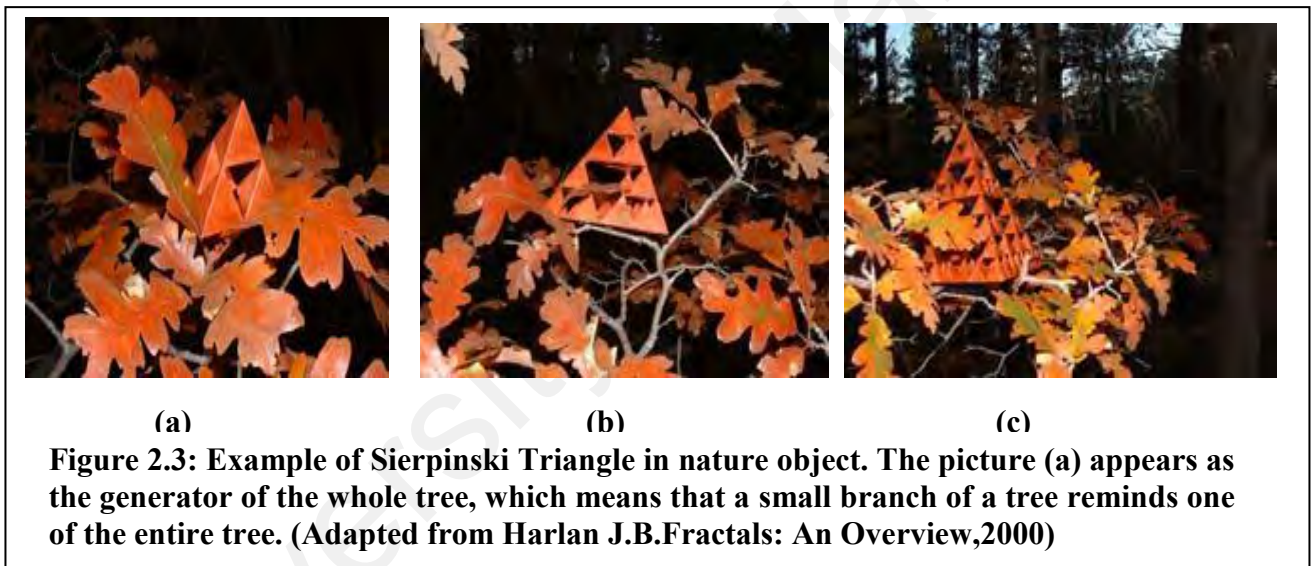
2.4 Fractals in Real World

There are many fields that can be permeated in fractal geometry such as nature and biological sciences. Moreover, there are many approximate fractal structures which look alike that can be found in this universe. In addition, the fractal geometry has become one of the most important techniques in computer graphics. In this section, the illustrations of fractal concepts adapted in real world are revealed.

2.4.1 Fractals in Nature

Figure 2.3 basically represents the fractal geometry of Sierpinski Triangle with statistical self-similarity in nature fractal structure. Although the fractal geometry uses different shapes from nature fractals, yet they share the same characteristics which is display of complex structure over an extended, but finite scale of range.

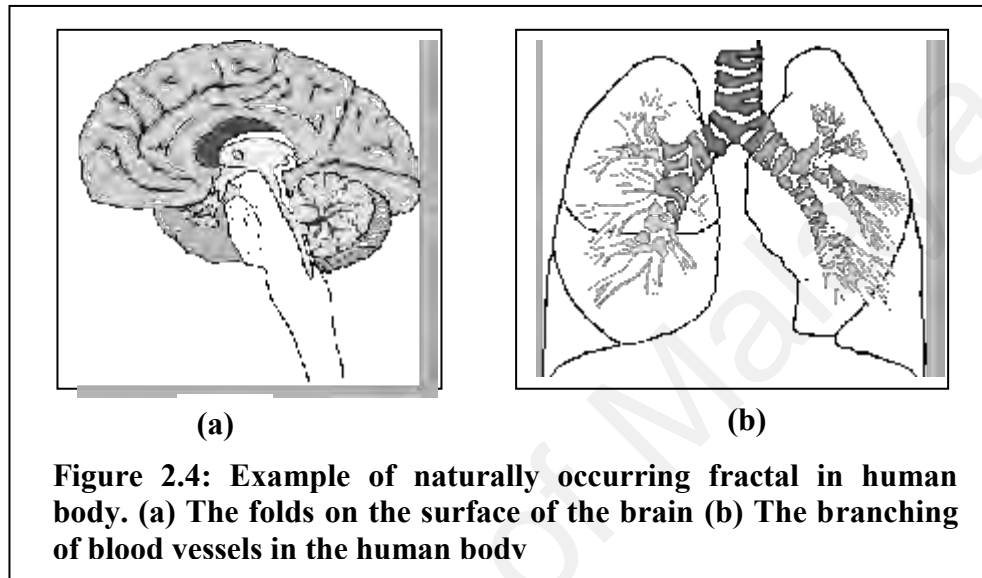
There are many other nature objects occurring fractals such as clouds, mountains, river network and plants. All these nature structures cannot be accommodated by Euclidean geometry as nature objects are not of simple structures but are, in fact, structures which exhibit irregularity and complexity. According to Connors (1997), fractal geometry is a new language used to describe, model and analyze complex forms found in nature. Trees and ferns are fractal objects in nature and can be modelled on a computer using a recursive algorithm. Figure 2.3 shows a good example of recursive nature whereby a branch from a tree is a miniature replica of the whole: not identical, but similar in nature.



2.4.2 Fractals in Biological Science

Traditionally, the scientists have modelled nature using Euclidean geometry representation of nature objects such as heart rate as sine wave and cell membrane as curve. However, fractal geometry, in the new mathematics field is changing the face of science. Scientists have recognized the complex system of the biological system using the fractal geometry. Biological systems and processes are typically characterized by many levels of substructures

that posses such characteristics as self-similarity, irregularity and invariance length. In recent years, scientists continue to use fractal geometry to model and analyse implications in human physiology (West and Golberger, 1987), ecology (Lehle, 1983) and many other sub disciplines of biology.

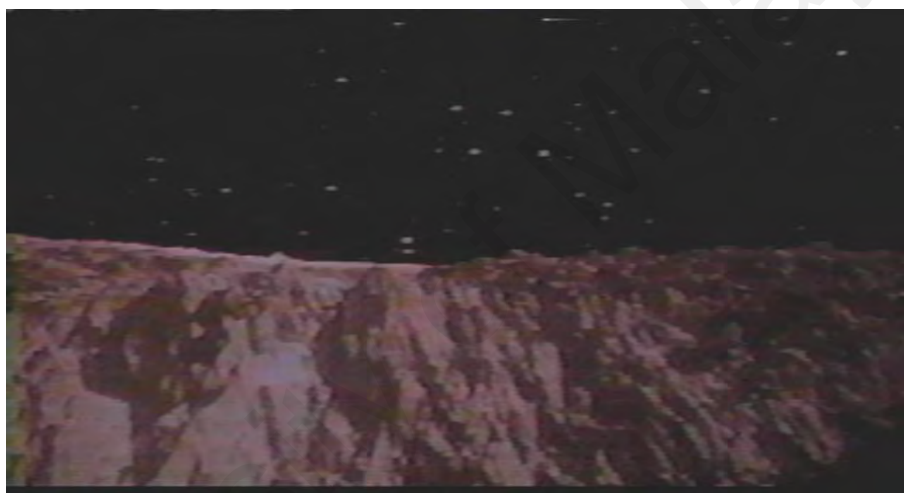


According to Kenkel and Walker (1993), fractal geometry may prove to be a combining theme in biology since it permits generalization of the fundamental concepts of dimension and length measurement. However, it is important to know that a nature object is not a strict mathematical fractal geometry. As mentioned in the previous section, nature fractal objects exhibit statistical self-similarity behavior, which means that in most biological systems there is a lower limit to self-similarity and also the addition of nature element of randomness to its fractal structure as depicted in Figure 2.4.

2.4.3 Fractals in Computer Graphic

Recently, fractal geometry has been used to generate many beautiful fractal images. The generation of fractals using Formula Iteration can be a good example of generating fractal in the context of computer graphics. Fractals are images created out of the process of a

mathematical exploration of the space in which they are plotted. Mostly the fractal pattern is produced using iterative equation process. There are many fractal gallery in the net to show their own collection of fractal images. Furthermore, fractal images have been used for image creation in science-fiction movies such as Star Wars, Star Trek and LOTR. Figure 2.5 is a fractal image from a clip of Star Trek II: The Wrath of Khan. The mountain is an example of a fractal-generated landscape that is used to show the birth of the "Genesis Planet" .



**Figure 2.5: An example of fractal in computer graphic used in science-fiction movie Star Trek.
(Adapted from HSHI, Fractal: An Introduction, 2000)**

2.5 Fractal Dimension

Fractal dimension is a quantitative measure but it gives and differentiates a qualitative features of a geometric object. Fractal dimension is used to distinguish different types of fractals. For example there are different types of the Sierpinski such as Sierpinski Gasket (Triangle) and Sierpinski Carpet (Square); and both of these fractals have different fractal

dimension values. Although these fractals were produced by a similar procedure, the result was a complicated object for one procedure to another. Hence, the measurement of fractal dimension is summarization of the overall complexity of fractal object. According to Kaye (1989), when the complexity of structure increases with magnification, it may be useful to use fractal dimension to describe the structure of the fine particle.

2.5.1 Notion of Dimension

Notion of dimension gives a precise parameterization of the conceptual or visual complexity of any geometry object. Basically the dimension is formalized in mathematics as the intrinsic dimension of a topological space. As for example the Euclidean object with n -space R^n , has topological dimension n . Topologically, a single dot has a topological dimension equal to zero, a line segment has dimension of one, surface has dimension of two and cube has dimension three. Moreover, topological dimension is always integral and it deals only with the qualitative shape of an object.

However there is a notion that allows the object with dimension other than integers. This notion is known as Hausdorff dimension. According to Mandelbrot (1983), a fractal is by definition a set for which the Hausdorff dimension strictly exceeds the topological dimension. An accurate way to measure the dimension of complicated set such as fractal is by using Hausdorff dimension.

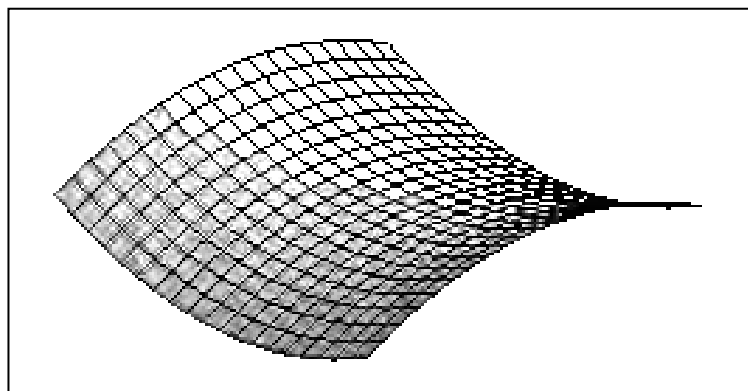


Figure 2.6: An example of space 'A' in a unit of square

For example, to define Hausdorff dimension for space 'A' in figure 2.6, number of little squares that are required to cover space 'A' and the size length of the little square are related using power law as equation (2.1).

$$N = s^d, \quad (2.1)$$

where variable N represents the number of little squares, s is the size length of the little square and d, represents the dimension of the object. Hence to get the dimension of space 'A', the dimension of the scaling law can be written as in equation (2.2).

$$d = \frac{\ln N}{\ln s} \quad (2.2)$$

Hausdorff dimension is quite similar to topological dimension where a line has Hausdorff dimension of 1 and n -dimensional Euclidean space has a Hausdorff dimension of n . However, Hausdorff dimension is not always a natural number. Hausdorff dimension quantifies the degree to which a trace 'fills' the plane or space. As for example a planar curved surface is topologically two-dimensional, while a fractal surface has Hausdorff dimension, d with the range of $2 \leq d \leq 3$.

2.5.2 Fractal Dimension Computation

There are many methods available to measure fractal dimension. For this research, a method which is suitable to measure medical images is considered. Therefore, several methods are reviewed namely Richardson method, Minowski method, Mass method and Box counting method. The methods are compared and the suitable method is selected to be incorporated in FGS.

Richardson method is one of the earliest method to measure fractal structure found by Louis Fry Richardson in the early 1960. It started when Richardson pointed out a question ‘How long is the coast of Great Britain’ (Kaye, 1989). Thus, Richardson devised a method to estimate the measure of the coastline of Great Britain. A polygon is used to estimate the coast perimeter as depicted in Figure 2.6. Different side length of polygon λ_1 , λ_2 and λ_3 is used to estimate the coastline of Great Britain. Richardson method is suitable for analyzing curves in a planar field. However, according to Long (1992), the Richardson method tends to enclose the outermost points of the structure’s boundary and slightly underestimates the length. As a result, the underestimate of boundary perimeter will severely influence the calculation of fractal dimension.

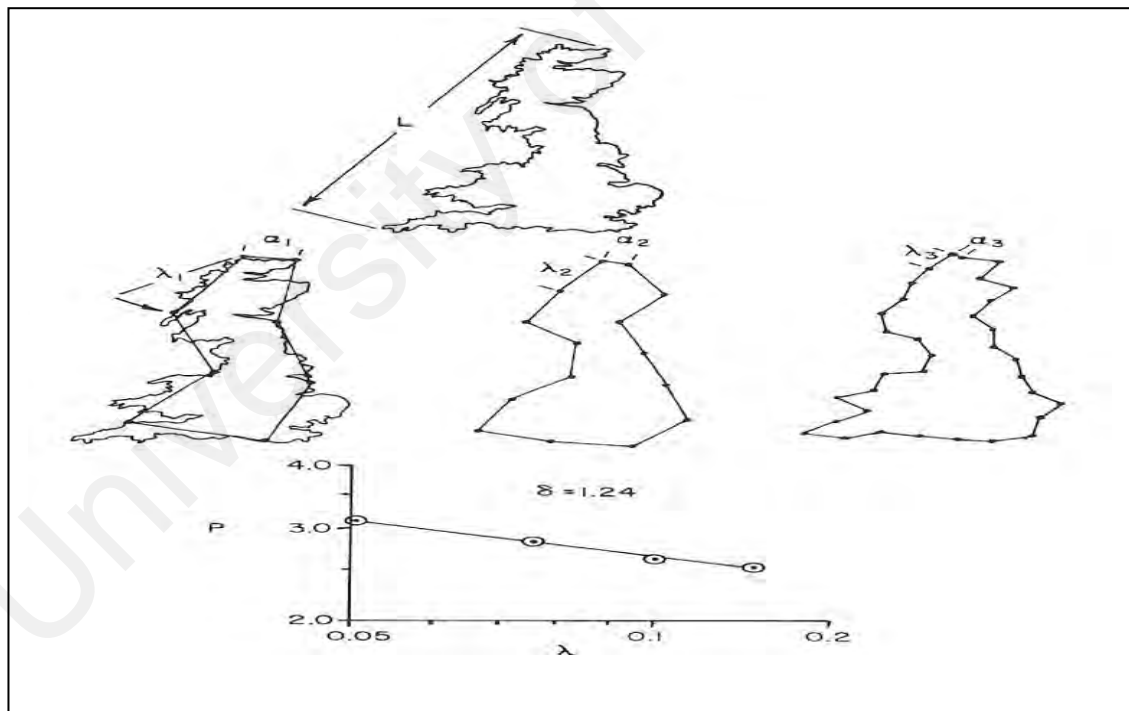


Figure 2.7: Richardson method in estimating the coastline of Great Britain (Adapted from Kaye; A Random Walk Through Fractal Dimension, 1989)

The next method is Minkowski method which is also known as Minkowski Sausage Logic. This is because circles are drawn around each point on the boundary and these circles merge

to form a ribbon overlaying the boundary as depicted in Figure 2.7. As the ribbon is straightened out, it looks like a sausage. Fractal dimension value of the boundary is estimated by dividing the area of the sausage with its breath (Cherbit ,1990). This method applies the use of circles of a predetermined radius. This method is suitable for the textural and structural analysis of a structure. However, according to Flook (1982), it can be over estimated due to expanded extremities of the sausage with free ends.

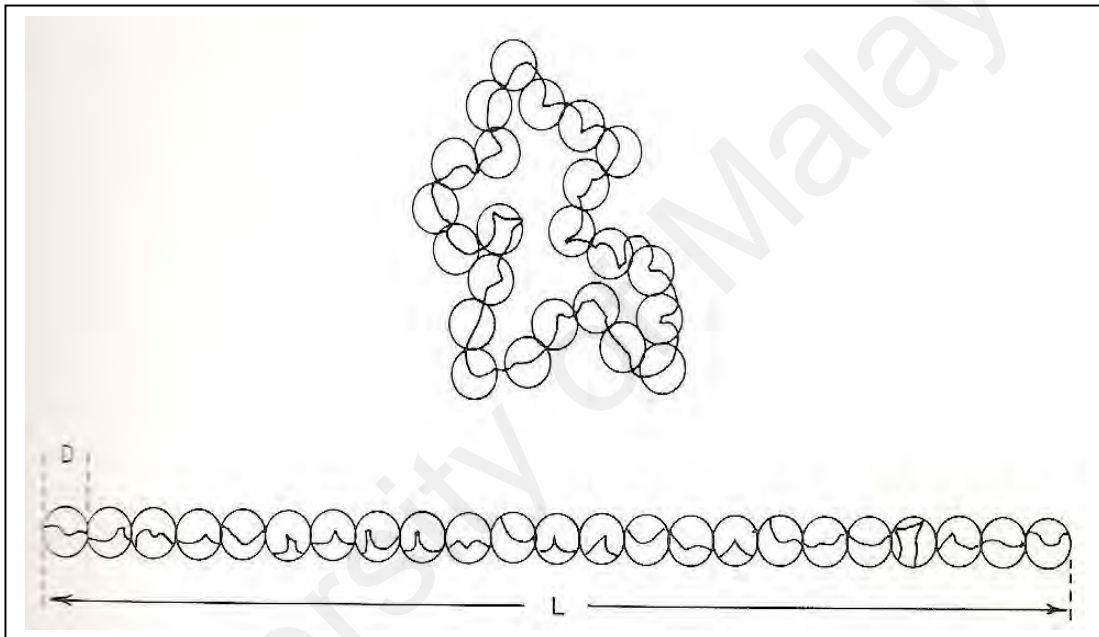


Figure 2.8: Minkowski sausage method
(Adapted from Kaye; A Random Walk Through Fractal Dimension, 1989)

Mass method is also known as the Scholl method. The computation of fractal dimension is by measuring the mass, m in circle of increasing radius r starting from the center of the set. A graph of logarithm, m versus logarithm, r is then plotted. If the graph is a straight line with a positive slope, one can conclude that the set is a fractal (Kaye,1989). As the radius increases beyond the point in the set far from the center, m remain constant and the dimension is trivially zero. Mass method studies a structure in a radial fashion. This method is suitable for the application of structural analysis but not for textural analysis

The final method is box-counting method (BCM) which is one of the best methods to measure fractal dimension. It is similar to mass method. According to Longley and Batty (1989), box-counting method can be used to measure the fractal dimension of a curve. Furthermore, according to Peitgen et al. (1988), this method can be applied to overlapping curves and structures lacking strict self-similar properties. Generally this method is based on a serial of grid boxes of size λ overlapping the fractal object. The grid boxes containing the mass of the object are considered in the estimate dimension of the structure. The data of box size, λ and box count are plotted over a log-log graph to obtain the fractal dimension of the object.

2.6 Fractal Analysis in Medical Field

Refining to the second main aim of this research project which deals with fractal application in biomedical field, this section reviews the use of fractal in biomedicine as the next step towards closer scrutiny in the application of fractal and its importance. There are several reasons why fractal seems to have attracted interests in biomedical research. According to Mandelbrot (1983), a fractal object is a part which is identical to the whole' For example there have been suggestions that nature structures with variable degrees of self-similarity arise as a consequence of deterministic growth rules. Thus it is perhaps that numerous links have been demonstrated in physics, biology and mathematic using fractal geometry.

According to Weibel (1994), fractal geometry provides an alternative important concept which has application in shape and texture characterization and consequently in diagnosis. The application of fractal analysis in medical image analysis has been developed since 1970 (Goldberger, 1990). Fractal mathematics has the power to evaluate numerically qualitative

changes in images or signals (Huang, 1994). Thus, it is particularly suitable to characterize irregularity, complexity and roughness from the quantitative properties of the medical images. The fractal properties of these images are therefore important variables in understanding the nature of biological materials. Moreover, mentions that fractal analysis is able to describe very complex images as long as they involve a certain degree of self-similarity (statistically or otherwise) at different scales (Goldberger, 1990). Thus, the property of fractal dimension in fractal analysis is not telling us the actual size of the images, however it measures overall 'complexity' of medical images.

2.6.1 Osteoporosis and Trabecular Bone Structure

To illustrate the application of fractal analysis in biomedical field for this research, the structure of trabecular bone is analyzed using the FGS prototype. The structure of trabecular bone exhibits fractal characteristics of self-similarity, irregularity and complexity in structure at any scale variance. Typically, the trabecular and the marrow spaces between them look very similar in any scale of range. Fractal index of trabecular bone can be related to bone strength. To refine the models of bone strength, apart from the dependence on the mineral content in the particular bone, it is important to consider the arrangement of the architecture of the bone structure. Since the trabecular bone structure exhibits the properties of fractal, it can be characterized by the numerical parameter, known as fractal dimension.

One of the applications of fractal analysis in the field of biomedical is in the prediction of osteoporosis based on architecture of trabecular bone. At a given age, bone mass results from the amount of bone acquired during growth. Beside that, osteoporosis is a major

health concern for our growing elderly population (Lau, 2004). In fact early diagnosis of bone degenerative process is important prevention action among osteoporotic patients. Thus, in this research we focus on the fractal analysis of texture applied to trabecular bone radiographs that can help to improve the diagnosis of osteoporosis.

Kleerekoper M Villanueva, Stanciu, Sudhaker and Parfitt (1985) defined texture as “a global pattern arising from the repetition, either deterministically or randomly, of local sub patterns”. Trabecular bone exhibits a repetitive branching pattern. The structural integrity of trabecular bone is an important factor characterizing the biomechanical strength of the vertebra, and is determined by the connectivity of the bone network and the trabeculation pattern. Applying fractal analysis to trabecular bone structure can represent an interesting approach to bone quality by exploring trabecular organization. Moreover the analysis of trabecular bone using fractal technique can overcome to predict fracture risk, monitor therapy and to diagnose osteoporosis. Therefore, the vital contribution of this study is to explore bone structures. Medical experts require more refined models in measuring the architecture of trabecular bone.

In conclusion, fractal dimension measurement is used to analyze and measure the ‘complexity’ of trabecular bone architecture. As discussed in section 2.5.1, the concept of fractal dimension measurement is based on Hausdorff dimension which is a ‘filling factor’ concept. This means that the more trabecular architecture tends to fill the space, the more complex it would be and vice versa. Therefore the fractal surface of trabecular bone architecture has Hausdorff dimension D where $1 \leq D \leq 2$. Trabecular bone structure that has fractal dimension which reaches the value of 2 can be concluded as having high bone strength.

2.7 Summary

This chapter identifies various types of fractal patterns based on its iteration. Moreover the description of fractal characteristics and fractal applications in real world are introduced. This chapter also illustrates several methods to measure fractal dimension. The application of fractal analysis in medical field is highlighted. In other words, this research has an important focus on the analysis of trabecular bone structure via fractal concept.

University of Malaya

CHAPTER 3

PROBLEM ANALYSIS AND SOLUTION APPROACHES

This chapter covers the analysis of the problems identified and the solution approaches to solve the identified problems.

3.1 Classification of Problems

Previously in section 1.2, the general identification of problems for this research project has been addressed. The problem are classified into three main categories namely a) generation of each types of fractal, b) identifying the method of calculating fractal dimension and c) analyzing fractal application in biomedical field. Based on the problems identified there are some questions encountered that need to be dealt with in this research.

a) Classifying the generation of each type of fractal

This research project concentrates on three types of iterations, which are Formula Iteration, IFS Iteration and Generator Iteration. Thus, the following questions need to be answered to get better understanding on the application of each type of fractal.

2. What are the types of fractal produced for every iteration?
3. What are the algorithms in generating the fractals?
4. What are the contributions from the original algorithms for each type of iteration?

(I) Identifying the method of calculating fractal dimension

An appropriate method needs to be used in measuring the fractal dimension of the fractals generated by FGS. The chosen method must be suitable for applications in various

disciplines especially in biomedical field. Thus, in trying to achieve the accuracy and reliability in the system, the following questions need to be examined:

- 2) Which method is relevant for the calculation fractal dimension of both fractals generated by FGS and also object in nature?
- 3) How accurate is the fractal dimension measured by this prototype system based on the fractal's theory?

c) Analyzing fractal application in biomedical field

An important part of the study is to analyze the fractal application for objects in nature to reflect real world applications. Hence this research study is further emphasized to focus on the fractal application in biomedical field. The study proceeds with an application of fractal analysis in medical images using FGS. There are several problems that are encountered which are:

- 2) How can medical image be characterized as fractal pattern?
- 3) What are the contributions of fractal analysis towards biomedical field?

3.2 Proposed solutions approaches

Based on the problem statements, there are three modules proposed in this research. The first module is the generation of each type of fractal. In fractal theory there are specific types of fractals based on how the fractals are created. Different types of fractal have different approaches and algorithms to generate the fractal. This is to meet one of the main aims of the research that is to emphasis on how different fractals are computer-generated using the specific algorithms. A prototype (FGS) is developed to generate fractals for three types of iterations namely Formula Iteration, IFS Iteration and Generator Iteration.

The second module of FGS is to calculate the fractal dimension of each type of the fractal generated. As established in the mathematical theory of fractal, there are fractals that have fixed numerical values of fractal dimensions, which are Koch Snowflake and Sierpinski Triangle. Hence to confirm the accuracy and reliability of the FGS prototype developed the fractal dimension value of fractal generated by FGS will be compared with the theoretical values.

The third module is based on the second aim of this research project, which is fractal application in biomedical field. The focus here is on branching structure in the human body. Therefore this module is focused on the application of fractal analysis in trabecular bone structure using FGS. Trabecular bone structure exhibits the properties of fractal (Messent, 2005). Hence, it can be characterized by the fractal dimension value. The analysis will be based on gender and patients with range age of 25 to 81 years for comparative studies.

3.3 Fractal Algorithms

This section elaborates the answers to the issue on a) Generation of each type of fractal. The algorithm implemented in this work is based on the formulation by Crownover (1995). However, there are some changes done to the algorithm due to some weaknesses found during development. As the algorithm is executed using a form of computer-generated process, it has created complex, repetitive, mathematically based geometric shapes and patterns.

3.3.1 Formula Iteration

As mentioned in section 2.2.1, Julia set and Mandelbrot set are the fractals to be generated in presenting Formula Iteration. Both fractals use the same algorithm for the generation but different parameters are used. These fractals are created by mapping each pixel to a rectangle region of the complex plane with quadratic formula $f(z) = z^2 + c$ where z and c are complex numbers. Complex number is expressed as $z = x + yi$. A point c on the complex plane is chosen. The formula expression of $f(z) = z^2 + c$ is expressed as $f(z) = (x + yi)^2 + (c_1 + c_2 i)$. Each point in complex plane then represents the starting point (x_0, y_0) of the series, z_0 for the result of quadratic equation. The resultant value of $f(z)$ is then substituted for z in the next iteration and the output is again evaluated. Generally, a series of complex numbers are produced.

$$z \rightarrow z^2 + c \rightarrow (z^2 + c)^2 + c \rightarrow [(z^2 + c)^2 + c]^2 + c \rightarrow \dots$$

The computation of the formula is based on the separation of real number and imaginary numbers equations such as shown in equations below.

$$X = x^2 - y^2 + c_1 \quad (3.1)$$

$$Y = 2xy + c_2 \quad (3.2)$$

The resultant value of $Z = X + Y_i$ should have one of two following properties:-

- i) The sequence remains bounded (prisoner set)
 - The points within any circle around the origin, which is never left by the sequence.
- ii) The sequence becomes unbounded (escape set)
 - The points of the sequence depart any circle around the origin

The escape set and prisoner set are based on the bailout value. If the resultant of $R = \sqrt{X^2 + Y^2}$ exceeds the bailout value, then the point is an escape set. However if the R-value is less than bailout values then it is a prisoner set. Based on Crownover (1995) algorithm, the prisoner set point is plotted in white color and the escape set will be ignored and not plotted once it has been identified. Hence, modification has been made whereby various colors are added to indicate number of iteration that determines the escape set. The example of the algorithm with maximum number of iteration as 30 for this step is as follows: -

8 bit RGB Module

LOOP A

For (R < bailout value)

Palette (i) = RGB (255,255,255) \implies Prisoner set

LOOP B

For (R > bailout value)

For (i < 5)

Palette(i) = RGB (0, i * 4, 0) \implies Escape set in black

For (i < 10)

Palette(i) = RGB (i * 4, 255 - i * 4, 0) \implies Escape set in green

For (i < 20)

Palette(i) = RGB (255 - i * 4, 0, i * 4) \implies Escape set in red

For (i <=30)

Palette(i) = RGB (i * 4, i * 4, 255) \implies Escape set in blue

whereby 'i' indicates number of current iteration. The points in complex plane are calculated using the quadratic equation and the resultant value of R is plotted by colors that depend on how many iterations it has executed to determine whether the point is prisoner set or escape set. Loop 'A' represent the algorithm in determining prisoner set, in which the points are plotted in white color. The point is determined as a prisoner point when the resultant value, R is less then the bailout value until the iterations exceed the maximum

number of iterations. However loop 'B' represents the escape set whereby blue points indicate the nearest of escape set points to the prisoner set which means that the resultant value, R exceeds the bailout value when the iteration is at the maximum number of iterations. The outer most layers consist of points in black colors where the resultant values of these points exceed the bailout value for just a few numbers of iterations. However there are also points in red color which indicate the points is escape set in the middle of iterations before it reach maximum number of iterations. The user will determine the maximum number of iteration. The higher the number of iterations the more accurate the fractal pattern will be generated; however this will increase the processing time.

Formula Iteration algorithm is used to generate Julia set and Mandelbrot set fractals. However, the parameters used to generate Julia set and Mandelbrot set are different. Table 3.1 shows the comparison of parameters between Julia set and Mandelbrot set.

Table 3.1: Comparison of parameters in Julia set and Mandelbrot set

Julia set	Mandelbrot set
<ul style="list-style-type: none"> • Randomly choose each point in complex plane for starting value of z • c represents constant point • Plot the point based on the resultant value of starting point z which has been chosen randomly 	<ul style="list-style-type: none"> • Starting point of the calculation is $z = 0$ • c is randomly chosen after each determination of prisoner or escape set. • Plot the point based on the resultant value of c

3.3.2 IFS Iteration

The concept of generating fractal using IFS Iteration algorithm is based on substitution of initial object with identical ones as described by a generator. The generation of Sierpinski

Triangle fractal is one of the examples using IFS Iteration algorithm. Let N be the stage of various incarnations in generating the Sierpinski Triangle.

The first step is to shrink down the shape to half of the original dimensions and the area of new triangle is exactly one fourth of the original area. Make two other copies of the new triangle with smaller shape and arrange the new three triangles to form a single full-sized stage 1 as depicted in Figure 3.1.

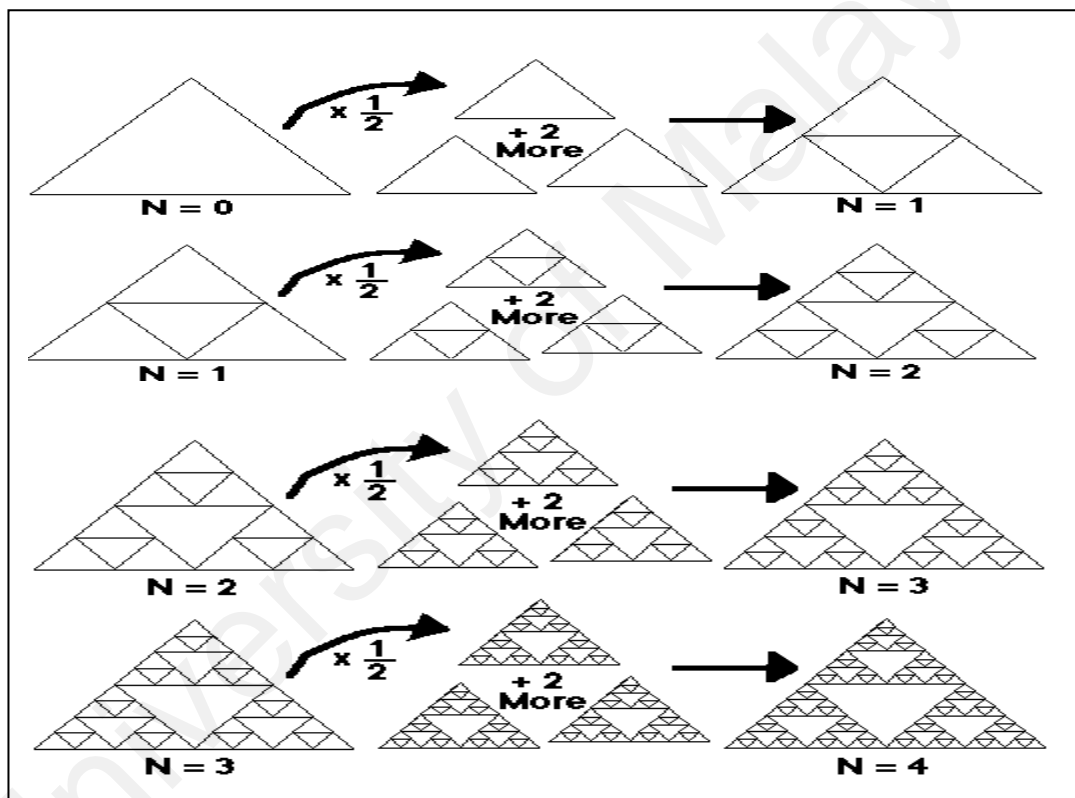


Figure 3.1: Procedure of Generating Sierpinski Triangle

The procedure is repeated for the next stage. Figure 3.1 shows the creation of Sierpinski Triangle in various stages. In other words, the area of original triangle is normalized to 1, the first iteration removes $1/4$ of the area. Next the second iteration removes a further $3/16$ of the area and goes on with N -th iteration removes $3^{N-1}(1/4)^N$ of the area. At an infinite number of iterations, there will be no area at all in the holes of Sierpinski Triangle.

To generate Sierpinski Triangle start with three points that hold the coordinates of the triangle corners, which are top, left and right coordinates. The minimum and maximum values of coordinate x and y are determined as the limit for the display. For each iteration, the generator is replaced by using affine transformations as shown in Figure 3.2. The new points of x and y coordinates of Sierpinski Triangle are obtained by transforming the previous points with randomly selected affine transformations. Each affine transformation represent new three triangles with smaller shape on top, left and right of original triangle.

$$\begin{array}{l}
 T_1 \left(\begin{bmatrix} x_1 \\ x_2 \end{bmatrix} \right) = \begin{bmatrix} 1/2 & 0 \\ 0 & 1/2 \end{bmatrix} \begin{bmatrix} x_1 \\ x_2 \end{bmatrix} + \begin{bmatrix} 0 \\ 0 \end{bmatrix} , \\
 T_2 \left(\begin{bmatrix} x_1 \\ x_2 \end{bmatrix} \right) = \begin{bmatrix} 1/2 & 0 \\ 0 & 1/2 \end{bmatrix} \begin{bmatrix} x_1 \\ x_2 \end{bmatrix} + \begin{bmatrix} 1/2 \\ 0 \end{bmatrix} , \\
 T_3 \left(\begin{bmatrix} x_1 \\ x_2 \end{bmatrix} \right) = \begin{bmatrix} 1/2 & 0 \\ 0 & 1/2 \end{bmatrix} \begin{bmatrix} x_1 \\ x_2 \end{bmatrix} + \begin{bmatrix} 1/2 \\ \sqrt{3}/4 \end{bmatrix} .
 \end{array}$$

Figure 3.2: Affine transformations used in generating Sierpinski Triangle

Based on the original algorithm by Crowover (1995), the initial point to generate Sierpinski Triangle is randomly chosen. However there is a difficulty to generate the fractal if the initial point is randomly chosen. The point for the next iteration is plotted randomly based on the transformation type. Modification has been done to the algorithm where the initial point is determined as fixed point in the middle of the original triangle instead of randomly chosen.

Referring to Figure 3.3 let P be the initial point. P is then fixed in the middle of the largest white space of the triangle. Therefore for the next step, it is easier to determine the next point with randomly choice of the transformations and the new point approximately

occupies the same position of P with respect to the half-size of the triangle as depicted in Figure 3.3. However the initial point P is discarded and not plotted. Every new point generated is plotted in each three triangles of top, left and right coordinates.

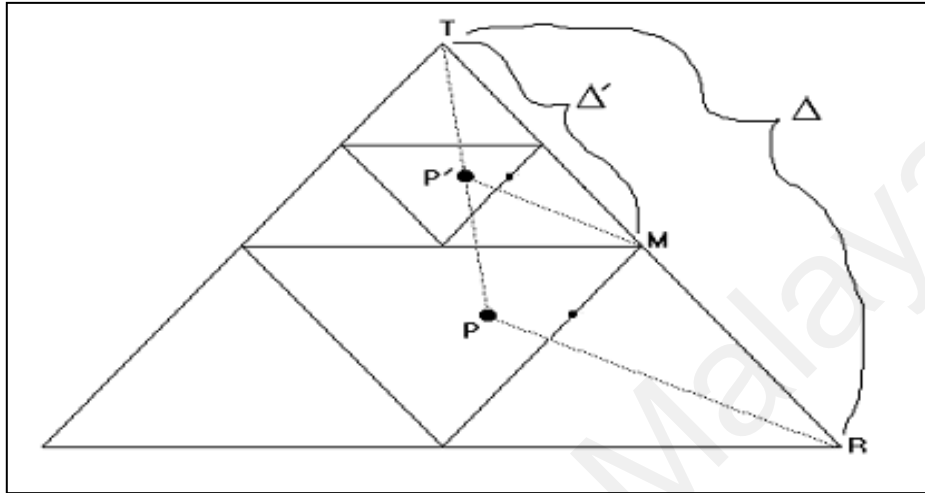


Figure 3.3: Initial point of Sierpinski Triangle is plotted

The sequence in generating Sierpinski Triangle as follows: -

$$Y = T_1(Y_0) \text{ or } T_2(Y_0) \text{ or } T_3(Y_0)$$

where $T_i = \begin{pmatrix} X1 & 1/2 & 0 & X1 & 0 \\ X2 & 0 & 1/2 & X2 & 0 \end{pmatrix}$ presents the point in Sierpinski Triangle and T is the transformation that will be randomly selected.

3.3.3 Generator Iteration

The procedure of generating fractal using Generator Iteration is by continuously substituting certain geometric shape with other shapes. Koch Snowflake is one of the examples of fractal that is generated using Generator Iteration algorithm. Based on Crownover (1995), there is no specific algorithm to generate Koch Snowflake due to any choice of shape. For illustration, the generation of Koch Snowflake is by substituting the base, with a triangle to Koch Curve, which is the generator. The construction of Koch

Curve starts with a line segment, the base as depicted in Figure 3.4. Then the middle one-third of the line segment is substituted with two line segments, each one-third in length of the base.

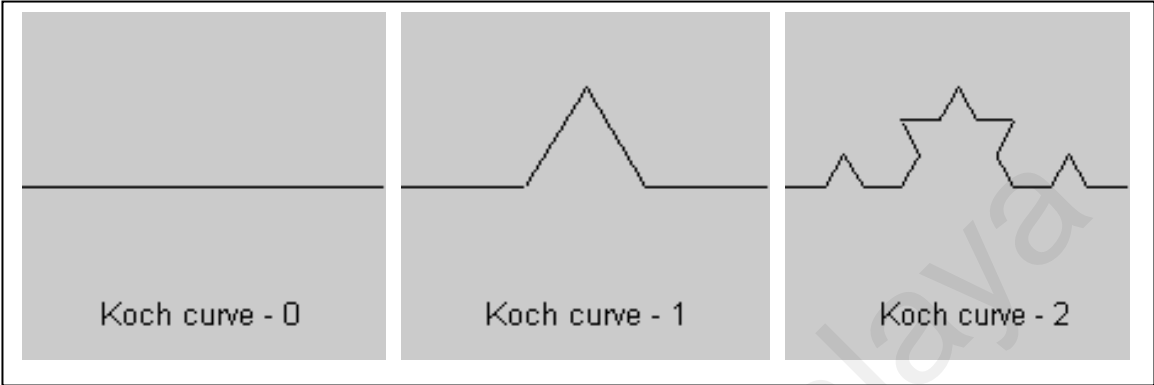


Figure 3.4: Construction of Koch Curve

The triangle in Koch Snowflake is divided into three line segments, which will be substituted with Koch Curve. This procedure will be processed iteratively as depicted in Figure 3.5.

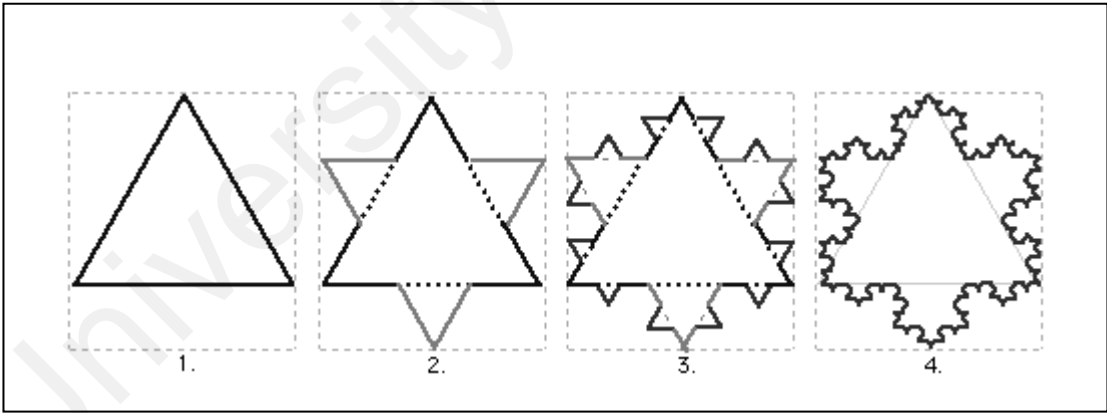


Figure 3.5: Process of Koch Snowflake

The line segments are identified as top, left and right. There are five points assigned to each line segment as depicted in Figure 3.6.

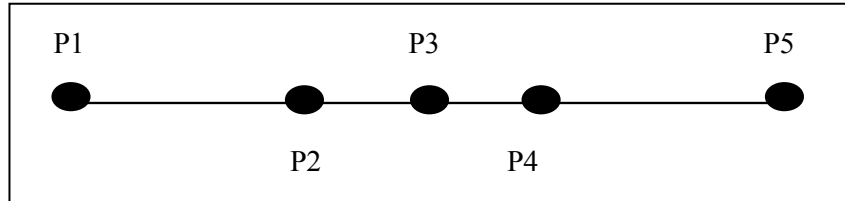


Figure 3.6: Five points in line segment

Each point represents the (x, y) value. Each line segments is divided into 3 sections of equal length. The algorithm is as follows: -

$$\Delta = p5 - p1 \text{ (axial distances between end points)}$$

$$p2 = p1 + \Delta / 3 \text{ (one third of the line segment)}$$

$$p4 = p1 + \Delta * 2/3 \text{ (two third of the line segments)}$$

$$p3 = (p1 + p5) / 2 + T * \Delta \text{ (p3 point substitutes the base line segment to generator)}$$

where T is the generator of line segments, with value

$$T = \sqrt{3} / 6$$

Once the above algorithm is executed, the line segment will be replaced by Koch Curve as shown in Figure 3.7.

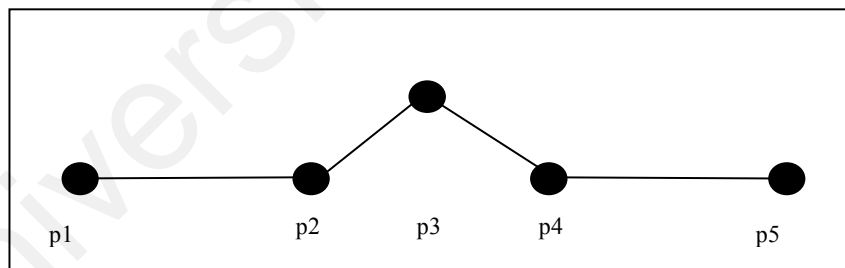


Figure 3.7: p3 point as generator

Based on the Figure 3.7, p2 and p4 points represent the one-third of left and right portions of the line segment. p3 point represents the centre point of line segment that will be substituted with the generator. This algorithm is applied to each line segment of top, left and right. The procedure is iteratively executed. As a result Koch Snowflake has infinite length since the length of each line segment in the triangle increases by one-third for every

iteration performed. However the area is bounded by the original triangle. In other words, Koch Snowflake is a curve of infinite length in a finite area. From the point of view of Euclidean geometry, the Koch Snowflake is an unusual object where normally objects occupy finite length and area in finite space.

3.4 Fractal Dimension Measurement

As previously discussed in section 2.5.2 there are several methods to measure fractal dimension. This section provides the answer to problem statement in section 3.1.b that is various methods are compared in their approaches and applications.

3.4.1 Comparison of Various Fractal Dimension Measurement Methods

There are four fractal dimension measurement methods, which have been briefly explained, namely Richardson method, Minowski method, Mass method and Box-Counting method (BCM).

Richardson method is suitable for analyzing curves in a planar field. A set of algorithm is developed to direct the steps in traversing the boundary of a structure. However, this application is more easily done manually compared to computer system development. According to Long (1994), the Richardson method tends to enclose the outermost points of the structure's boundary and slightly underestimate length. As a result, the underestimation of boundary perimeter will severely influence the calculation of fractal dimension. In addition, Richardson method is not suitable to analyze object involving other objects scattered within an image.

On the other hand, Minowski Sausage method is suitable for the textural and structural analysis of a structure. However, according to Flook (1982), it can over estimate due to expanded extremities of the sausage with free ends.

Mass method is suitable for the application of structural analysis but not for textural analysis. Hence it is not suitable for a complex pattern such as pattern in medical image structure.

The advantage of BCM is that it can be applied to both textural and structural analysis of a structure. In addition, the mesh grid also allows the analysis of objects scattered in an image. Furthermore this method can be used to analyze the irregularities in surfaces filling the space volume.

An evaluation has been done to select a suitable method to apply in FGS. This evaluation is based on the criteria of easy for application, flexibility and method that is suitable for medical image analysis. This means that the method selected must be relatively simple and accurate to develop using computer-processing and facilitate users to understand the concept. Moreover it must be flexible to measure any fractal pattern. The third criterion to evaluate is the suitability of the methods to analyze medical images. This is to achieve the second main aim of this research, which is to analyze medical images using fractal analysis. Table 3.2 shows the evaluation table of each method.

Table 3.2: Evaluation of the method to determine fractal dimension

	Ease of Application	Flexibility	Suitability
Richardson	NO	NO	NO
Minowski	YES	NO	YES
Mass	YES	NO	NO
BCM	YES	YES	YES

After considering the advantages and disadvantages of these methods, box-counting method (BCM) is selected as the method to calculate fractal dimension for FGS. Due to computer technology, BCM is easy and flexible to implement and the computer simulation helps users to understand the concept. BCM is a flexible method to measure any fractal pattern and any image that exhibits fractal characteristics specifically medical images. This is an important justification to consider in achieving the second aim of the research, which is to analyze medical images using fractal analysis.

3.4.2 Box-counting Method

BCM makes the use of regular mesh grid for analyzing the image, to compute the coverage of the image inside the rectangular boxes. Various sizes of mesh grid are used and accordingly the amount filled boxes are counted in analyzing the image.

Initially parallel vertical and horizontal lines are used to generate the mesh grid. Line method is used to generate the vertical and horizontal lines in the rectangle region. This method allows the mesh grid to resize rapidly and standardizes the size of mesh grid based on number of pixels. This is because BCM requires changing the size of the rectangular boxes in data acquisition phase.

The next step is to detect whether the image components exist within the boxes of mesh grid. It is important to note that for BCM only the boxes of the mesh grid containing the image are considered. The image can be measured by utilizing the information contained in each pixel in the region. The boxes containing binary value of 1 are selected. In other words, boxes that contain white color structure will be selected and counted. The algorithm for this step is as follows:

```
For < pixels of the i-th grid box>
  For pixel 1 to vertical box
    For pixel 1 to horizontal box
      Loop
        If the current pixel(x,y) represents structure pixel value of 1 then add box count
        Go to the next box i
      End Loop
```

The algorithm will continuously scan the entire boxes in the region, resulting in the box count for the grid boxes containing the image based on the box size. The box count is collected successively for different box sizes.

The next step is the calculation of fractal dimension value. The data of box sizes and corresponding filled box counts, which have been collected, are then used as input to obtain fractal dimension value of the image analyzed. The value is determined based on the gradient of the least squares regression line, which can be obtained by plotting of the log-log graph of $N(s)$ versus s as in Figure 3.8 where $N(s)$ represents the amount of filled boxes counted, which contain the image to analyze and s represents the corresponding box size. Mathematically, a gradient is given as follows: -

$$\text{Gradient} = \frac{S_{xy}}{S_{xx}} \quad (3.3)$$

where:

$$S_{xy} = \sum x_i y_i - n \bar{x} \bar{y} \quad (3.4)$$

$$S_{xx} = \sum \bar{x}_i^2 - n \bar{x}^2 \quad (3.5)$$

$$\bar{y} = \frac{\sum y_i}{n} \quad ; \quad \bar{x} = \frac{\sum x_i}{n} \quad (3.6)$$

Value n indicates the total values of coordinate points (x,y) . The fit of the data to the regression line and the number of data points determining the line are two important aspects to determine the confidence of the estimation value of the gradient. The higher number of observations improves the confidence of the estimated value as it decreases inter variability in the measurement as the scale of measurement decreases.

Relating to the equation above, the data that need to be considered in calculating the gradient (fractal dimension value) are n , $\log N_i(s)$, $\log s_i$, $(\log N_i(s))^2$ and $(\log s_i)^2$. The gradient of the best-fit line gives the value of the fractal dimension parameter.

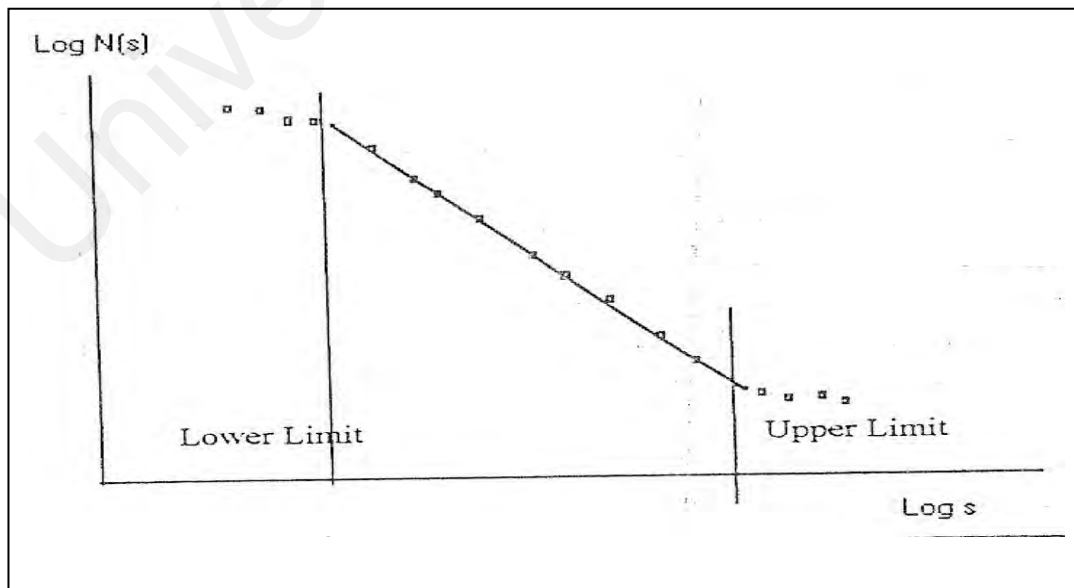


Figure 3.8: The upper and lower bound limit to define fractal dimension

Referring to Figure 3.8, upper and lower limits of (N,s) which are not traversed by the regression line need to be identified. The limits are identified as bounds for the plots, which form a plateau and the scattering of plots due to insignificant change in box counts and extreme values of box sizes.

3.5 Application of Fractal Analysis in Trabecular Bone Structure

Due to fractal-like pattern of bone structure, fractal analysis is used in the prediction of osteoporosis based on architecture of trabecular bone. According to Bonjour et al. (2001), osteoporosis is a systemic skeletal disease characterized by low bone mass and microarchitectural deterioration of bone structure. Thus, to illustrate the application of fractal analysis in biomedical field in this research project, the structures of trabecular bone radiographs are analyzed that can help to improve the diagnosis of osteoporosis. This section elaborates on the solution of the problem as stated in section 3.1.c, which is examining fractal application in biomedical field.

Typically, the trabecular and the marrow spaces between them look very similar at any scale of range. Hence, trabecular bone structure can be categorized as fractal pattern as it has fractal characteristics. Fractal index of trabecular bone can be related to bone strength. The normal medical practice is to study the mineral content in the particular bone. To refine the model it is important to consider the arrangement of the architecture of the bone structure which can be related to bone strength.

For this research project, 53 CT-scan images of lumbar spine of 27 males and 26 females with ages between 25 to 81 years old are used for fractal analysis application. It is

important to note that none of the patients had medical consultation history of metabolic bone disease or bone fractures so that the experiments and analysis are unbiased. The purpose is to analyze and measure the ‘complexity’ of trabecular bone architecture based on fractal dimension measurement. The concept of fractal dimension measurement is based on Hausdorff dimension, which is “filling factor” concept, which means that the more trabecular structure tends to fill the space, the more complex it would be and vice versa. It is closely linked to the bone strength of the patients. The higher value of fractal dimension indicates a higher density of the bone structure.

The CT-scan images of lumbar spine axial scan were taken using a CT scanner machine, GE LightSpeed 16 slice at 140 kVp and 133 mA, with slice thickness 5 mm. The scan field of view (FOV) is 33.6 cm. Each CT-scan image is standardized by magnification factor (MF) of 6.2 with window values of width 483 and length 326. No deconvolution was performed on the image since blurring was minimal. Therefore the images are focused on the bone structure itself and not on the soft tissue. However, there is no direct digital output of the CT-scan images from the scanner machine. Therefore the CT-scan images were captured using digital camera Casio 5 mega pixel on illuminator. Then the images were transferred and stored to the computer in a standardized size of 640 x 480 pixels.

Before analyzing the CT-scan images, the images need to be processed and converted to binary format. This is because as previously mentioned; BCM in FGS only measures the image of binary format. Image processing tool from MATLAB 7 is used to process the CT-scan images.

The standardization of the image processing is a key point to get better images, particularly concerning the determination of the region of interest (ROI) because the calcaneus has been

shown to be very heterogeneous in terms of trabecular bone structure by CT-scan image. Therefore in this research project, users required to have a reasonable knowledge of the fractal theory and experience in analyzing the medical images. The first module of FGS which is to generate different types of fractals helps in better understanding of fractal images. There are procedures used to gain standardization of binary image of trabecular bone structure as follows: -

- Conversion of CT-scan image to grayscale
- Selecting region of interest (ROI)
- Conversion of image to binary format

3.5.1 Conversion of CT-scan Image to Grayscale

As mentioned previously, the CT-scan image is captured using digital camera and stored into computer. However the image captured is in truecolor image. Hence the image needs to be converted to grayscale to standardize the intensity value for each CT-scan images between the ranges of 20 to 245, which are determined empirically during the execution. This is to get a precision and sharpness of the structure of the image when converted to binary format. Figure 3.9 shows the procedure diagram in converting an image of CT-scan to a grayscale image of trabecular bone structure. "Figure 1" in the screen shots refers to the original image of CT-scan and "Figure 2" shows the grayscale image.

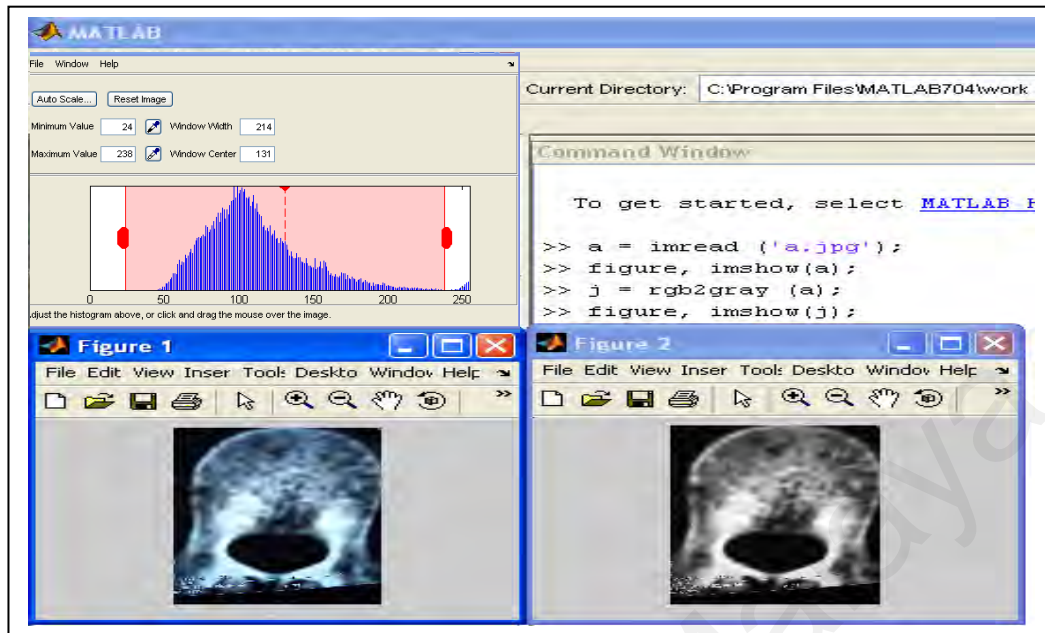


Figure 3.9: Conversion of a CT-scan image to a grayscale image

3.5.2 Selecting Region of Interest (ROI)

In measuring the fractal dimension value in medical image, the typical structure component of the image needs to be selected and measured. ROI represents the area of bone structure that needs to be measured for the fractal dimension value. Only the exact patterns, which resemble the whole structure, have close approximation for the fractal dimension value.

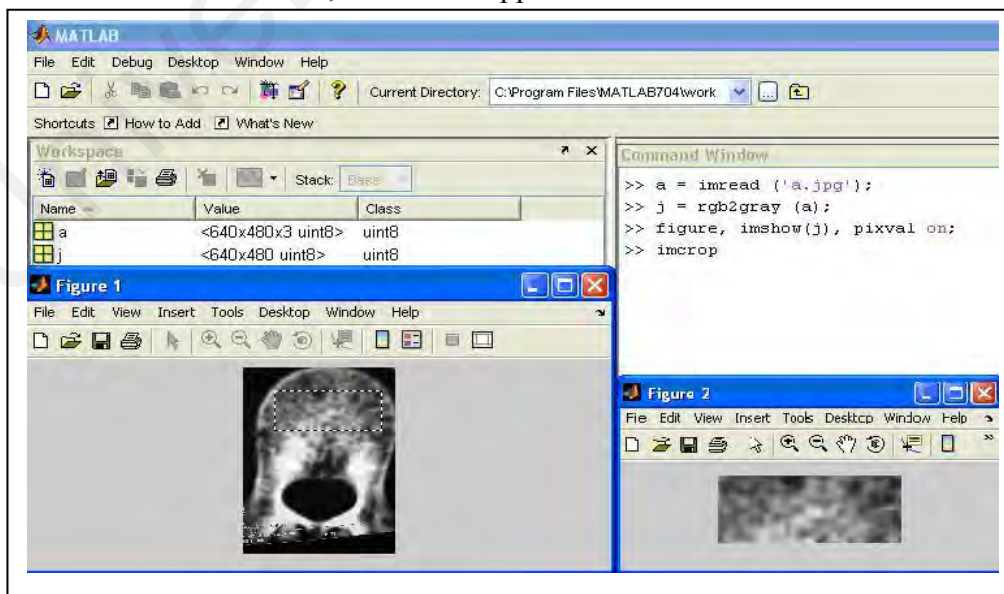


Figure 3.10: “Figure 1” shows the selection of ROI of the CT-scan image and “figure 2” is the result of output image after the cropping

In MATLAB, the ROI is presented as a rectangular shape. The rectangle is specified in terms of spatial coordinates, comprising four-element vector with the form x-axis minimum, y-axis minimum, width and height. ROI depends on the appearance of fractal pattern in the images. The selection is based on the maximum area with the appearance of fractal pattern that can be measured for the fractal dimension value. For this research project, the size of the image is standardized to 400 X 250 pixels for further analysis.

3.5.3 Conversion of Image to Binary Format

The final procedure is to convert the ROI to binary format. In converting the grayscale image to binary format, a standardized value is required to determine the threshold value level. The lowest representative value between 0 and 1 should be determined for the threshold value. In this research the threshold value level is 0.2. Lower values than 0.2 will cause no bone detection for the old age group. All images should have bone structure for the analysis.

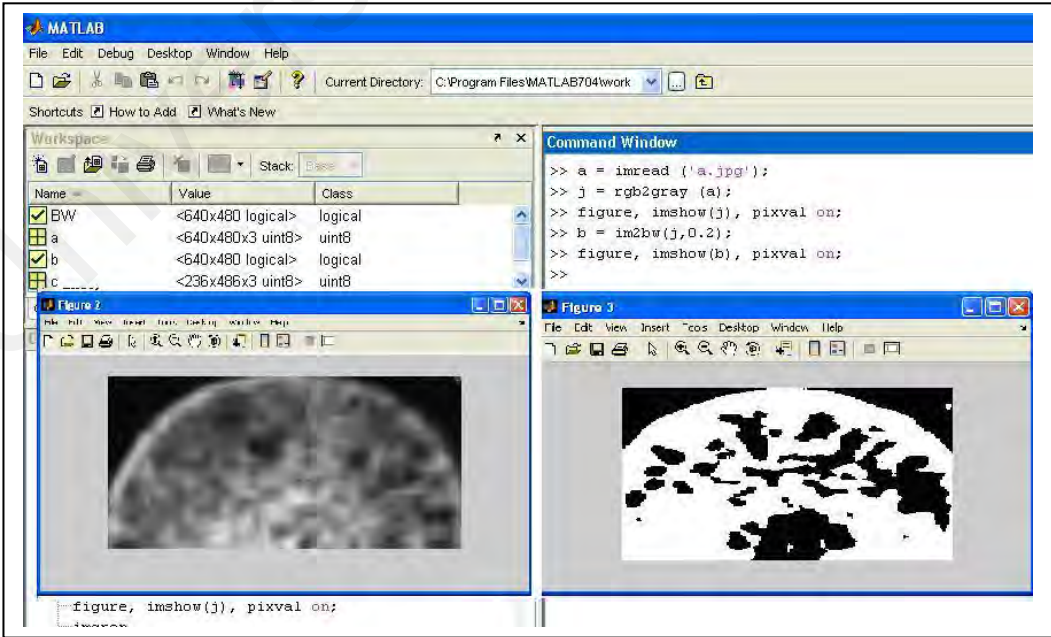


Figure 3.11: Conversion of grayscale image to binary format.

The value 0.2 represents the minimum value that indicates the detection of the bone structure, which needs to be analyzed. Figure 3.11 shows the conversion of a ROI of medical image from a grayscale to a binary image. The white structure represents the bone structure to be measured.

3.6 Summary

Based on the analysis of problem statements, the main solution is to develop a system called Fractal Generation System (FGS), which consists of three main modules. The modules are to generate various types of fractals based on its iteration, to measure the fractal dimension value and the application of fractal analysis on medical images.

CHAPTER 4

REQUIREMENT ANALYSIS AND DESIGN

This chapter presents the requirement analysis conducted based on the solution approaches described in chapter 3 and also the design of FGS. Requirement analysis is a process of transforming a problem definition from a fuzzy set of facts and myths into a coherent statement of system's requirement (Bahrami, 1999). The phase in this chapter is divided into two sections, which are requirement analysis and system design.

4.1. FGS Requirement Analysis

Requirements analysis focuses on the functional and non-functional requirements needed by FGS. Functional requirements are behavioral requirements which address FGS features or functionalities. Non-functional requirements are non-behavioral requirements which are concerned with system attributes, or constraints that should be taken into FGS implementation.

4.1.1 Functional Requirements

In Chapter 3, the proposed features for FGS were identified. The functional requirements for FGS are based on the identified features. There are three modules in FGS, which are Fractal Generation, Fractal Dimension Measurement and Fractal Analysis of Medical Images. The following gives a description of functionalities for each module of FGS:

I. Fractal Generation

- There are four types of fractals that can be chosen for fractal generation.

- Relevant parameter needs to be inserted before generating the fractal.
- A user is able to save the fractal pattern generated and also to reset.

II. Fractal Dimension Measurement

System only allows image in binary format to be measured

- System displays the information of image imported such as size and dimension of image and date of image modification.
- System places the image on the rectangular region and a mesh grid is overlapped on the image based on its minimum and maximum number of box size.
- The system calculates the mesh box containing white structure and collects the data of number of boxes and the corresponding box size.
- A scattered X-Y graph is generated and fractal dimension value is obtained.

III. Fractal Analysis of Medical Images

- A number of image processing stages need to be performed on a medical image to convert it to binary format.
- The area of structure that needs to be analyzed is identified.
- The resultant of fractal dimension values are measured, compared and analyzed.

4.1.2 Non-Functional Requirements

Non-functional requirements are attributes that need to be considered in developing the FGS. The non-functional requirements include:

I. Usability

- FGS provides a simple user interface to ensure that users can easily operate the system, prepare inputs and interpret output.

II. Expandability and scalability

- FGS can be expanded for future purposes.
- FGS should be easy to be modified in the future.

III. Maintainability

- FGS can easily be maintained by authorized users.

IV. Portability

- FGS should accurately produce a fractal pattern and the value of fractal dimension.

4.2 System Design

System design is a process of transforming the requirement analysis into technical representation of the system. For this research project, structural analysis modeling and object-oriented analysis modeling are used in system design to explain and describe the framework of FGS.

4.2.1 Structural Analysis Modeling

The primary objective of structural analysis modeling is to develop a modular system structure and to represent the data structure and defining interfaces that enable data to flow throughout the system. Structural analysis modeling for FGS is subsequently explained through data flow diagram (DFD).

DFD is a graphical presentation to visualize the data processing of a system. Figure 4.1 shows the top-down DFD level '0' of FGS.

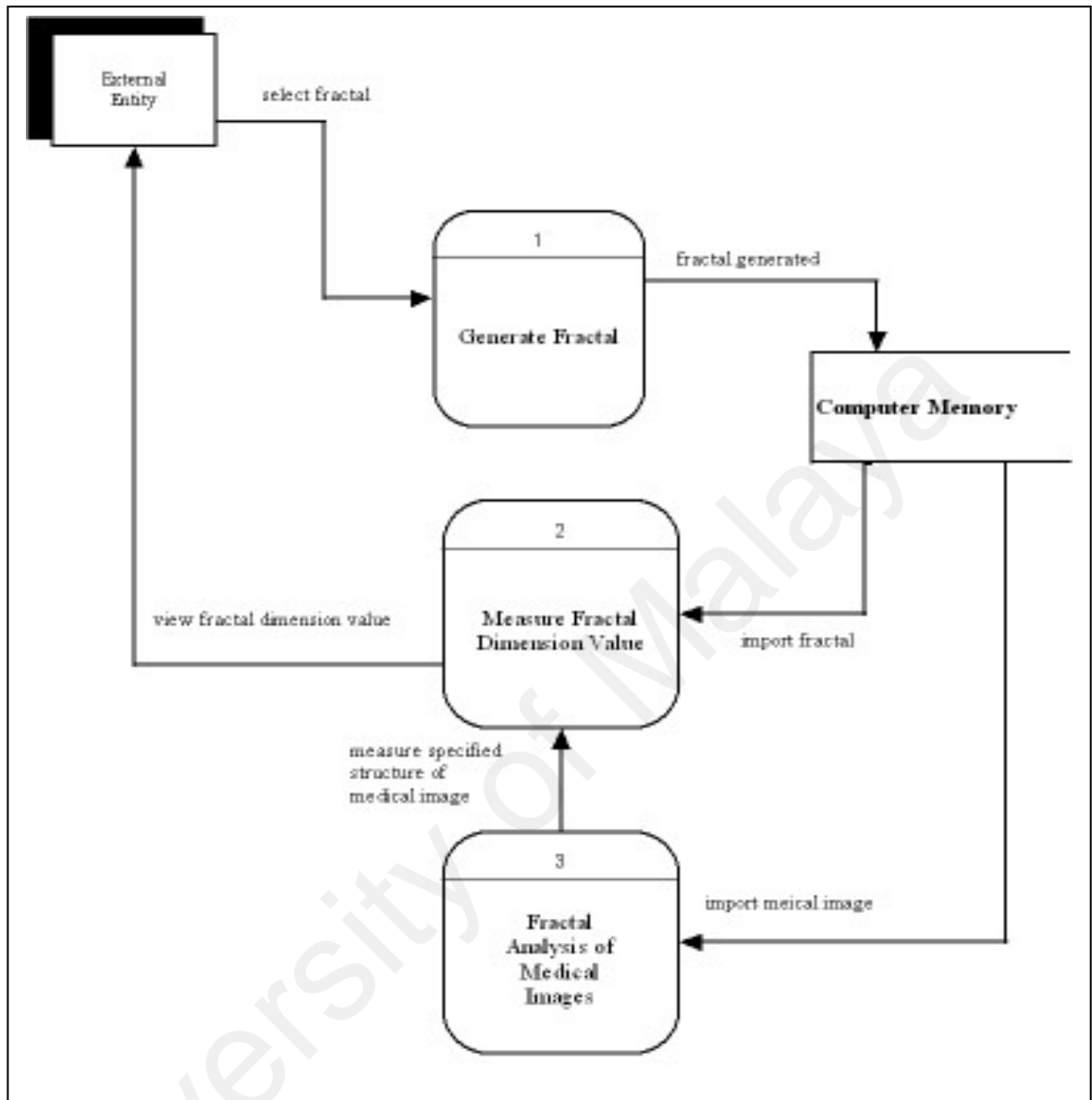


Figure 4.1: DFD Level '0' of FGS

DFD level '0' represents the general view of FGS. Based on the figure, there are three data processes in the diagram which are 1) Generate Fractal, 2) Measure Fractal Dimension Value and 3) Fractal Analysis of Medical Images. Initially a user will select one of the various types of fractals to be generated. Once the system generates a fractal it will be saved to computer memory. The fractal image from the computer is imported before fractal dimension value can be measured. To analyze medical images, the image need to be imported from computer. The process to analyze the medical images will be done in this

stage; however the measurement of the fractal dimension value will be done in the data process number 2. Finally the system will display the results to be viewed by the user. Figure 4.2, 4.3 and 4.4 show DFD diagrams of level 1, 2 and 3 to specify each data process in level '0'.

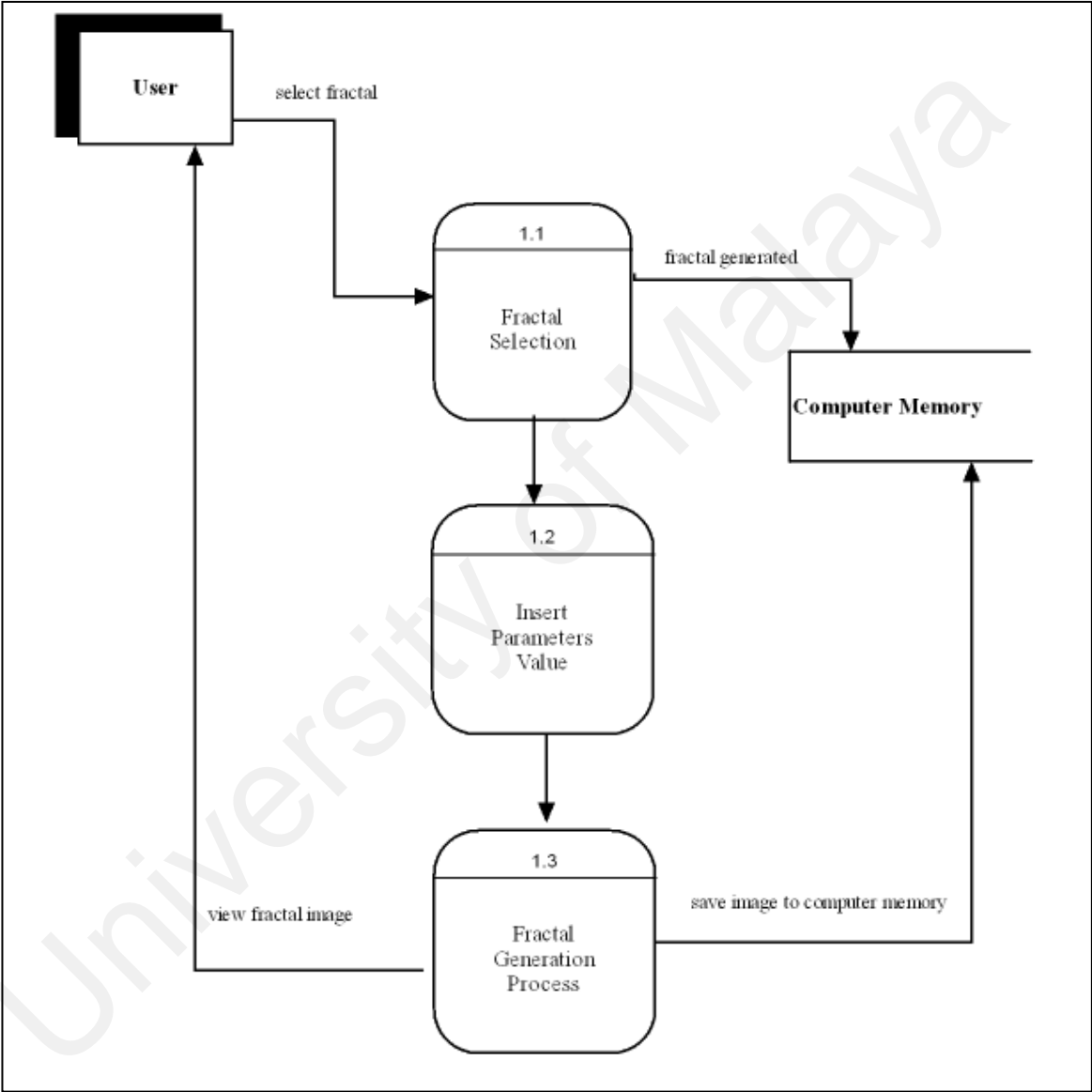


Figure 4.2: DFD Level '1' of FGS

Figure 4.2 shows DFD level '1' which represents the procedure to generate fractal. A user needs to select a specific type of fractal to be generated, and then the user needs to insert the parameters required by the system. Once the parameters are inserted, the FGS will

generate fractal pattern in the complex plane. The fractal pattern can be stored in computer memory.

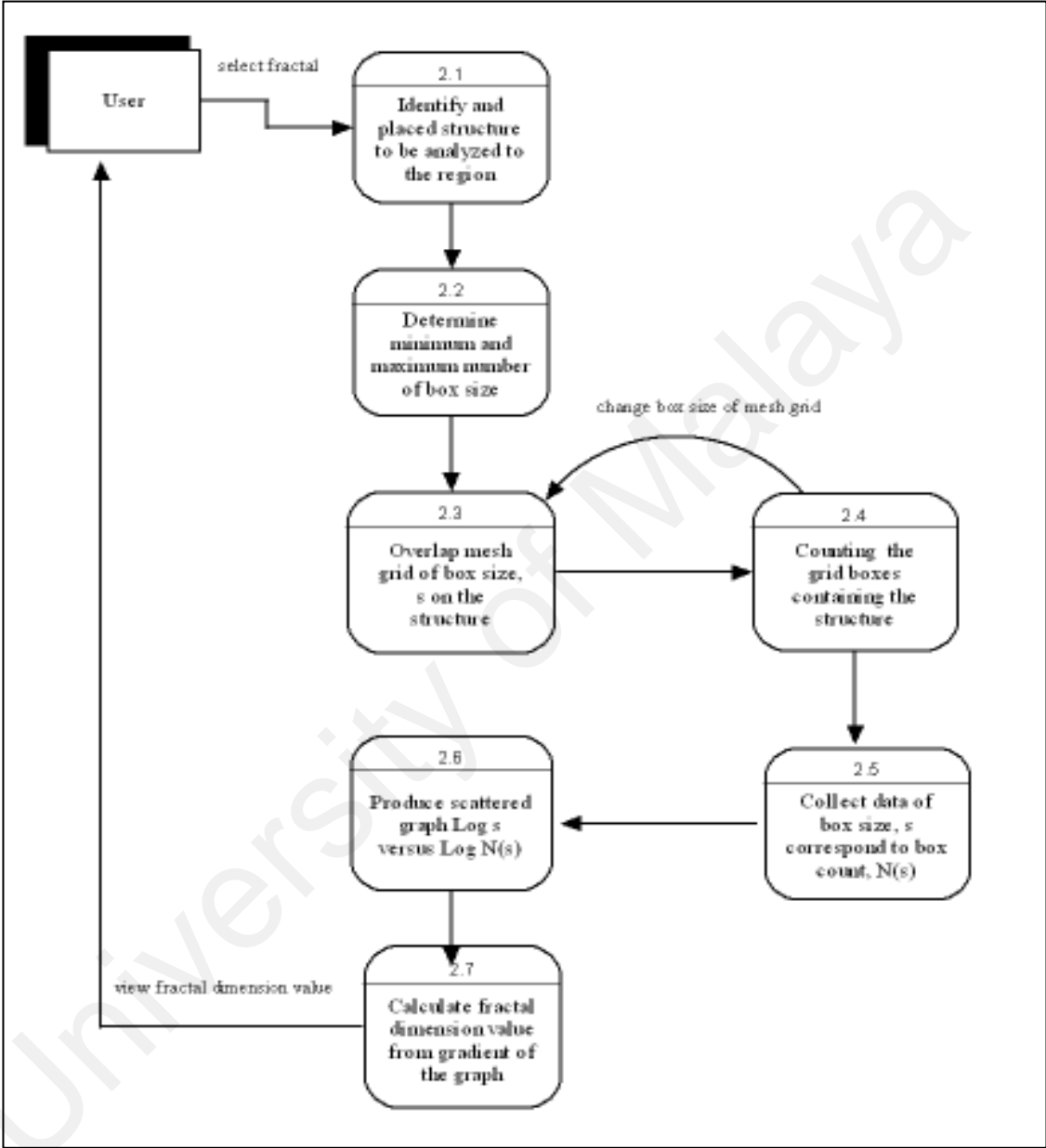


Figure 4.3: DFD Level '2' of FGS

Figure 4.3 shows the DFD level '2' of FGS. The diagram is based on data process number 2 of DFD Level '0', which is the measurement of fractal dimension value. A user initially selects the fractal to be measured and identify the structures that need to be analyzed. Then the structure is placed in the rectangular region. The user needs to determine the minimum

and maximum number of box sizes. Then the system will overlap the structure with mesh grid box. The next step is to count the boxes which contain the structure. This step is continuously executed until the maximum number of box size is reached. The system will collect data of box size, s corresponding to the number of box count, $N(s)$. From the collection data, FGS will produce a scattered graph of logarithm value of box size, $\text{Log } s$ versus number of box count in logarithm form, $\text{Log } N(s)$. Fractal dimension value is obtained based on the linear regression gradient of the graph.

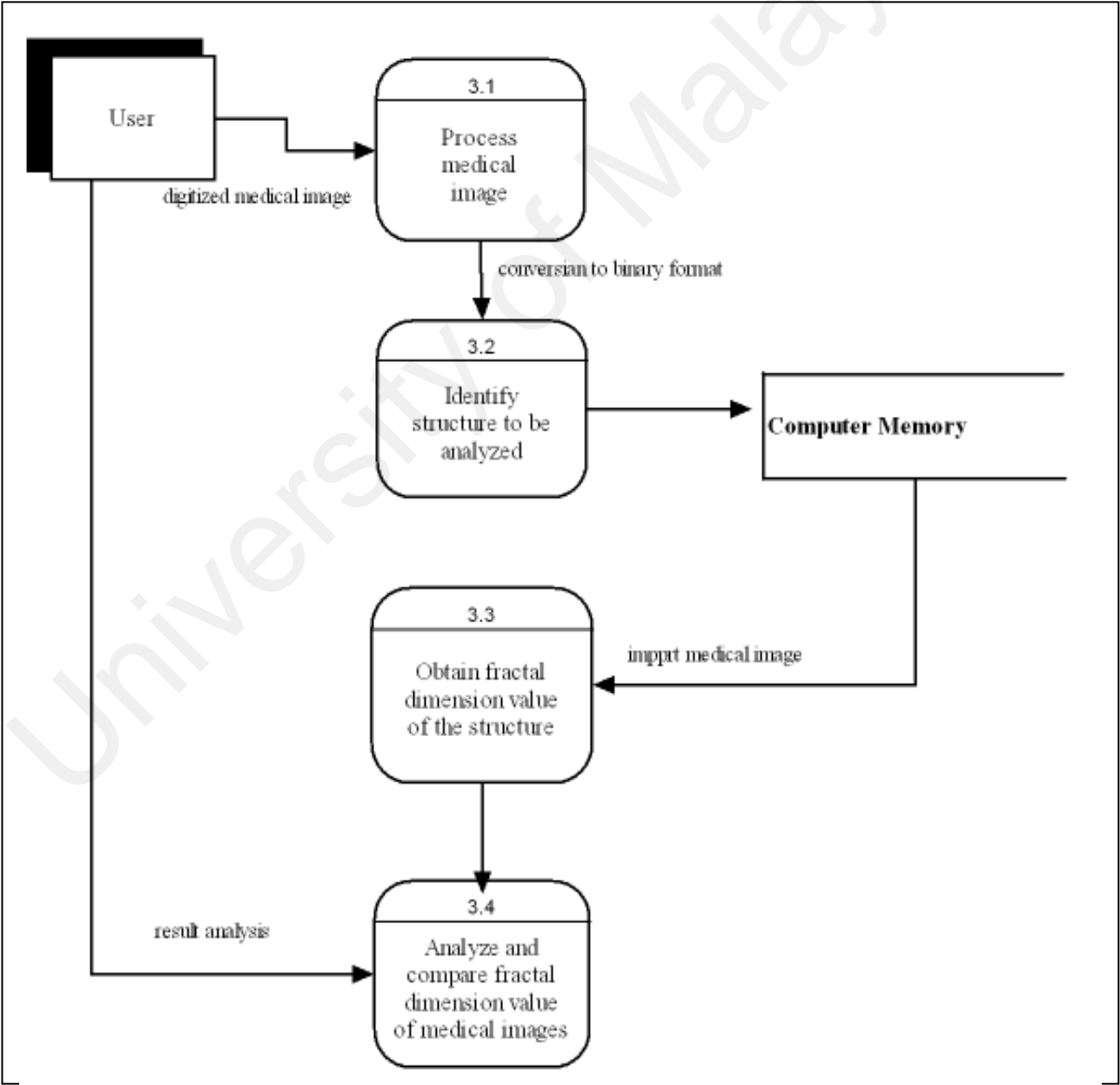


Figure 4.4: DFD Level '3' of FGS

Figure 4.4 represents DFD level '3' for fractal analysis of medical image. Before the medical image can be analyzed, the image need to be digitized and processed as previously explained in section 3.5.1. Once the image has been processed, a user needs to identify the region of interest to represent the area of structure in the medical image, as not the whole structure of medical image will be analyzed. Then the image is stored in computer memory. FGS will import the processed medical image to measure the fractal dimension value. Values obtained will be compared and analyzed by users.

4.2.2 Object-oriented Analysis Modeling

Object-oriented analysis modelling applies object-modeling techniques such as use case and UML diagrams to analyze and define the collaboration in fulfilling the requirements in the system. Hence use case, class diagram and sequence diagram are used to graphically illustrate the FGS system.

4.2.2.1 Use Case Diagram

Use case diagram is a scenario used to describe the user-computer system interaction. There are three modules proposed in FGS, which are I) Fractal Generation, II) Fractal Dimension Measurement and III) Fractal Analysis of Medical Image. Use case for FGS is described based on the three modules of FGS. There are two actors involved in FGS, user and system. Figure 4.5 shows the use case diagram of FGS.

From the figure below, the system only involves two use cases, which are fractal generation and fractal dimension measurement. The fractal analysis of medical images use case uses the relationship of <<extends>> to interact with fractal dimension measurement use case.

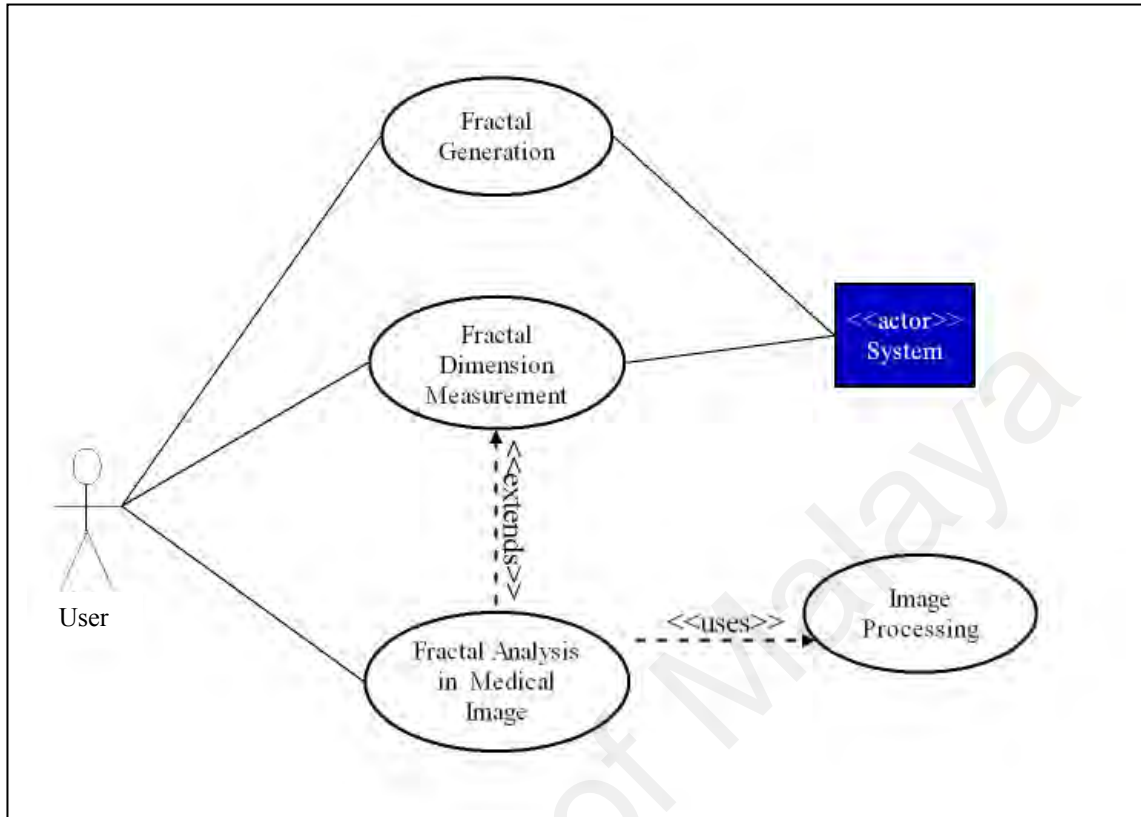


Figure 4.5: Use case diagram of FGS

This means that the analysis of medical images is done by measuring the fractal dimension value of each medical image and compares the values to return the analysis results. Prior to that, the images need to be processed for conversion to binary format. Hence there is relationship of <<uses>> to image processing use case. In this scenario, certain procedures are executed to digitize the medical image and execute a pipeline of image processing stages as explained in section 3.5.

4.2.2.2 Class Diagram

Class diagram illustrates the collaboration between classes in FGS application as depicted in Figure 4.6. The diagram is extended to illustrate the methods of each class and attribute type information.

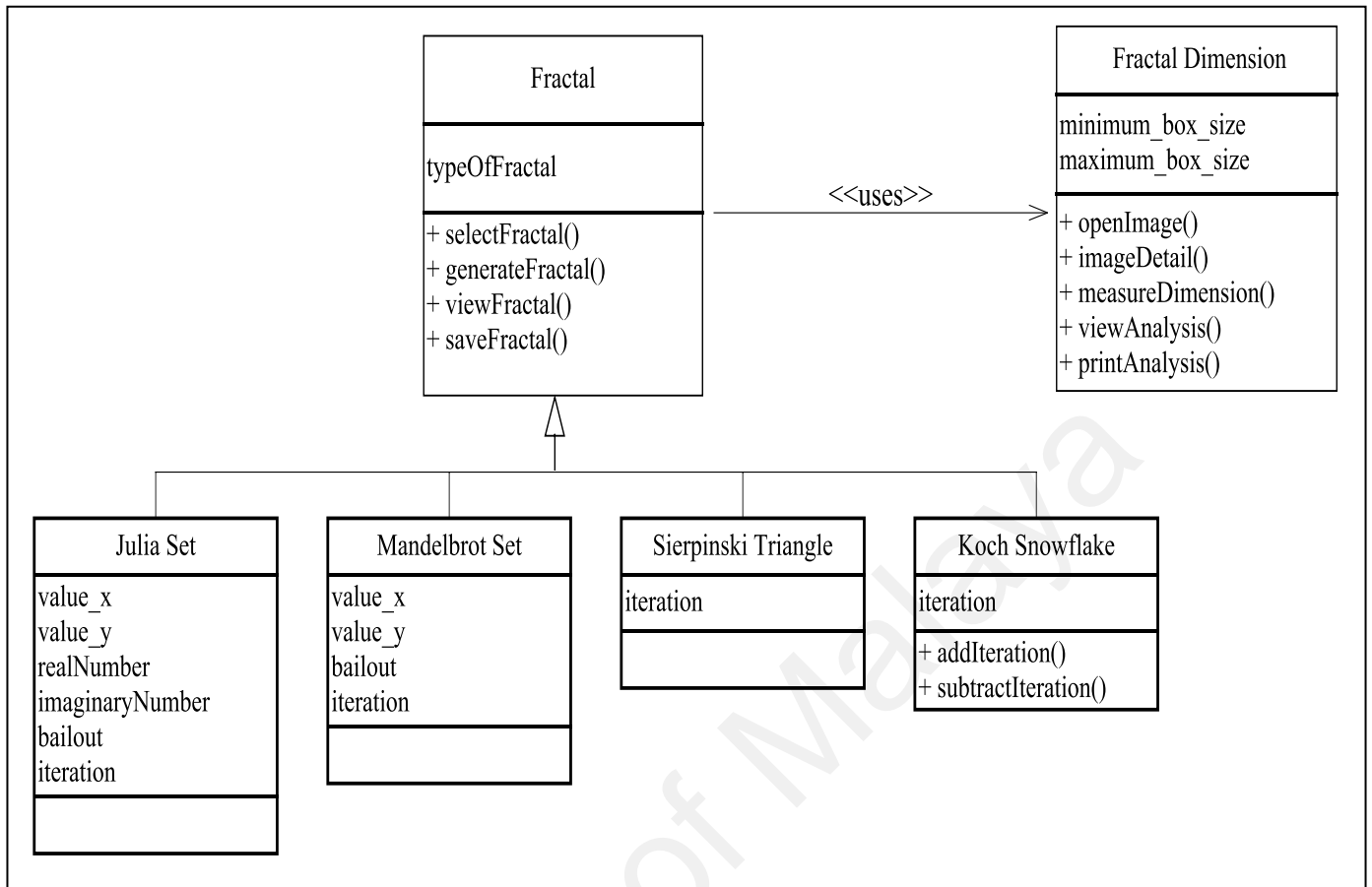


Figure 4.6: Class Diagram of FGS

Previously described in use case diagram (Figure 4.5), only two use cases are involved in FGS. Prior to that there are two classes in the class diagram, which are Fractal and Fractal Dimension. For Fractal, there is only one attribute which is typeOfFractal and four methods involved which are selectFractal(), generateFractal(), viewFractal() and saveFractal().

There are four sub-classes generalization from Fractal, which are Julia Set, Mandelbrot Set, Sierpinski Triangle and Koch Snowflake. These four sub-classes inherit all the methods in Fractal. However, the sub-classes have its own attributes in generating the fractal image.

There is a relationship between Fractal and Fractal Dimension in obtaining the fractal dimension value. Hence, the relationship <<uses>> is used to interact from Fractal class to Fractal Dimension class. Fractal Dimension class has two attributes which are

minimum_box_size and maximum_box_size. These attributes are used to determine the size of mesh grid that overlap the image and number of iterations of one application. There are five methods in Fractal Dimension class which are openImage(), imageDetail(), measureDimension(), viewAnalysis() and printAnalysis().

4.2.2.3 Sequence Diagram

Sequence diagram is a notation diagram that can represent the interaction of the actor and the operations initiated by them. The illustration of sequence diagram is based on use case diagram and class diagram. Figure 4.7 shows the sequence diagram of FGS.

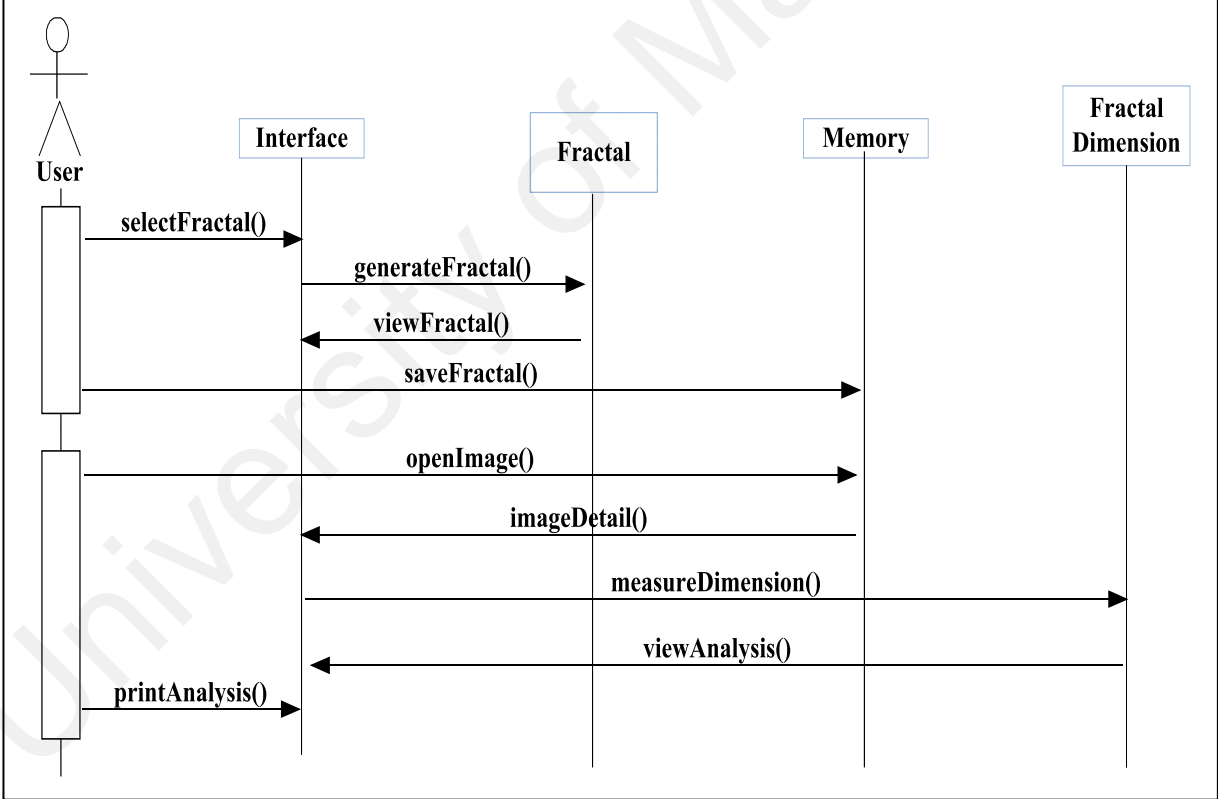


Figure 4.7: Sequence diagram of FGS

From the diagram, there is an actor, which represents the User, and Fractal Dimension and two agents, which are Interface and Memory. For fractal generation scenario, user needs to select any type of fractal using selectFractal() method.

Made with a Trial Copy of SmartDraw
 Buy SmartDraw! - purchased copies print this document without a watermark.
 Visit www.smartdraw.com or call 1-800-768-3729.

FGS generates the selected fractal through generateFractal() method. Then the fractal is viewed on the interface through viewFractal() method. User has an option to save the generated fractal in the computer memory using saveFractal() method.

To measure the dimension of the fractal, user needs to import the image from computer memory using openImage() method. Then the details of the image are viewed in the interface through imageDetail() method. In the next step, the system measures the dimension of the fractal image using measureDimension() method. After the measurement, FGS will view the analysis and the value of fractal dimension through viewAnalysis() method. User has option to print the analysis via printAnalysis() method.

CHAPTER 5

IMPLEMENTATION RESULTS AND DISCUSSION

This chapter discusses on the implementation and execution of FGS comprising two significant phases. The first phase is the fractal-generating phase, which generates four types of fractals, which are Julia set, Mandelbrot set, Sierpinski Triangle and Koch Snowflake. The second phase is the process for measurement of fractal dimension value. The details of the main features of FGS are explained in this chapter. Screenshots of the system are presented for better understanding. The main screen of FGS is shown in Figure 5.1.

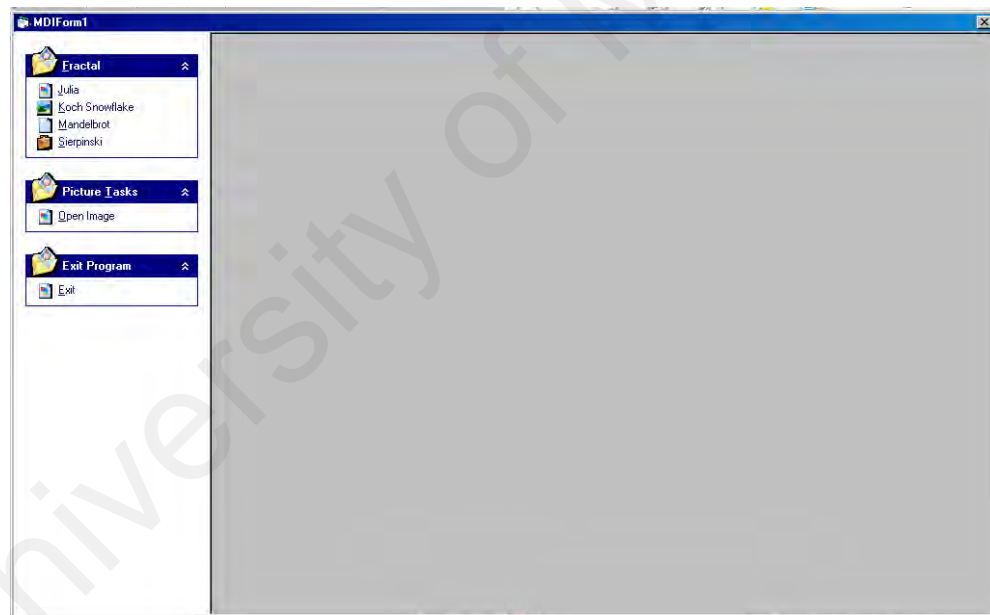


Figure 5.1: Main Screen

Based on the figure above, on the left segment there are three main menu options. The first option is the list of types of fractals that can be generated. The second menu option is 'open image' menu. This part is to import the image from computer memory that needs to be

analyzed and to measure the fractal dimension value. The final menu option is to stop and exit the program.

5.1 Fractal Generation Phase

In this module there are three types of iteration, with Julia set and Mandelbrot set which represent Formula Iteration, Sierpinski Triangle, which represents IFS Iteration and Koch Snowflake, which represent Generator Iteration

5.1.1 Julia set

Figure 5.2 shows the interface of FGS to generate Julia set fractal. There are several parameters that are required to be set before generating Julia set fractal. The x -axis and y -axis minimum and maximum parameters specify the coordinates in the complex plane.

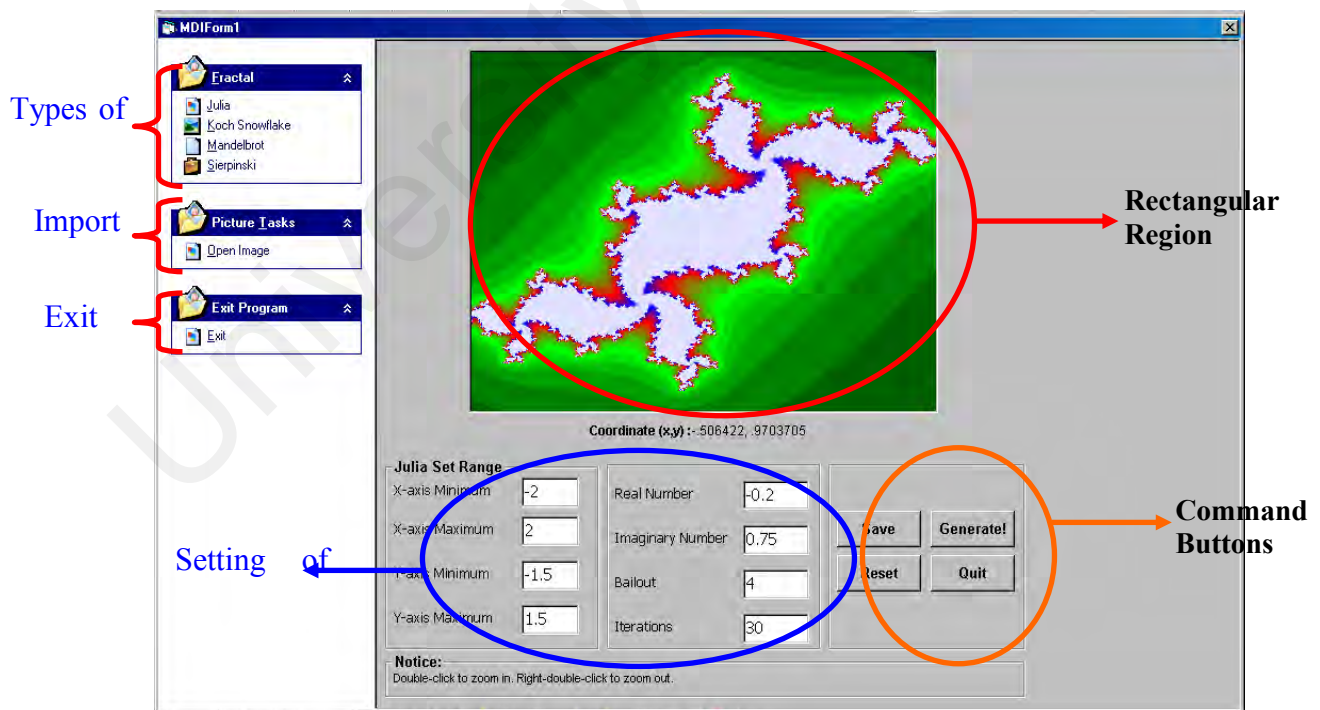
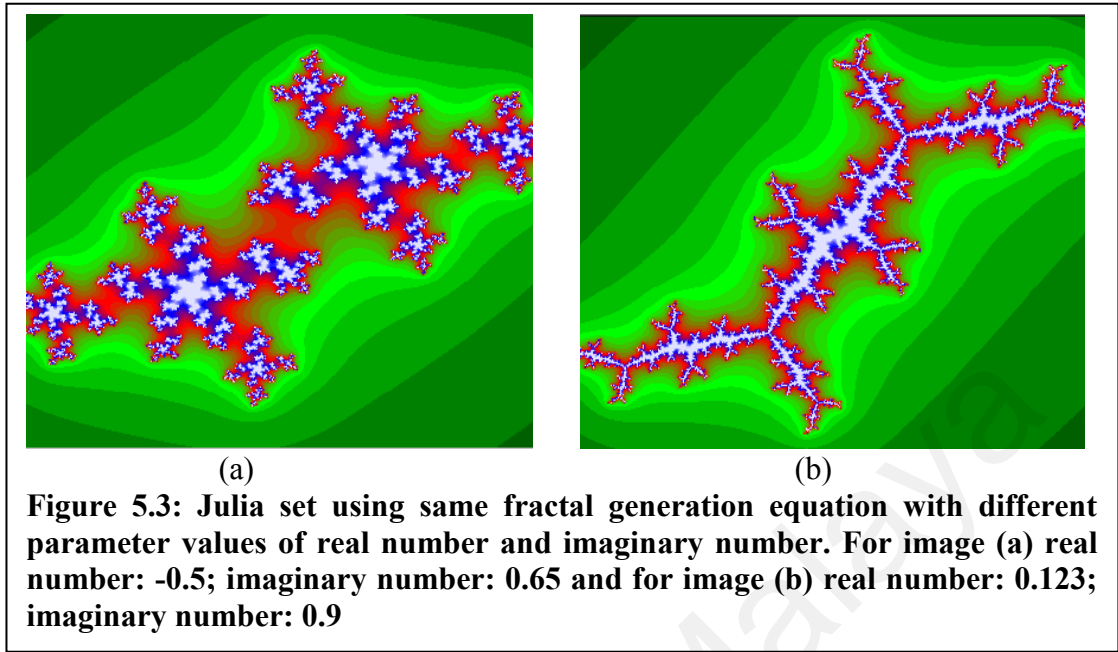


Figure 5.2: Fractal image of Julia set

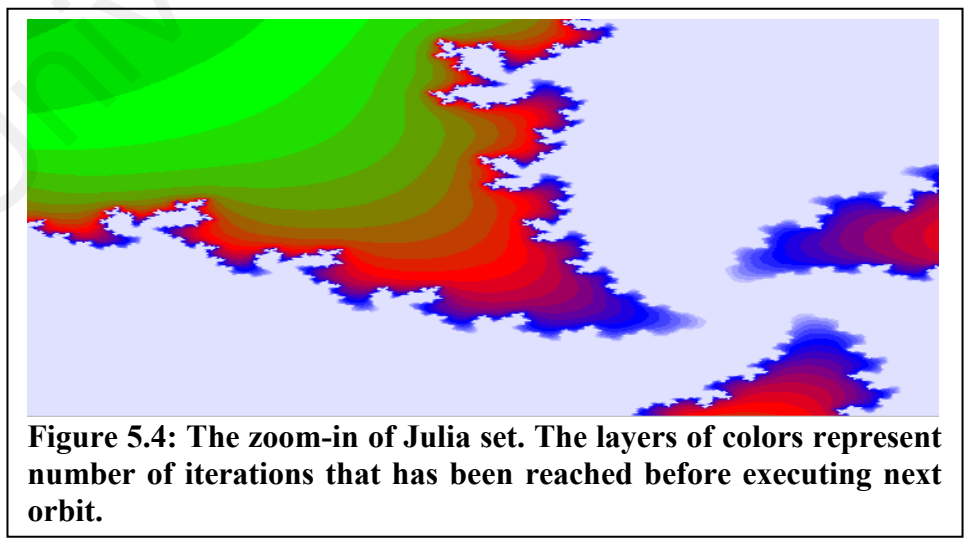
The real number and imaginary number parameter represents parameter, c used in fractal generation equations section 3.3.1. Different real number and imaginary number will produce different shapes of fractal images as depicted in Figure 5.3 and more examples in Appendix I.

The bailout parameter is to set control during the execution whereby it determines whether the evaluated point is in a prisoner set or escape set of Julia set. For this system the default bailout value used is 4. Bailout value should be set to 4 or larger (Frederik, 2003) for good results. Larger values tend to smoothen the outside areas. The last parameter is the iteration parameter, which sets the maximum number of iteration. For better generation of Julia set, number of maximum iterations must be within 20 to 120 iterations. For maximum iterations less than 20 iterations the colors of outside layers of Julia set are not smoothly generated. Iterations more than 120 will make the generation of Julia set very slow and require a lot of time and memory.

The next step is to generate the fractal by clicking the 'Generate' button that is located on the bottom right of the interface. Thus FGS will execute the algorithm iteratively in the complex plane and will produce the fractal image of Julia set. The fractal image is displayed in the complex plane window as depicted in Figure 5.2 and Figure 5.3. The image can be saved and stored into computer memory by pressing the 'Save' button. The 'Reset' button is to clear and refresh the complex plane and the parameters in the system. The 'Quit' button is to exit Julia set sub module and consequently choose another sub module to generate fractal.



The fractal image generated can be zoomed in up to four times for closer view of the image as shown in Figure 5.4. One needs to double click on the complex plane to zoom in and right double click to zoom out. As the fractal image is zoomed, there are a few layers of colors that represent the number of iterations of escape set. Based on Figure 5.4, the green layer is the outer layer of escape set, which means that only at a few times of iterations the resultant value of complex variable, R has exceeded the bailout value.



The blue layer shows that the escape set is really close to Julia set (prisoner set) where the iterations at number of maximum iteration for the resultant value to exceed bailout value. The most inner layer of points is the closest points to Julia set. As the white layer structure are the points of Julia set. There are two conditions that can determine the point is a Julia set (prisoner set). First condition is when the resultant value is less than the bailout value for the first few iterations and the second condition is when the iteration of is at the maximum number of iteration, yet the resultant value of the equation is still less than bailout value.

5.1.2 Mandelbrot set

Figure 5.5 shows the interface to generate fractal of Mandelbrot set. Similar to Julia set, the Mandelbrot set is a fractal generated using Formula Iteration. The difference of parameters between Julia set and Mandelbrot set are explained in Table 3.1.

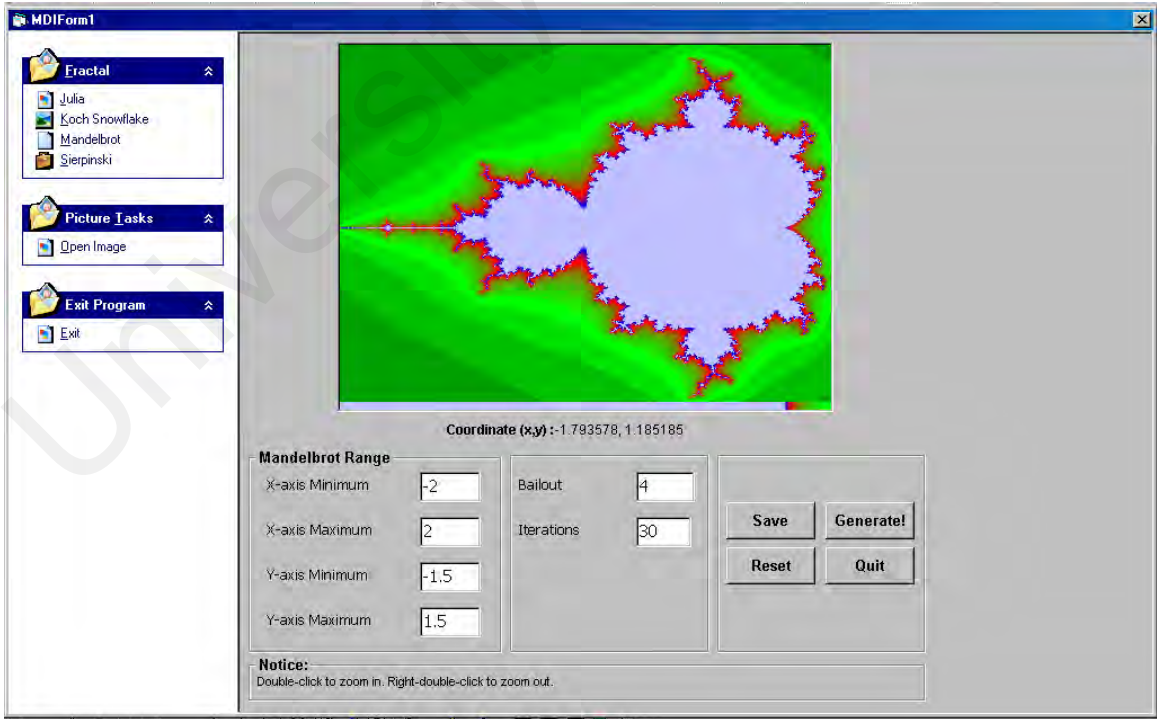
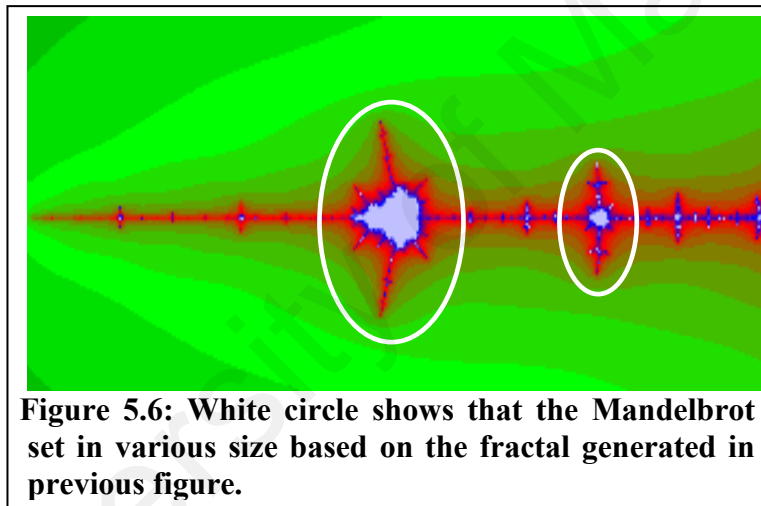


Figure 5.5: Fractal image of Mandelbrot set

Unlike Julia set fractal, Mandelbrot set does not have the parameters, c of real number and imaginary number. This is because generation of Mandelbrot set fractal starts with z equalsto zero. The system will repetitively choose the points of (x, y) on the complex plane presented as variable c . Thus, Mandelbrot set has a variety of variable c .

The unique characteristic of Mandelbrot set fractal is that as one looks closer at the pattern in the image, there are many Mandelbrot sets which appear in different sizes. In Figure 5.6, the white circle illustrates the Mandelbrot set in various size based on the fractal generated in the previous figure.

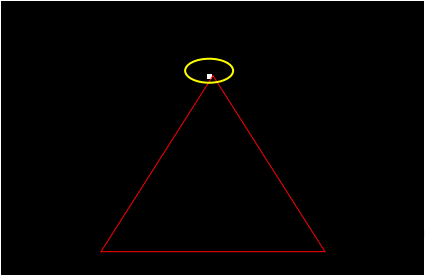
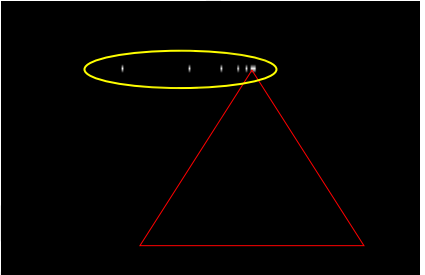
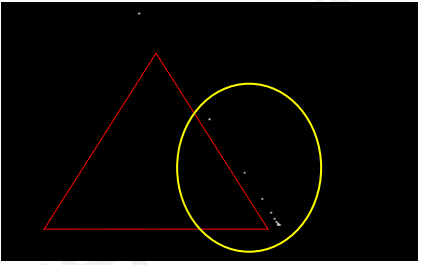
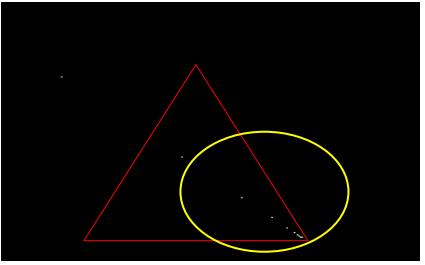
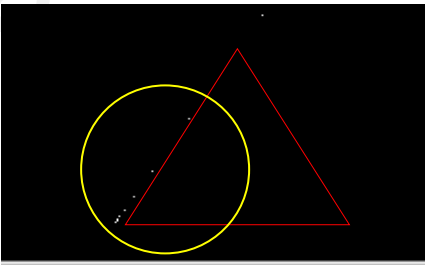
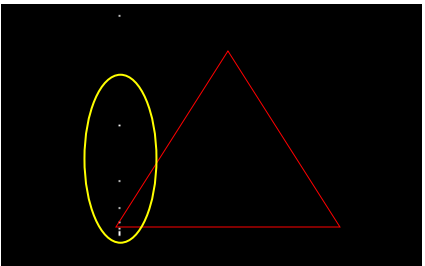


5.1.3 Sierpinski Triangle

Next fractal generated using FGS is Sierpinski Triangle which is perfectly self-similar fractal. The generation of Sierpinski Triangle is by using random approach. The initial point to generate Sierpinski Triangle is fixed. However this initial point is discarded and not plotted. For this research the initial point is determined in the middle of original triangle. Then the system randomly selects transformations to generate the next point. As previously explained in chapter 3, three affine transformations represent new three smaller

triangles of top, left and right. Table 5.1 shows the generation of Sierpinski Triangle points using specific transformation of T1, T2 and T3 with and without initial point.

Table 5.1: Generation of Sierpinski Triangle using separately of affine transformations T1,T2 and T3

Transformations	With Fix Point	<u>Without Fix Point</u>
<u>T1</u>		
<u>T2</u>		
<u>T3</u>		

The fractal that is generated using one transformation will produce points only one side of the triangle as the three transformations represent top, left and right. From the table above, the generation of Sierpinski Triangle is in order of the triangle shape if the initial point is used. However the Sierpinski Triangle points will be deviated if there is no initial point

used. Figure 5.7 shows the generation of Sierpinski Triangle using all three transformations that are randomly selected. The figure also shows the comparison of Sierpinski Triangle with and without initial point. The red circle indicates the points that deviated from the triangle when generating the fractal without initial point.

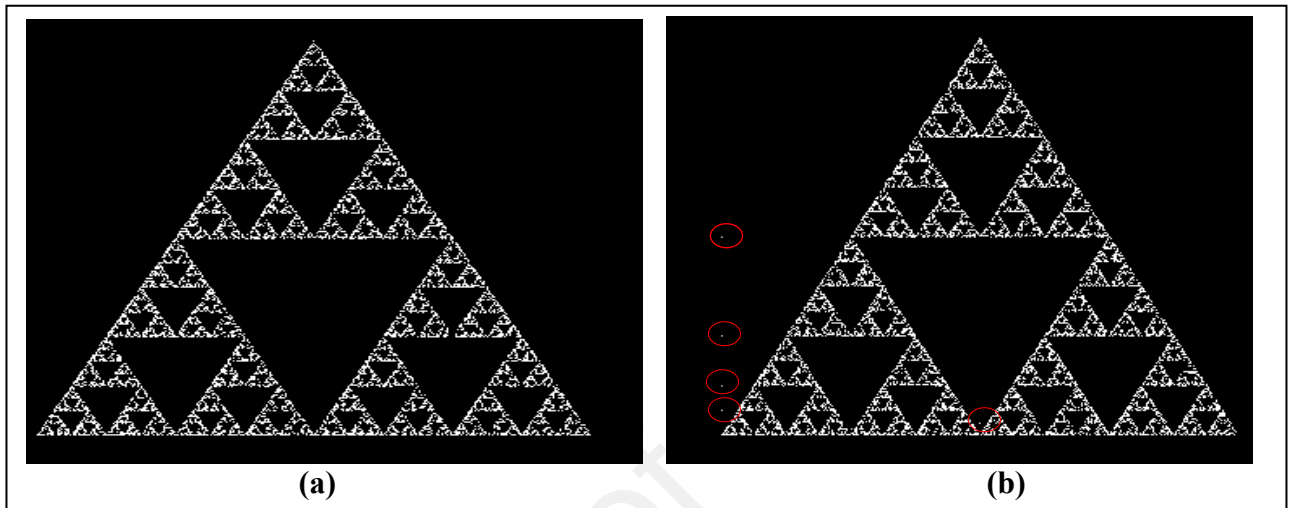
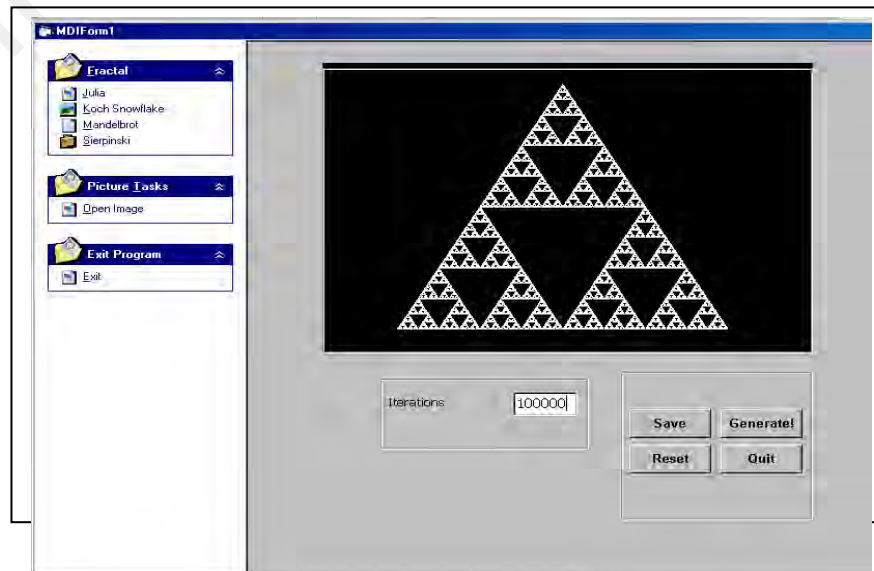


Figure 5.7: Figure (a) shows the generation of Sierpinski Triangle with initial point. Figure (b) shows the generation of Sierpinski Triangle without initial point.

Figure 5.8 is the screenshot of Sierpinski Triangle via FGS for 100000 iterations. The initial point is fixed, hence the only parameter that needs to be inserted is number of iterations, which means that, this parameter represents number of dots that appears to fill the Sierpinski Triangle.



5.1.4 Koch Snowflake

Koch Snowflake is generated based on Generator Iteration. The generation of Koch Snowflake is based on substitution of every base with another shape called generator. Figure 5.9 represent Koch Snowflake fractal generated using FGS.

Based on the figure, the iteration shows number of substitution between the base and the generator. The plus (+) button is to increase the substitution of the current base to generator. The minus (-) button is to decrease the substitution. Parameter of iteration is automatically changed due to the increment or decrement of the substitution. Figure 5.10 shows the sequence of generating Koch Snowflake via six iterations.

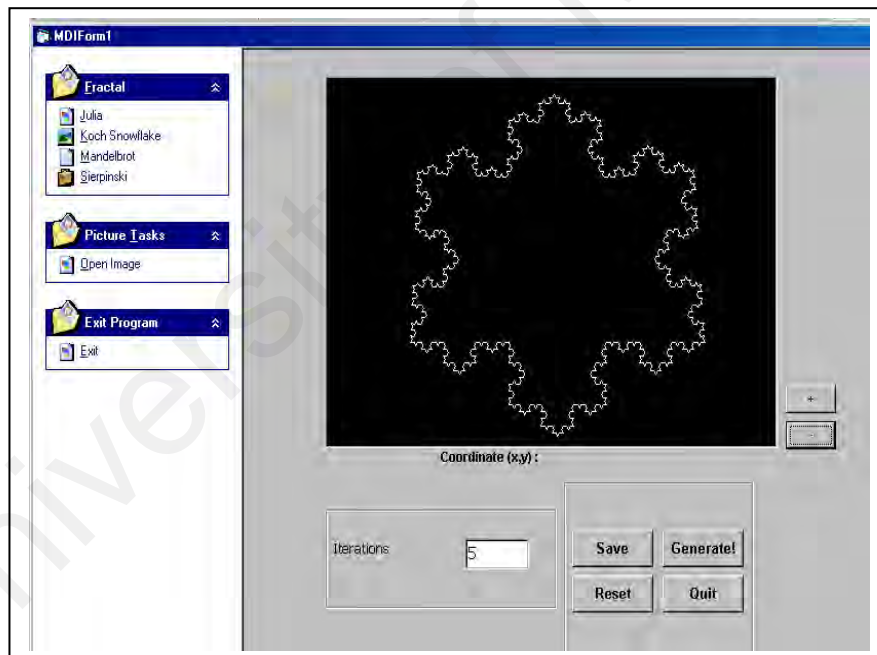


Figure 5.9: Fractal image of Koch Snowflake

Figure 5.10 shows the base or the initial shape of Koch Snowflake as an equilateral triangle. Step 2 shows that the initial shape is substituted with generator by pressing the plus (+) button, which means that, every line segment in the equilateral triangle has been replaced with Koch Curve line that works as generator. One keeps on adding the generator

to the line segment by pressing the plus (+) button. From the figure it can be concluded that the image will be more complex as more iteration of substitution has been executed.

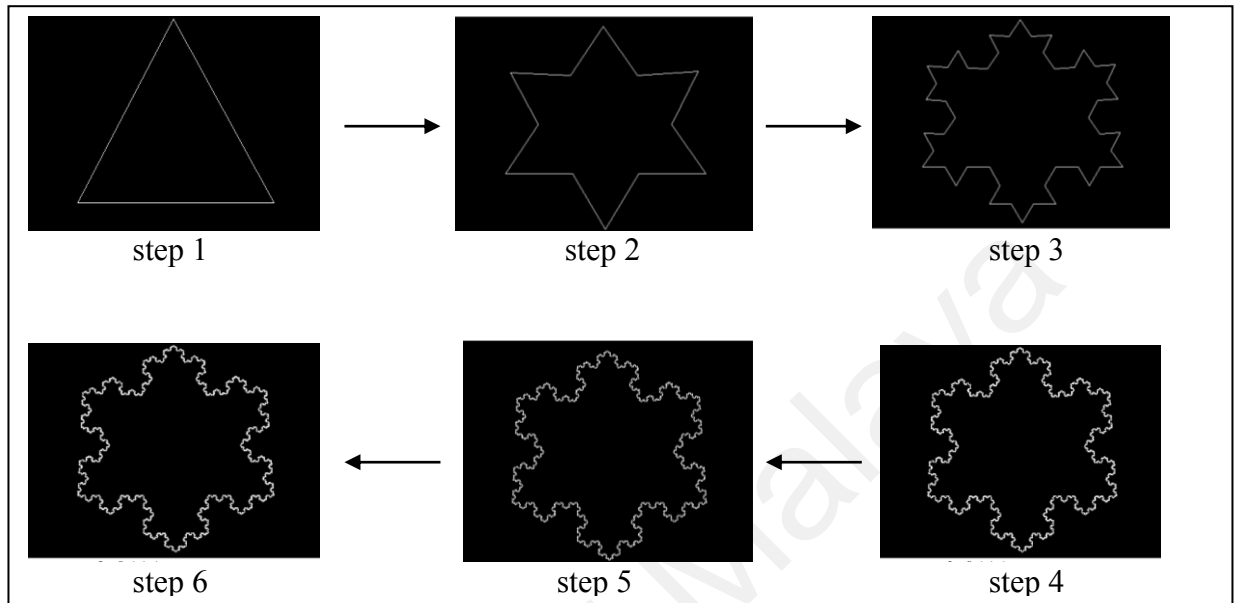


Figure 5.10: The sequence of Koch Snowflake generation

5.2 Fractal Dimension Phase

Fractal dimension phase is a division where all the generated fractals are characterized to obtain the value of fractal dimension. Moreover, this phase is used to measure and analyze medical images. There are two main functions involved within this phase:

1. Data acquisition phase
2. Fractal dimension calculation phase

Before the features above can be utilized, users have to load up an image to the system by selecting 'Open Image' label on the main menu option on the left side of the screen. The image that needs to be utilized must be in binary type of image. This is because as

mentioned in section 3.4.1, FGS only allows the binary image to be measured. This image then will be displayed at the rectangular region of the interface. There is also information of the image shown in the bottom left of the screen such as type, size and the latest date of modification of the image. For this research project, MATLAB tool is used to convert the image to binary type of image.

5.2.1 Data acquisition phase

The data acquisition phase involves the overlapping of mesh grid on the structure of image. The next step is the data gathering of the box size and box count value of the mesh grid containing the image structure. The box size value can be altered by choosing the minimum and maximum box size under the label 'Grid properties' as in Figure 5.11.

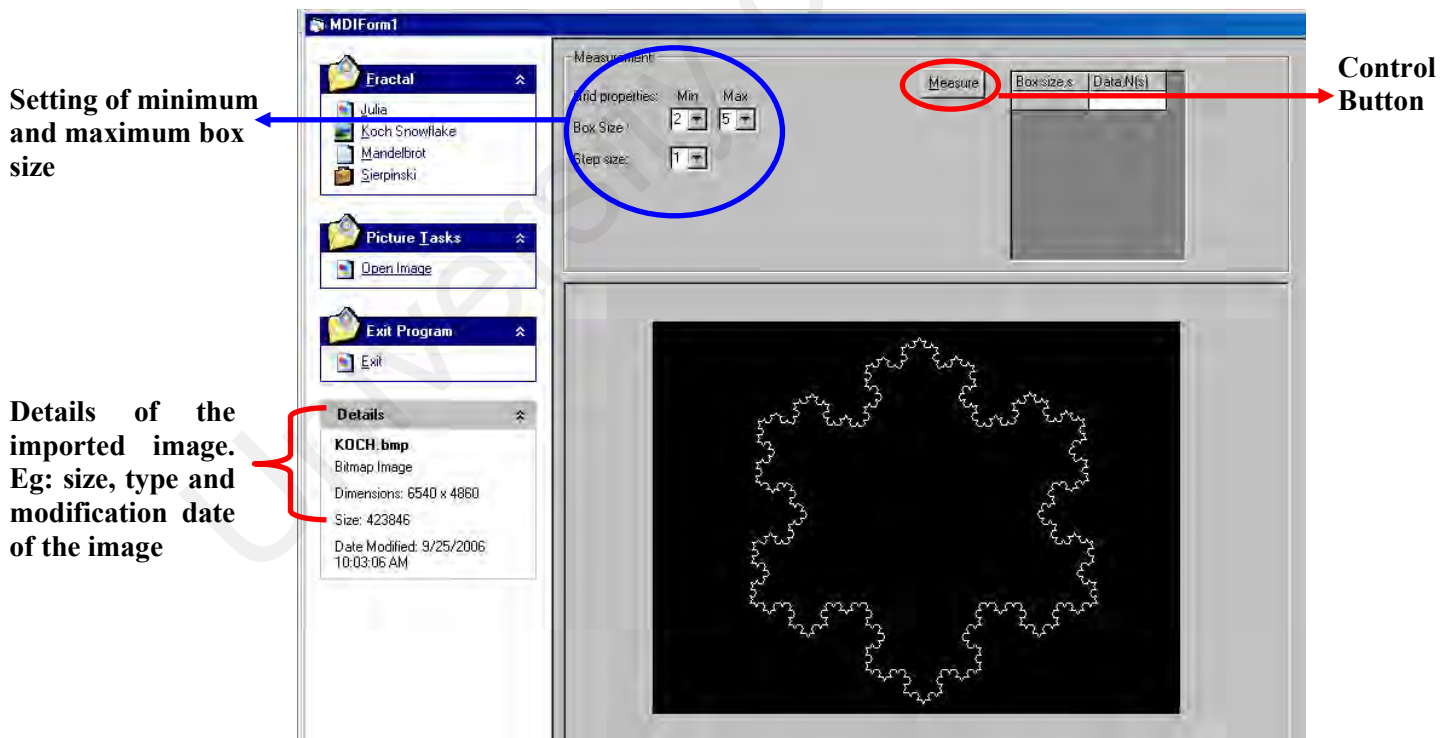


Figure 5.11: Screen shot for data acquisition phase

For this system, the box size is based on the pixel length. For instance a box size of 10 would result in a mesh grid with boxes of the length equal to 10 pixels. ‘Measure’ control button instructs FGS to compute the value of box count containing the white structure of the image corresponding to the box size. The command causes the boxes containing the structure to be counted and simultaneously shows up the counted boxes in yellow. Figure 5.12 shows FGS interface after the measurement of the structure. The data collection of box count with corresponding box size are stored in a table at the upper right of the screen from minimum to maximum box size. The next step is the fractal dimension calculation phase.

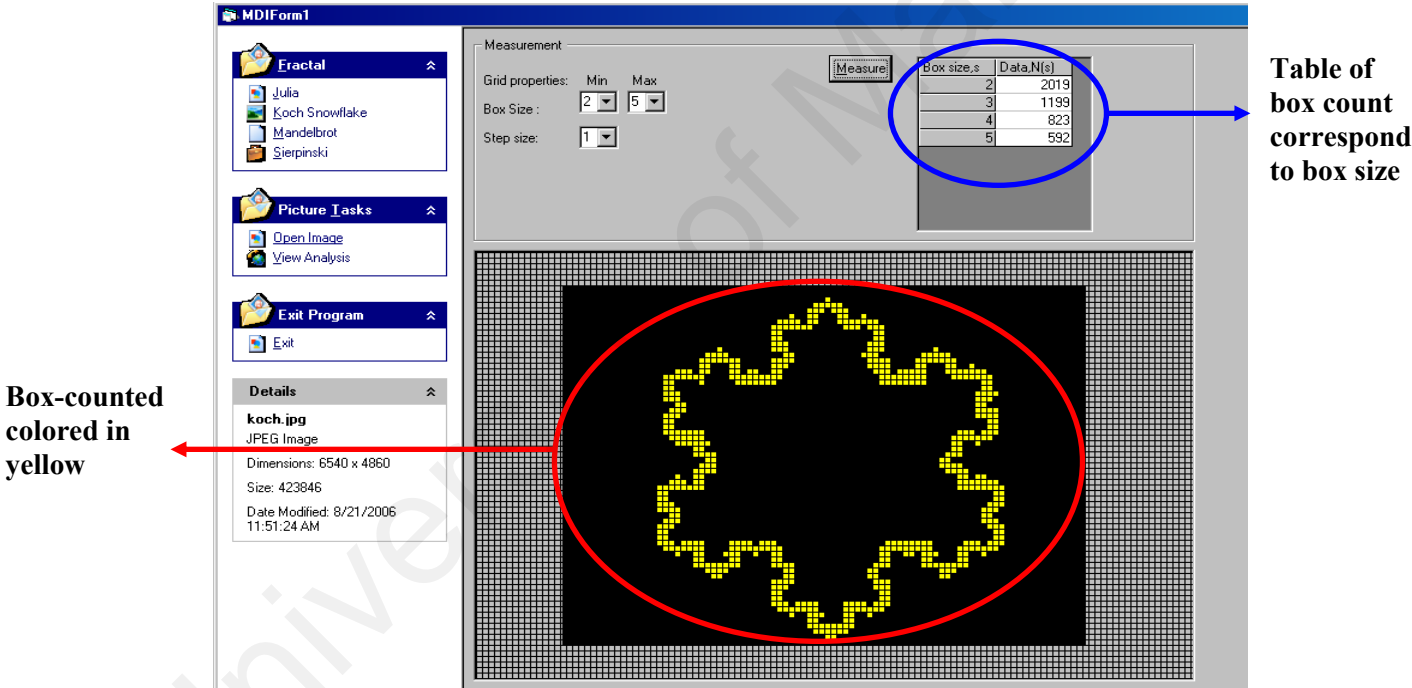


Figure 5.12: The system interface after the structure measurement

5.2.2 Fractal dimension measurement

The data collection obtained from the previous phase as in section 5.2.1 is the input of this phase, which is to calculate the value of fractal dimension of the image. Once the data acquisition phase is done, selecting the ‘View Analysis’ label as depicted in Figure 5.13 causes the interface of fractal dimension measurement phase to appear. The table on the

bottom left of the interface shows the average values of box counts corresponding to the box sizes and simultaneously logarithm values of box sizes and box counts are tabulated with a scatter plot of $\text{Log } N(s)$ versus $\text{Log } s$.

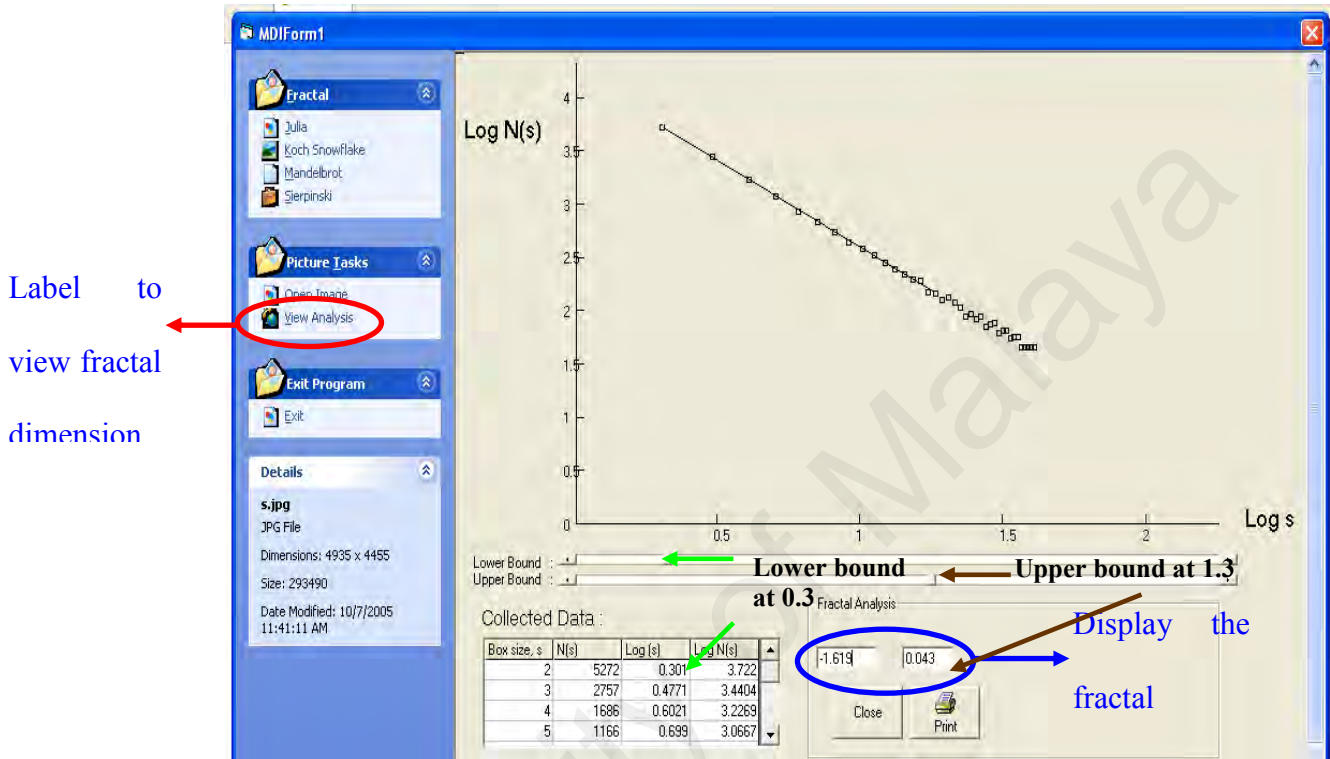


Figure 5.13: The system interface for fractal dimension calculation phase.

The value of fractal dimension determined which is based on the gradient of the least squares regression line is displayed on the frame labeled 'Frame Analysis'. Before a user can finalize the value of the fractal dimension, the user must first determine the upper and lower bounds, which define the fractal behavior of the image. The lower bound is used when the plot forms a plateau in the region of smaller values of $\log s$, which is beyond the representative region of the graph. The upper bound is determined when the plots develop a scattering behavior at the high values of $\log s$ due to insignificant change in box counts during the calculation. Based on Figure 5.13, the lowest $\log s$ is indicated by a green arrow (with no indication of a plateau in this example). Hence, the starting plots start at 0.3 and the lowest level of $\log s$ can be accepted as the lower bound. However, there is a slight


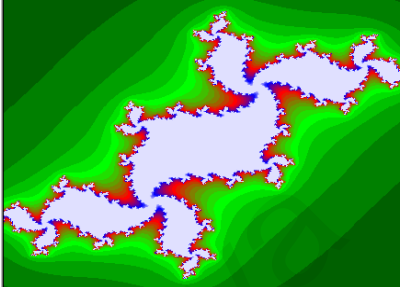
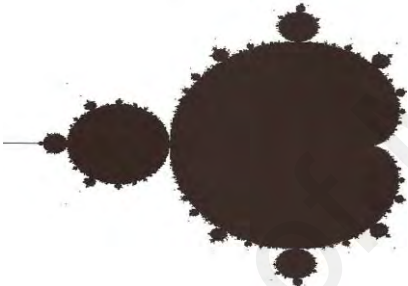
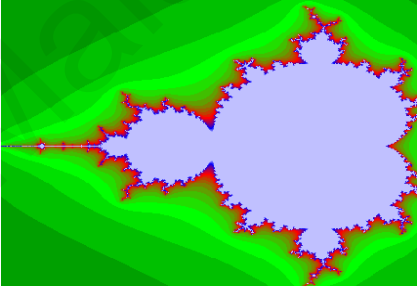
scattering behavior in the region of the extreme end indicated by $\log s \geq 1.3$ as shown by a brown arrow. Therefore the upper bound is set by this value. The value of fractal dimension will change once a user drags the scrollbars of the lower bound or upper bound. The white dotted lines guide the user to indicate the region, within which the plots are accepted. The fractal dimension value of the image is finalized once the user has the lower bound and upper bound. Based on the figure above, the finalized value of the fractal dimension is 1.619 ± 0.043 .

5.3 System Validation

The implementation of FGS is discussed in the previous sections 5.1 and 5.2. Section 5.1 illustrates the generation for each type of fractal and section 5.2 demonstrates the calculation of fractal dimension using the Box Counting method. However, to answer the problem statement of section 3.1.2 (question 2) the system must be validated for its reliability and accuracy, which are based on the geometric patterns of the fractals generated and the fractal dimension values obtained.

As previously mentioned, the algorithms to generate the fractals are adopted from Crownover (1995) with some enhancements. Fractals from Formula Iteration apparently do not have the theoretical analytical value of fractal dimension directly from its mathematical formulation and it depends on the dimension metric utilized and the parameter used. Hence to show the reliability of fractal generated by Formula Iteration, the fractal patterns of Julia set and Mandelbrot set taken from Crownover (1995) and fractal patterns generated by FGS is compared as in Table 5.2. To compare the images, the formula from Crownover (1995) is used which is $z^2 - 0.20 + 0.75i$ to generate Julia set and Mandelbrot set with different parameter values for Julia set and Mandelbrot set.

Table 5.2 Comparison of fractal images obtained by Crownover (1995) and FGS.

Type of Fractal	Crownover (1995)	FGS
Julia set		
Mandelbrot set		

From Table 5.2, it can be seen that the fractal patterns generated by FGS are agreeable to the images from Crownover (1995). Moreover for FGS, there are layers of colours to represent the escape set.

To test the accuracy of fractal patterns generated using IFS Iteration and Generator Iteration, FGS was tested to compare the fractal dimension values of Koch Snowflake and Sierpinski Triangle obtained by FGS with the theoretical values. These two fractals have theoretical fractal dimension values derived mathematically based on Hausdorff 'scaling dimension technique'. Table 5.3 summarizes the theoretical fractal dimension values for Koch Snowflake and Sierpinski Triangle.

Table 5.3 Analytical fractal dimension values for Koch Snowflake and Sierpinski Triangle

Types of Fractal	Scaling of fractal elements	Fractal dimension value
Sierpinski Triangle	3 parts scaled by 1/2	$(\log 3) / (\log 2) = 1.585$
Koch Snowflake	4 parts scaled by 1/3	$(\log 4) / (\log 3) = 1.262$

Sierpinski Triangle and Koch Snowflake generated from FGS are measured to obtain the fractal dimension values based on BCM and compared with the theoretical values. The values of box size, s and box count, $N(s)$ Triangle and Koch Snowflake fractals are tabulated in Table 5.4 and Table 5.5. Table 5.4 shows the collection of data acquisition of Sierpinski Triangle comprise with Sierpinski Triangle image as in Figure 5.14 and scattered graph plot to measure fractal dimension is as in Figure 5.15. The data acquisition collection of Koch Snowflake is depicted in Table 5.5 with Koch Snowflake image in Figure 5.16 and the scattered graph of Koch Snowflake in Figure 5.17. From the scattered plot of $\log N(s)$ versus $\log s$, the fractal dimension value is determined based on the gradient of the least square regression line. The value of Sierpinski Triangle fractal dimension using FGS is 1.619 ± 0.083 , with the percentage of relative difference 2.14% different from the theoretical value. The resultant value of Koch Snowflake fractal dimension using FGS is 1.301 ± 0.046 of 3.09% difference from the theoretical value. The results show that the fractals generated by FGS can be numerically accepted with good accuracy of low percentage in relative differences. At large box sizes, the box count tends to scatter. This is due to the selection of insignificant boxes into count. Users can obliterate the scatter points by dragging the lower bound or upper bound to fix the best regression line.

Table 5.4 Sierpinski Triangle data acquisition

Box size, s	Box count, N(s)	Log (s)	Log N(s)
2	5272	0.301	3.722
3	2757	0.4771	3.4404
4	1686	0.6021	3.2269
5	1166	0.699	3.0667
6	851	0.7782	2.9299
7	677	0.8451	2.8306
8	541	0.9031	2.7332
9	442	0.9542	2.6454
10	383	1	2.5832
11	327	1.0414	2.5145
12	279	1.0792	2.4456
13	245	1.1139	2.3892
14	216	1.1461	2.3345
15	197	1.1761	2.2945
16	188	1.2041	2.2742
17	150	1.2304	2.1761
18	144	1.2553	2.1584
19	126	1.2788	2.1004
20	134	1.301	2.1271
21	118	1.3222	2.0719
22	108	1.3424	2.0334
23	88	1.3617	1.9445
24	94	1.3802	1.9731
25	83	1.3979	1.9191
26	88	1.415	1.9445
27	71	1.4314	1.8513
28	74	1.4472	1.8692
29	76	1.4624	1.8808
30	61	1.4771	1.7853
31	64	1.4914	1.8062
32	64	1.4914	1.8062
33	55	1.5185	1.7404
34	56	1.5315	1.7482
35	56	1.5441	1.7482
36	45	1.5563	1.6532
37	45	1.5563	1.6532
38	43	1.5324	1.6358
39	42	1.5301	1.6245
40	40	1.5254	1.6145
41	36	1.6128	1.5563
42	38	1.6232	1.5798
43	38	1.6335	1.5798
44	39	1.6345	1.5911
45	39	1.6532	1.5911
46	30	1.6628	1.4771
47	30	1.6628	1.4771
48	31	1.6812	1.4914
49	31	1.6812	1.4914
50	30	1.699	1.4771

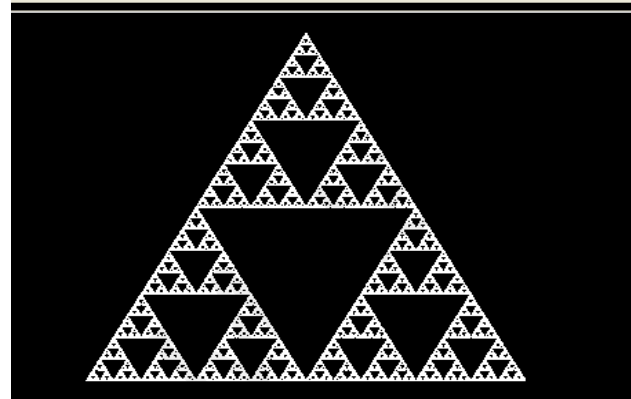


Figure 5.14: Sierpinski Triangle

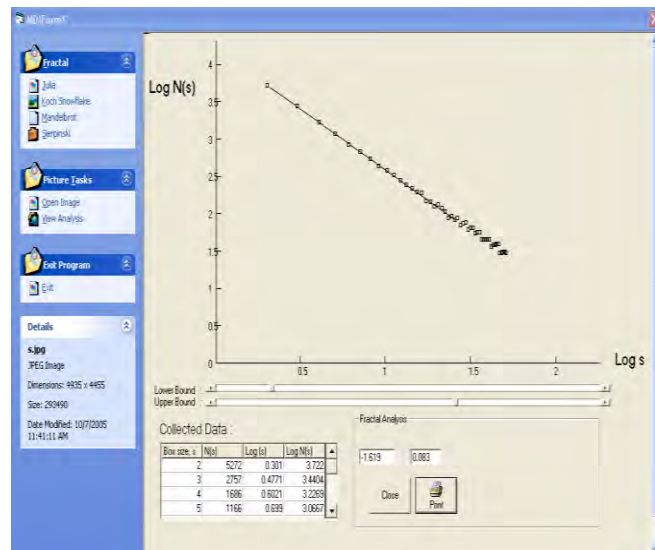


Figure 5.15: Scatter plot to obtain fractal dimension value of Sierpinski Triangle

Table 5.5 Koch Snowflake data acquisition

Box size,s	Box count, N(s)	Log (s)	Log N(s)
2	2019	0.301	3.3051
3	1199	0.4771	3.0788
4	823	0.6021	2.9154
5	592	0.699	2.7723
6	483	0.7782	2.6839
7	382	0.8451	2.5821
8	322	0.9031	2.5079
9	274	0.9542	2.4378
10	240	1	2.3802
11	214	1.0414	2.3304
12	188	1.0792	2.2742
13	165	1.1139	2.2175
14	161	1.1461	2.2068
15	137	1.1761	2.1367
16	132	1.2041	2.1206
17	121	1.2304	1.0828
18	116	1.2553	2.0645
19	105	1.2788	2.0212
20	91	1.301	1.959
21	91	1.3222	1.959
22	87	1.3424	1.9395
23	85	1.3617	1.9294
24	79	1.3802	1.8976
25	70	1.3979	1.8451
26	69	1.415	1.8388
27	69	1.4314	1.8388
28	67	1.4472	1.8261
29	55	1.4624	1.7404
30	57	1.4771	1.7559
31	57	1.4914	1.7559
32	55	1.5051	1.7404
33	58	1.5185	1.7634
34	52	1.5315	1.716
35	46	1.5441	1.6628
36	47	1.5563	1.6721
37	42	1.5682	1.6232
38	45	1.5798	1.6532
39	37	1.6021	1.5682
40	38	1.6129	1.5798
41	38	1.6232	1.5798
42	38	1.6232	1.5798
43	38	1.6335	1.5798
44	39	1.6345	1.5911
45	35	1.6532	1.5441
46	35	1.6628	1.5441
47	35	1.6721	1.5441
48	35	1.6812	1.5441
49	31	1.6902	1.4914
50	30	1.699	1.4512

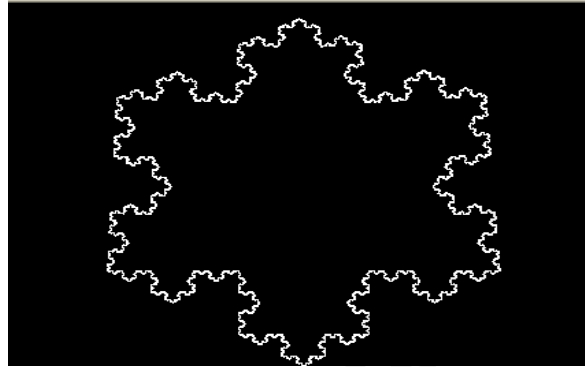


Figure 5.16: Koch Snowflake

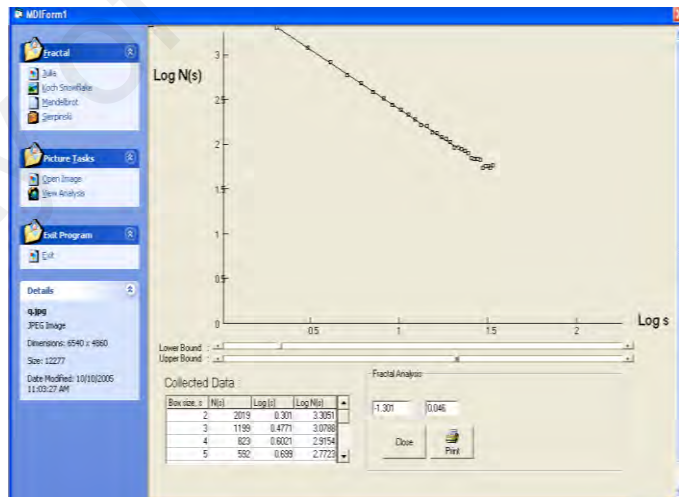


Figure 5.17: Scatter plot to obtain fractal dimension value of Koch Snowflake

Following the system validation, the next stage is fractal analysis on medical images, which is presented in Chapter 6.

5.4 Summary

This chapter illustrates the implementation results of FGS. Basically there are two main modules in the system; comprising of a module to generate various types of fractals and a module to measure the fractal dimension value. However the third system component, which is the application of fractal analysis in trabecular bone structure, is discussed in Chapter 6.

University of Malaysia

CHAPTER 6
RESULTS AND DISCUSSION OF FRACTAL ANALYSIS
IN TRABECULAR BONE ARCHITECTURE

To achieve the second main aim of this research, FGS was tested to measure the fractal dimension values of trabecular bone structures. Previously in section 2.3, the properties of biological structures in terms of fractal patterns have been discussed. This chapter explains and illustrates the medical fractal analysis application to measure the degree of roughness and complexity of trabecular bone structures. Moreover, the relation of fractal analysis of trabecular bone structure and bone strength is discussed with reference to the influence of gender and age.

6.1 Bone Mineral Density (BMD) and Bone Architecture

Osteoporosis is characterized by low bone mineral density (BMD) and architectural changes of bone tissue leading to bone fragility and increased fracture risk (Lori, 2004). Bone fractures are linked to osteoporosis. Current approach to osteoporosis diagnosis in clinical practice is based on bone mineral density (BMD) by mean of dual-energy x-ray absorptiometry (DXA). BMD is certainly strongly related to osteoporosis (Messent, 2005). National Institutes of Health (2005) states that BMD measurement is used to predict fracture risk by the measurement of the amount of mineral bone tissue in a given area, usually calculated as grams per square centimeter. According to World Health Organization (WHO) study group (1994), age increment causes BMD value to decrease due to the decrement of the bone mass and mineral bone tissue. Figure 6.1 shows a graph presentation of BMD values versus fracture risk at different ages. Based on the figure the BMD value

decreases when the age increases. The percentage of fracture risk probability increases when the age increases.

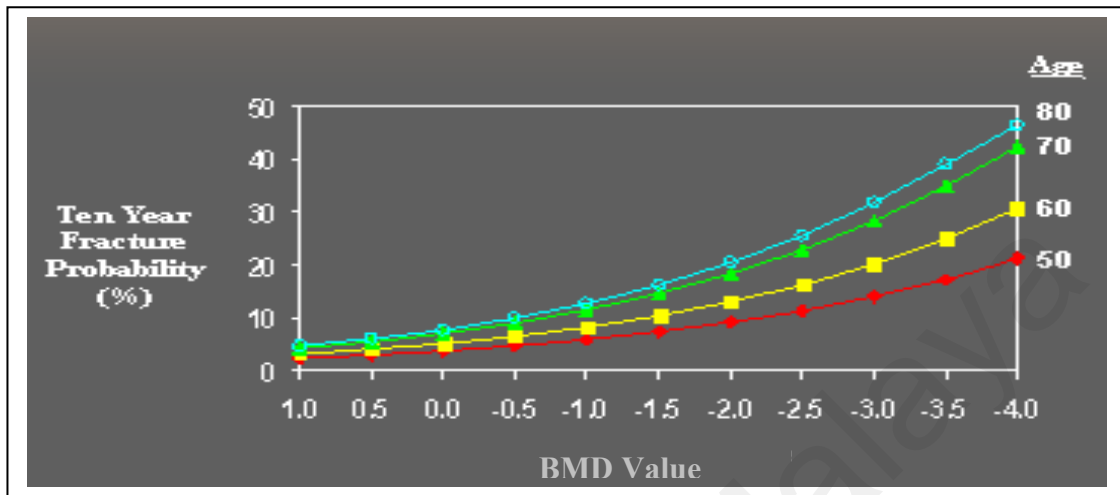


Figure 6.1: Graph presentation of BMD value and age versus fracture risk. (Adapted from Kanis JA et al. Osteoporosis Int. 2001;12:989-995)

However, BMD measurement seems to be a poor predictor for bone fracture risk in some cases. This is because there are wide biological variations seen in bone fracture among patients with the same bone mineral density. According to Ralph and Pharm (2005), analyses of clinical trials show an inconsistent relationship between increased spinal BMD and a decrease risk of vertebral fracture.

According to McCubbrey (1991), the bone architecture is increasingly an important factor in determining bone strength and consequently fractures risk. During ageing, a period of rapid loss in bone strength is much greater than the reduction of BMD (Parfitt, 1985). Thus strength depends not only on bone mass, but also on the continuity of the trabecular network. Bergot et al. (1988) state that the trabecular network in human vertebrae loses continuity due to a preferential thinning and loss of horizontal trabeculae. Such patterns of bone loss can be characterized by the trabeculation pattern and the connectivity of the bone

network, an indication of which can be obtained from the fractal analysis associated with fractal dimension.

6.2 Fractal Analysis in Trabecular Bone Structure

In this section, the results in analyzing the trabecular bone structures are illustrated and explained. The key purpose of analyzing the architecture of trabecular bone is to determine the bone strength based on the value of fractal dimension. For this research study, there are 53 CT-scan images of 27 males and 26 females with the age range from 25 to 81 years. The patients are divided into three groups of different stages which are puberty stage, encompassing patients between 25 to 35 years old, pre-menopausal stage with patients 38 years and below 49 years and lastly the post-menopausal stage consisting of patients above 50 years. Appendix II a, b, c, d, e and f show the example of trabecular network patterns in CT-scan images for each stage. Previously in chapter three (section 3.5), image processing of CT-scan images using MATLAB tool is explained. The following step is to analyze each processed CT-scan image using FGS in obtaining the fractal dimension value. Fractal dimension values are compared to study the effects of age, gender and the state of the three stages. Figure 6.2 shows an example of a CT-scan image before and after it has been processed using MATLAB image processing tool.

Image (a) as shown in Figure 6.2 is the CT-scan image that has been captured and stored in computer memory. The next step is the conversion of the grayscale image to which result from the image processing using MATLAB tool as depicted in image (b). The final image (c) represents the cropping of region of interest (ROI) of trabecular bone structure in binary format. This final image format is in a suitable form to measure and analyze using FGS in measuring the fractal dimension (F_D) value.

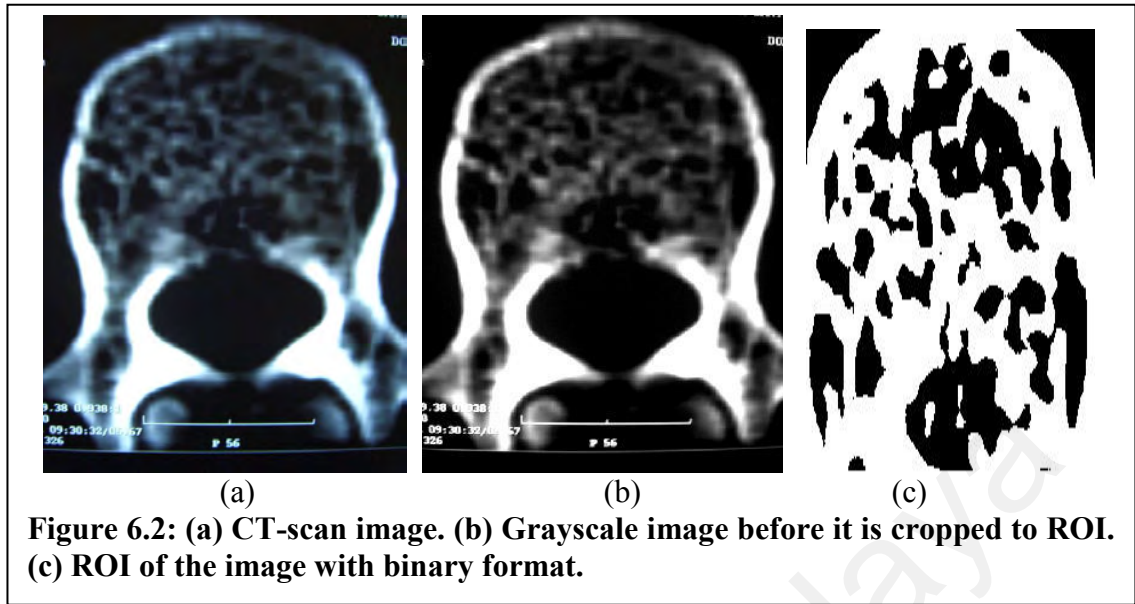


Table 6.1 represents the overall results of F_D value for 53 CT-scan images. Based from the values in Table 6.1, shows that male has stronger and compact bone structure compared to female due to the value of F_D . However the value decrease when the age increases for both male and female.

Table 6.1: Fractal dimension values for patients in the age range from 20 to 80

Age	MALE				FEMALE			
	(1)	(2)	(3)	(4)	(1)	(2)	(3)	(4)
20s	1.891	1.855	1.843	1.864	1.851	1.857	1.827	1.836
30s	1.817	1.809	1.812	1.826	1.773	1.7698	1.762	1.751
40s	1.735	1.783	1.772	1.75	1.721	1.714	1.681	1.709
50s	1.746	1.714	1.735	1.746	1.693	1.684	1.681	1.675
60s	1.716	1.725	1.698		1.696	1.684	1.667	
70s	1.705	1.689	1.692	1.684	1.682	1.67	1.687	1.674
80s	1.693	1.665	1.69	1.675	1.668	1.685	1.654	

Figure 6.3 to Figure 6.9 illustrate the average results using graph presentations that compare box count values between male and female based on each age group. The blue regression line () represents male data and the pink regression line () represents female data. Each regression line presents data collection of box counts corresponding to box sizes on trabecular bone structure using log graph. The box count is an indication of the proportion of filled bone structures on the bone architecture.

(a) Puberty Stage

As seen from the graph in Figure 6.3, there is a negligible difference in box count values between males and females for patients with age range of 25 to 29 years. At this stage, both males and females have strong bones. However, according to Seeman (1997), bone size and thickness in male are larger than female in general situations.

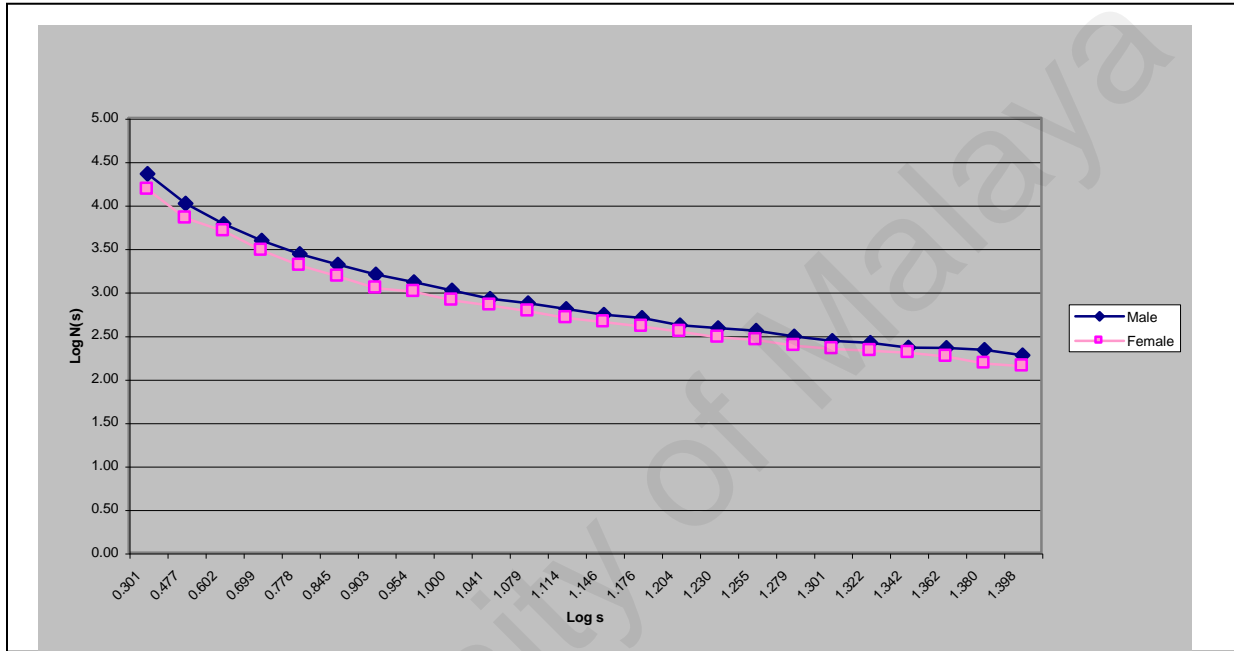


Figure 6.3: Box count values for patients with age range from 25 to 29 years; male $F_D = 1.863$ and female $F_D = 1.843$

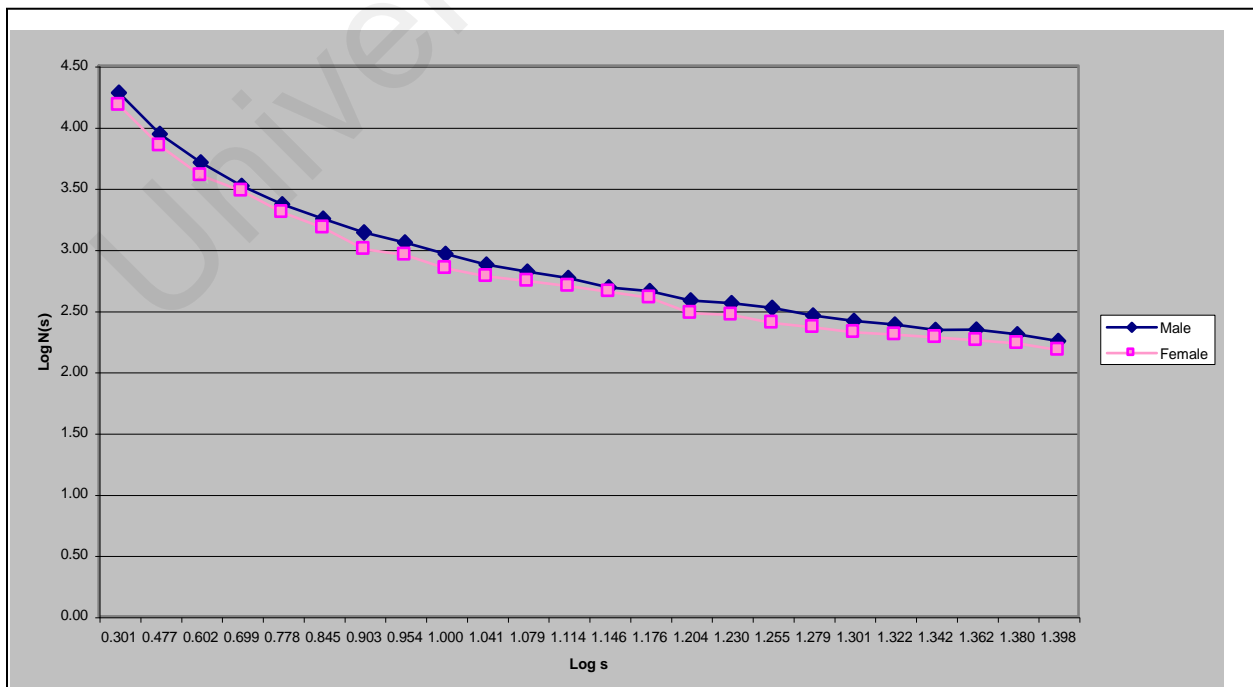


Figure 6.4: Box count values for patients with age range from 30 to 35 years; male $F_D = 1.816$ and female $F_D = 1.781$

Hence it is expected that the fractal dimension value is higher in males than females as also obtained in Figure 6.3 up to Figure 6.9. Figure 6.4 shows a slight decrement of box count values for females compared to males with the range age of 30 to 35 years.

(b) Pre-menopausal Stage

In this stage, the bone strength in females tends to reduce more compared to males. This may be due to the lack of calcium during pregnancy, low endogenous level of estrogen, low weight, low body mass index (BMI) and early menopause in females. Figure 6.5 illustrates such situation whereby there is a more marked difference of box count values with higher



Figure 6.5: Box count values for patients with age range from 38 to 48 years; Male $F_D = 1.760$ and female $F_D = 1.746$

(c) Post-menopausal Stage

There is a great loss of bone strength for several years in females during post menopausal stage. According to Lori (2004), from 25 million people in the United States, 80% of osteoporosis patients are women. However, one woman in eight men over the age of 50 has

an osteoporosis-related fracture during their lives. In post-menaoposal stage of age range 50 to 67 years, there is a marked difference of box count values between males and females.



Figure 6.6: Box count values for patients with age range from 50 to 58 years; Male $F_D = 1.735$ and female $F_D = 1.726$

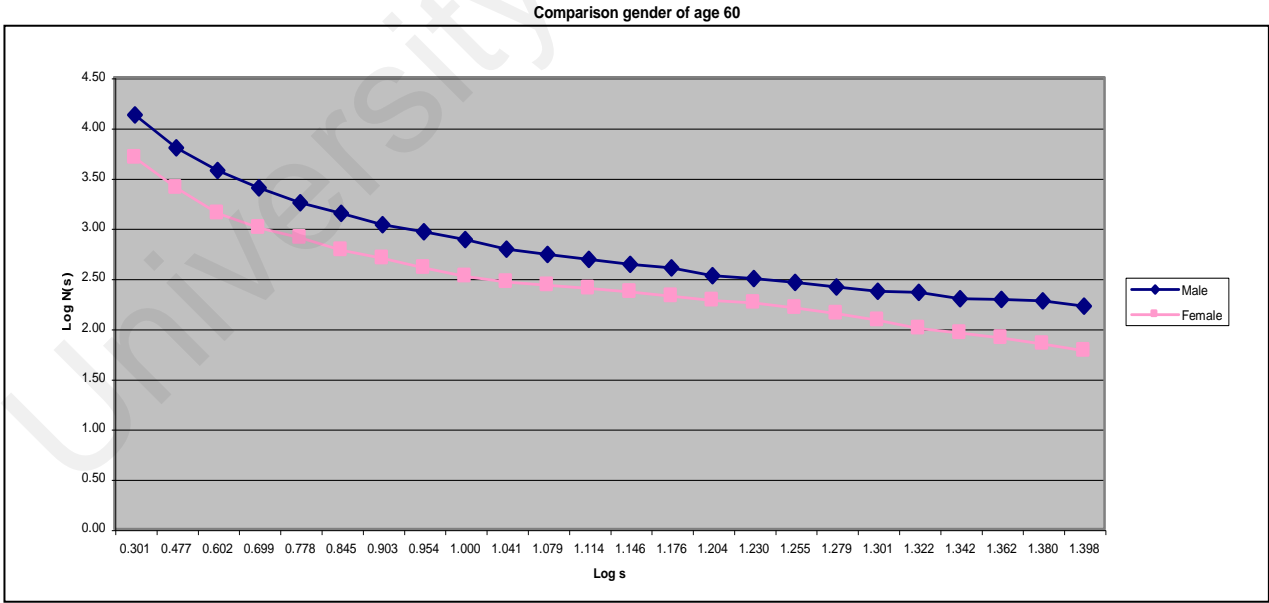


Figure 6.7: Box count values for patients with age range from 62 to 67 years; Male $F_D = 1.698$ and female $F_D = 1.682$

Males in age range of 50 to 67 years do not experience rapid reduction of bone structure as females do in the years of post-menopausal. The decline in the bone structure in males occurs relatively slow but by the age of 69 and above, bone architecture in males and females have approximately the same values of box counts as depicted in Figure 6.8.

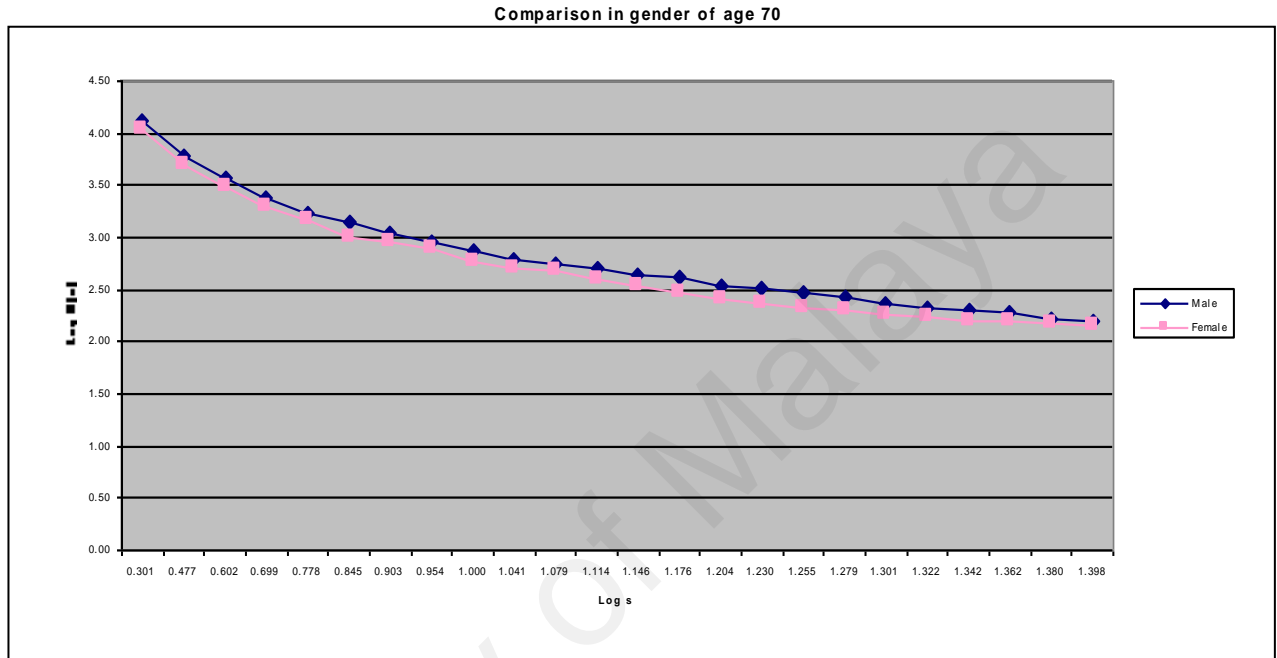


Figure 6.8: Box count values for patient with age range from 69 to 81 years; Male $F_D = 1.693$ and female $F_D = 1.678$

It shows that males start to lose bone strength around the age of 70. Excessive bone loss causes bone to become fragile and more likely to fracture. Fractures resulting from osteoporosis most commonly occur in the hip, spine, and wrist, and can be permanently disabling. Perhaps because such fractures tend to occur at older ages in men than in females, males who sustain hip fractures are more likely than women to die from complications.

These data are graphically presented in Figure 6.9, which represents the regression line for males and Figure 6.10, which represents the results for females with age range of 25 to 81 years. Each regression line has different color and symbol to represent different age group.

Fractal Analysis in Trabecular Bone of Male

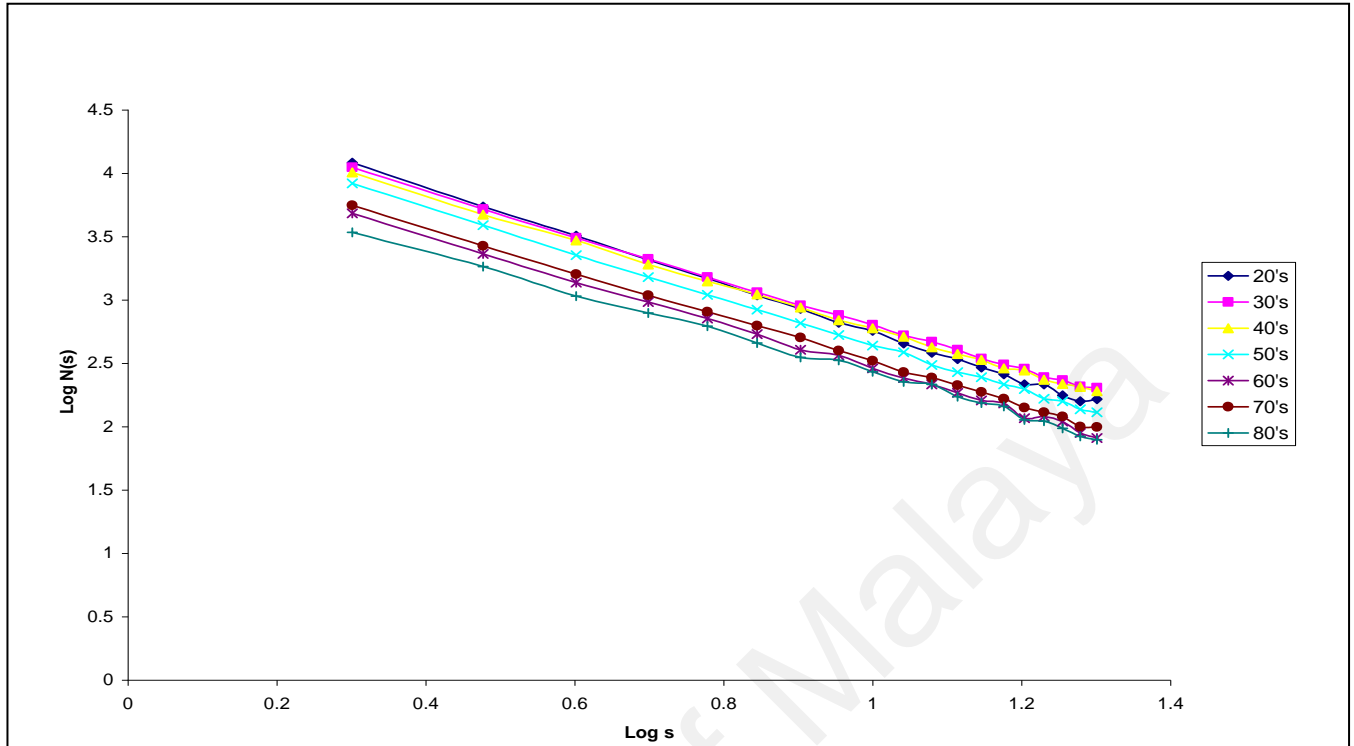


Figure 6.9: Measurement of trabecular bone structure for male patients with age range of 25 to 81 years.

Fractal Analysis in Trabecular Bone of Female

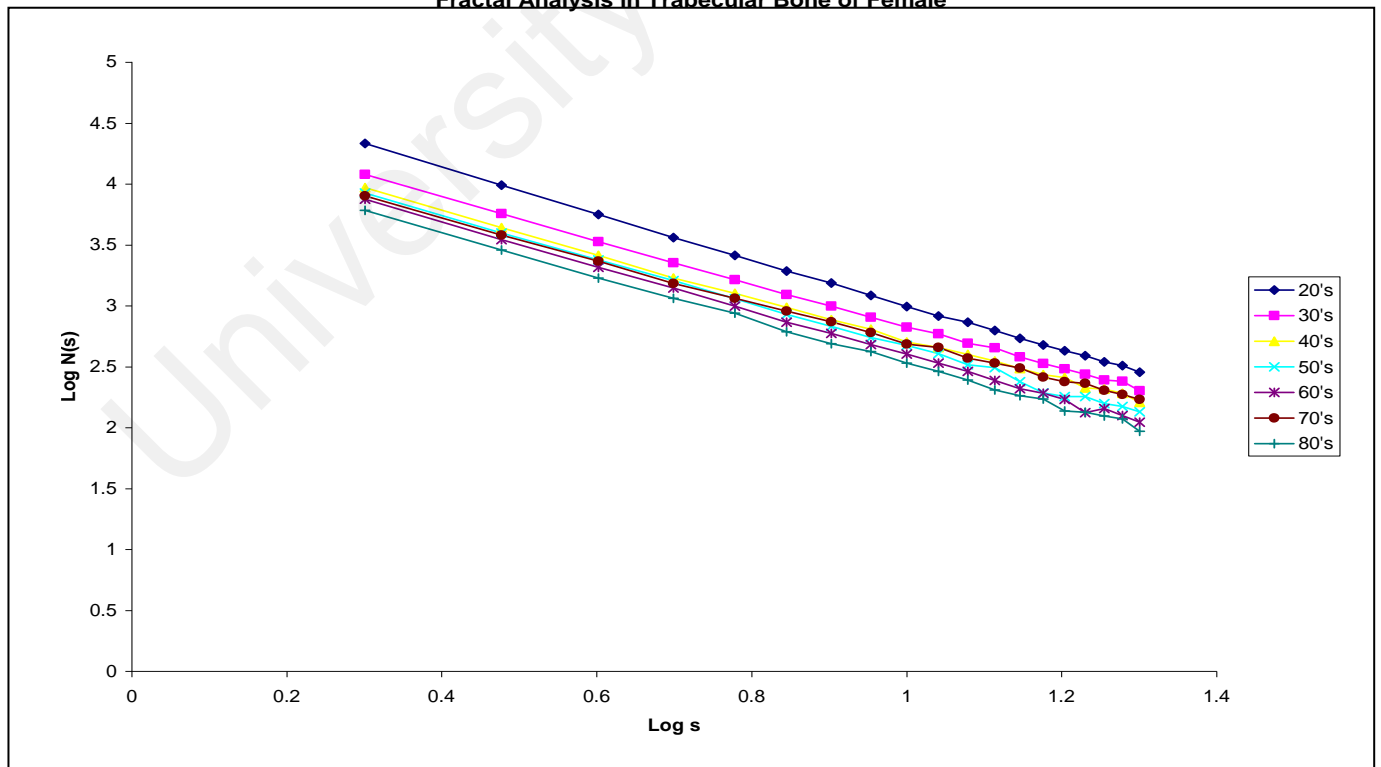


Figure 6.10: Measurement of trabecular bone structure for female patients with age range of 25 to 81 years.

From the table and graphs, we can also see the decrement of the fractal dimension values when the age increases for both male and female. This is due to an age-associated reduction in number of fine trabecular network (Lin, 1999).

6.3 Summary

From this study, it shows that fractal analysis of trabecular bone structure is a reliable alternative technique to characterize the architecture of trabecular bone. It is important to analyze the structural pattern of trabecular bone.

Male has stronger and compact bone structure compared to female. This is because F_D value in male is larger than female. However the value decrease when the age increases for both male and female. In puberty stage both males and females have strong bones but still the F_D value in female is a slight lower than male. During pre-menopausal stage, F_D value in female decreases drastically. This is due to the affect of hormone changing and early menopause. At post-menopausal stage, there is a great loss of bone strength for several years in females. However males start to show marked decrease in F_D value at the age of 70.

The main significance of this FGS module is for medical health planning by taking preventive measures accordingly. Bone analysis helps to identify patients at high risk of osteoporosis and the measurement on architecture of bone structure helps to detect low bone strength before a fracture occurs.

CHAPTER 7

SYSTEM EVALUATION

FGS was developed for practical implementations of the theories with some adaptation based on conceptual and mathematical modeling to generate different types of fractals. An important enhancement in the medical application is based on fractal analysis. In general, this section covers validation of FGS in terms of the generation of each type of fractal and the computation of the fractal dimension value. The system has fulfilled the criteria of precision and reliability. Thus, FGS has been tested to be able to generate four types of fractals, which are Julia, set, Mandelbrot set, Koch Snowflake and Sierpinski Triangle with high accuracy. Furthermore, FGS has been tested to be able to calculate the value of the fractal dimension with promising and reliable results. In this chapter, the strengths and the weaknesses of FGS are identified.

7.1 Strengths of FGS

The strengths of FGS are listed as follows: -

- (a) FGS is able to generate several types of fractal images, namely Julia set, Mandelbrot set, Koch Snowflake and Sierpinski Triangle as illustrated in Figure 5.9, Table 5.1 and Table 5.2. Refinement is done by generating colorful layers of Julia set and Mandelbrot set based on number of iterations. FGS offers users a better understanding to differentiate various types of fractals by using different algorithms for their simulations.
- (b) The user-friendly interface helps users to follow the instructions and execute the functions with ease. Furthermore the fractal generated can be saved in computer memory or it can be reset.

- (c) In importing image to the system, FGS provides the information on the image in terms of memory size, dimension and the last date that the image was modified.
- (d) FGS is able to measure fractal dimension using box-counting technique with high accuracy as computed and analyzed in section 5.3. Proving the accuracy of the system is a very important aspect of the system since in this research there is indepth analysis of medical images.
- (e) The data produced are clearly presented graphically and in the form of tables. The graph can be instantly generated corresponding to the data obtained in the form of Log N (box count) versus Log s (box size). In addition, there is a lower bound and upper bound, which can be modified in the graph. Furthermore, there is a white dotted line to guide users to determine the required region within which the plots are accepted. FGS can then calculate the gradient of the least mean square regression line and simultaneously display the value of fractal dimension.
- (f) FGS also has a potential application in medical field, which in this research, FGS is shown as a reliable tool for analysing trabecular bone structure of patients age range of 25 to 81 years by using CT-scan images by obtaining the fractal dimension values. The results show that fractal dimension values of trabecular bone structure decreases when age increase as it similarly found for BMD value in quantifying the bones.
- (g) FGS is a potential tool in diagnosing and analyzing potential patient of osteoporosis by comparing and measuring the fractal dimension values of the bone architecture.

7.2 FGS Weaknesses

In the development of FGS, all the main aims and objectives have been achieved successfully. However, there are few weaknesses encountered in the system, which are as follows:

- (a) The image that needs to be analyzed and measured for the fractal dimension must be in binary image. FGS does not have a module to process the image. Thus users need to use other external tool to process the image. In this research, software tool, MATLAB is used to process the image starting with conversion the CT-scan image to grayscale image, selecting the region of interest (ROI) and lastly to convert the grayscale image to binary image.
- (b) FGS has a difficulty to process large images. The system will hang when a bitmap file size larger than 200 kilobytes is used. However, FGS prototype can be practical in some applications for experimenting to produce good results.
- (c) Only one image can be executed at one time. FGS cannot support multiple images to be analyzed at one time.

CHAPTER 8

CONCLUSION AND FUTURE ENHANCEMENT

The overall research study is summarized in this chapter. The significant findings are concluded. Future enhancement is also discussed for further improvement in fractal contribution.

8.1 Conclusion

FGS was developed based on the three main iterations to generate fractals, which are Formula Iteration, IFS Iteration and Generator Iteration. Each iteration can generate various fractals such as Julia set and Mandelbrot set for Formula Iteration, Sierpinski Triangle for IFS Iteration and Koch Snowflake for Generator Iteration. Each fractal is based on specific algorithm and different parameters for its generation. However, all fractals share the same properties of self-similarity, scale independence, irregularity and complexity with varying degrees.

Fractal analysis is an important study as various object formations in nature are closely related to specific fractal patterns. Environmental occurrences such as snowflake, mountain and clouds are nature objects that have similar patterns to Koch Snowflake fractal. Sierpinski Triangle is categorized as a non-linear system that can be widely observed in branching systems of human body such as lung cast and bone structure. The irregular and complexity pattern of Formula Iteration (Julia set and Mandelbrot set) can be related to the dendrite pattern of human cell. Formula Iteration algorithm can be used in determining the abnormal pattern and detection of tumor in human cell.

FGS provides the function of calculating fractal dimension values. Box Counting Method (BCM) is chosen to measure fractal dimension as it fulfils certain criteria namely ease of application, flexibility and suitability which are required for its computer-based operationalization. FGS was tested on Koch Snowflake (Generator Iteration) and Sierpinski Triangle (IFS Iteration) fractals based on comparison of their fractal dimension values with exact theoretical fractal dimension values, which were derived mathematically. The testing showed that the system resulted in good fitting with the theoretical values as shown in Table 5.2. In addition all the four types of fractals generated by FGS based on the three iterations show good matching of FGS fractal structured patterns with the actual patterns.

The next stage of this research is the application of fractal analysis in medical field. The study was carried out on trabecular bone structure by calculating the fractal dimension values of trabeculae network in CT-scan images of patients ranging from 25 to 81 years. The purpose of this study is to compare the bone strength in terms of fractal dimension values with two main influencing factors, which are gender and age. The architecture of trabecular bone is useful to indicate an appropriate risk factor of osteoporotic fractures that can lead to a better diagnosis of osteoporosis.

The measurement of trabecular bone structure is based on 'filling factor' approach where amount of space filled by the bone structure is represented by the fractal dimension value to indicate bone strength. Values of fractal dimension decreases with age showing the increase in marrow spaces within the architecture of trabecular bone.

The patients are divided into three groups of different stages, which are puberty stage, pre-menopausal and post-menopausal. The research study shows that during puberty stage, both males and females have strong bones. However, fractal dimension value is higher in males

than females and this can be supported by the statement from Seeman (1997), claiming the bone size and thickness in male are larger than female in general situations. In pre-menopausal stage, the bone strength in females tends to reduce compared to males. This may be due to pregnancy, low endogenous level of estrogen and early menopause in females. There is a great loss of bone strength for several years in females during post menopausal stage. However the decline in the bone structure in males occurs relatively slow but by the age of 69 and above, bone architecture in males and females have approximately the same bone strength.

8.2 Future Enhancement

The drawback of this tool may be used to further examine FGS scalability. There are still a number of FGS features that need to be enhanced.

Currently FGS can generate four types of fractals based on the three iterations. Future system should consider additional fractal types that can be generated such as fractals that relate to chaos and L-systems. Hence, users can gain better understanding in studying the types of various fractals. More attractive and realistic fractal patterns can be generated by 3-dimensional technology.

For this research, MATLAB tool is used to process the images before feeding the processed image into FGS for further analysis. For future convenience, an additional module can be incorporated to process medical images. Thus users can easily process the images by extracting directly the required information from the images.

8.3 Summary

FGS has shown its capabilities in generating various types of fractals based on the appropriate iteration. These fractals can give some understanding in developing fractals using the algorithms. Different algorithms are used to create different fractal patterns. This makes fractal interesting to learn and study. Moreover, the complexity of fractal can be measured by the value of fractal dimension. Box-counting method is chosen to measure the fractal dimension value of the fractal. FGS has its strength in medical application. Trabecular bone structures were analyzed in terms of the determination of trabecular bone compactness. The results show that FGS has a potential to be used as an alternative tool in determining bone strength and prediction of osteoporosis risk affected by patient's age and gender.

BIBLIOGRAPHY

- Bahrami, A.(1999). *Object Oriented System Development*. McGraw-Hill, New York
- Bergot, C., Laval-Jeantet, A.M., Preteux, F. and Meunier, A. (1988). *Measurement of Anisotropic Vertebral Trabecular Bone Loss During Aging by Quantitative Image Analysis*. *Calcify Tissue Int*;43:143–149.
- Caligiuri, P., Giger, M.L., Favus, M.J., Jia, H., Doi, K. and Dixon, L.B. (1993). *Computerized Radiographic Analysis of Osteoporosis: Preliminary Evaluation*. *Radiology* 186:471-474.
- Cherbit, G. (1990). *Fractals*. Chichester, John Wiley and Sons
- Clayton, K. (1994). *Fractal Memory for Visual Form*. Society for Chaos Theory in Psychology and the Life Sciences, Berkeley, CA
- Connors, M.A. (1997). *Exploring Fractals*. Available from:
<<http://www.math.umass.edu/~mconnors/fractal/intro.html>>
- Crownover, R. (1995). *Introduction to Fractal and Chaos. In Iterated Function Systems, Dimension and Complex Dynamics*. London: Jones and Barlett Publisher International (p. 81-195).
- Cynthia, L. (1996). *Fractals*. Available from: <<http://math.rice.edu/~lanius/frac/>>
- Daniel, C., Pascal, G. and Erick, L. (2004). *Texture Analysis of X-ray Radiographs is Correlated with Bone Histomorphometry*. *Journal Bone Miner Metab* 23 : 24-29**
- Deering, W. and West, B.J. (1992). *Fractal Physiology*. IEEE Engineering in Medical and Biology 11 No. 2: 40-46.
- Edgar, G.A. (1990). *Measure, Topology and Fractal Geometry*. New York: Springer Verlag.
- Fielding, A. (1995). *Applications of Fractal Geometry to Biology*. Oxford University Press, Oxford.
- Flook, A.G. (1982). *Fractal dimensions: their evaluations and their significance in stereological measurements*. *Acta Stereologica*. Proceedings of the 3rd European Symposium on Stereology - 2nd part, 79-87.
- Frederik, S. (2003). *Ultra Fractal*. Available from:< <http://www.ultrafractal.com/>>.

- Gabriele, A.L., Danilo, M., Theo, F.N., Ewald, R.W. (2002). *Fractals in Biology and Medicine*. Berlin: Birkhauser Verlag.
- Geoffrey, D. (2001). *A Comparison of the Texture of Computed Tomography and Projection Radiography Images of Vertebral Trabecular Bone using Fractal Signature and Lacunarity*. Medical Engineering and Physics, 23 :313 –321
- Goldberger, A.L., Rigney, D.R. and West, B.J. (1990). *Chaos and Fractals in Human Physiology*. Sci Am 46:42-49
- Gray, S. B. (1992). *Fractal Math*. Journal of Computers in Mathematics and Science Teaching. 11 (1).31-38.
- Green, D.G. (1995). *Fractal and Scale*. Environmental and Information Sciences, Charles Sturt University.
- Harlan, J.B. (2000). *Fractal: An Overview*. Available from: <<http://www.brotherstechnology.com/docs/fractals.pdf>>
- Hastings, H.M. and Sugihara, G. (1994). *Fractals: A User's Guide to the Natural Sciences*. Oxford: Oxford University Press.
- Havlin, S., Buldyrev, S.V. and Goldberger, A.L. (1995). *Fractal in Biology Medicine*. National Library of Medicine 6:171-201
- Heinz-Otto, P., Hartmut, J., and Dietmar, S. (2004). *Chaos and Fractal: New Frontier of Science*. New York: Springer Publisher.
- High School Honors Institute (2000). *Fractal: An Introduction*. Available from:<<http://amath.colorado.edu/outreach/demos/hshi/2003Sum/Fractals.html>>
- Huang, Q., J.R. Lorch, and R.C. Dubes,(1994). *Can the fractal dimension of images be measured?*, Pattern Recognition, volume 27 , number 3pp. 339-349.
- Kaye, B.H. (1989). *A Random Walk Through Fractal Dimensions*. New York: VCH.
- Keith, C. (1997). *Concepts in Non Linear Dynamic and Chaos*. presented at the Society for Chaos Theory in Psychology and the Life Sciences; Marquette University, Milwaukee, Wisconsin.
- Kenkel, N.C. and D.J. Walker. (1993). *Fractals and ecology*. Abst. Bot. 17: 53-70
- Kleerekoper, M., Villanueva, A.R., Stanciu, J., Sudhaker, R.D. and Parfitt, A.M. (1985). *The Role of 3D Trabecular Microstructure in the Pathogenesis of Vertebral Compression Fractures*. CalcifTiss Int 37:594–597.
- Korvin, G. (1992). *Fractal models in Earth Science*. Amsterdam, Elsevier

- Lapidus, M. L. (2000). *Fractal Geometry and Number Theory*. New York: Birkhäuser.
- Lau, E.M. (2004). *Preventing Osteoporosis in Everyday Life*. 14: 430-434.
- Lewis, R.S (1996). *Fractal In Future. Fractal Geometry*. New York: St. Martin's Press (p.5-20)
- Lin, T., Majumdar, S. and Grampp, S. (1999). *Imaging of Trabecular Bone Structure in Osteoporosis*. *European Radiology*, 9:1781-1788
- Long, C.A. (1994). *Leonardo da Vinci's rule and fractal complexity in dichotomous trees*. *J. Theor. Biol.* 167: 107-113.
- Longley, P.A. and M. Batty. (1989). *On the fractal measurement of geographical boundaries*. *Geogr. Anal.* 21:47-67.
- Lori, W.T. (2004). *Design and implementation of an Osteoporosis Prevention Program*. *American Journal of Public Health* Volume 91, Number 7, p.1056
- Lorimer, N.D., Haight, R.G. and Leary, R.A.(1994). *The Fractal Forest: Fractal Geometry and Applications in Forest Science*. NC-170, US Department of Agriculture, Forest Service, St. Paul Minnesota
- Mandelbrot, B.,(1983). *The Fractal Geometry of Nature*. New York:Freeman and Company.
- Maurice, M.D. and Simon, K., (2003). *Hausdorff Dimension and Diophantine Approximation* to appear in "Fractal Geometry and Applications: A Jubilee of Benoit Mandelbrot", *Proceedings of Symposia in Pure Mathematics*, American Mathematical Society
- McCubbrey, D.A., Goldstein, S.A., Cody, D.D., Goulet, R.W. and Kuhn, J.L. (1991). *The Regional Density, Architectural, and Tissue Properties of Vertebral Trabecular Bone and Their Relation to whole Bone Fracture Properties*. *Adv Bioeng*;20:575–81.
- McGuire, P., (1991). *An Eye for Fractals: A Graphic and Photographic Essay*. Redwood City, CA: Addison Wesley Publishing Company
- McNamee, J.E. (1990). *Introduction to fractals in biomedical research*. *Ann Biomedical Engineering* 18: 109-110.
- Messent, E.A. (2005). *Fractal analysis in Knee Osteoarthritis (OA) is a More Sensitive Marker of Disease than Bone Mineral Density (BMD)*. *Classified Tissue International* 76:419-425
- Michael, F.B. (1988). *Fractals Everywhere*. San Diego: Academic Press Professional.

National Institutes of Health (2005). *The NIH Osteoporosis and Related Bone Diseases*. Available from < <http://www.osteoporosis.nih.gov/> >

Paul, B. (2002). *Self-Similarity*. Available from: <<http://local.wasp.uwa.edu.au/~pbourke/fractals/selfsimilar/>>

Peitgen, H.O. and Dietmar, S. (1988). *The Science of Fractal Images*. New York: Springer-Verlag.

Penn, A.I. (1999). *Estimating Fractal Dimension of Medical Images*. Available from: < <http://www.seas.gwu.edu/~medimage/GWIFMI2.html> >

Pentland, A.P. (1984). *Fractal-Based Descriptions of Natural Scenes*. IEEE Trans Pattern Ann Machine Intell PAMI 6:661–674.

Peterson, I. (1992). *Basins of froth: Visualizing the 'chaos' surrounding chaos*. Sci News 142: 329-330.

Pickover, C.A. (1998). *Chaos and Fractals: A Computer Graphical Journey*. New York: Elsevier Science

Ralph, E.S. and Pharm, D. (2005). *Uses and Limitations of Bone Mineral Density Measurements in the Management of Osteoporosis*. Medscape General Medicine.;7(2):3.

Richards, R. and Kerr, C. (1999). *The Fractals Forms of Nature: a resonant aesthetics*. Paper presented at the Annual Meeting of the Society for Chaos Theory in Psychology and the Life Sciences, Berkeley, CA.

Richardson, M.L. and Gillespy T.(1993). *Magnetic resonance imaging*. In: Kricun ME, ed. *Imaging of Bone Tumors*. Philadelphia, Pa: WB Saunders Co:358-446.

Bonjour, J., Rizzoli, R. and Ferrari, S. (2001). *Osteoporosis, Genetics and Hormones*. Journal of Molecular Endocrinology, 26: 79-94

Sandau, K. and Kurz, H. (1997). *Measuring fractal dimension and complexity-an alternative approach with an application*. J Microsc. Vol 186 Pt 2:164-176

Seeman, C.(1997). *Calcium Enriched Food and Bone Mass Growth in Prepubertal Girls: A Randomized*. Journal of Clinical Investigation 99 :1287 – 1294

Slijkerman, F. (2003). *Ultra Fractal*. Available from:<<http://www.ultrafractal.com>>

Team (1999). *ThinkQuest, Fractal Unleashed*. Available from:<<http://library.thinkquest.org/26242/full/tutorial/ch8.html>>

Teng, H.T (1995). *A Study of Fractal Sets in Dynamical Systems*. Jabatan Matematik, Fakulti Sains, Universiti Malaya.

Thatcher, A.R (1999). *The Long-Term Pattern of Adult Mortality and the Highest Attained Age*. Journal of the Royal Statistical Society, 162.

Teh, A.S. (2000). *Analysis of Computer Generated Fractal Dimension in Biomedical Science*. Fakulti Sains Komputer dan Teknologi Maklumat, Universiti Malaya.

Theiler, J. (1990). *Estimating Fractal Dimension*. Journal of the Optical Society of America A-Optics and Image Science 7, pp. 1055-1073.

Weibel, E.R., Nonnenmacher, T.F. and G.A. Losa (1994). *Fractals in biology and medicine*. Birkhäuser, Cambridge.

WHO Study Group (1994). *Consensus Development Conference: Diagnosis, Prophylaxis, and Treatment of Osteoporosis*. Am J Med ; 94:646-650.

Yuval, F. (1998). *Fractal Image Encoding and Analysis*. New York: Springer Verlag.

Zarinah, M.K.(1995). *Fractal Scenery Graphic System*. National Electronics and Computer Technology Center (NECTEC), National Research Council of Thailand.

University of Malaya